

University of Windsor

Scholarship at UWindor

Electronic Theses and Dissertations

Theses, Dissertations, and Major Papers

1-1-1983

A field investigation of the groundwater ridging hypothesis.

Premadasa M. Attanayake
University of Windsor

Follow this and additional works at: <https://scholar.uwindsor.ca/etd>

Recommended Citation

Attanayake, Premadasa M., "A field investigation of the groundwater ridging hypothesis." (1983).
Electronic Theses and Dissertations. 6776.
<https://scholar.uwindsor.ca/etd/6776>

This online database contains the full-text of PhD dissertations and Masters' theses of University of Windsor students from 1954 forward. These documents are made available for personal study and research purposes only, in accordance with the Canadian Copyright Act and the Creative Commons license—CC BY-NC-ND (Attribution, Non-Commercial, No Derivative Works). Under this license, works must always be attributed to the copyright holder (original author), cannot be used for any commercial purposes, and may not be altered. Any other use would require the permission of the copyright holder. Students may inquire about withdrawing their dissertation and/or thesis from this database. For additional inquiries, please contact the repository administrator via email (scholarship@uwindsor.ca) or by telephone at 519-253-3000ext. 3208.

A FIELD INVESTIGATION OF
THE
GROUNDWATER RIDGING HYPOTHESIS

by

Premadasa M. Attanayake

A Thesis
submitted to the Faculty of Graduate Studies
through the Department of Geology and Geological
Engineering in Partial Fulfillment of the requirements
for the degree of Master of Applied Science at the
University of Windsor

Windsor, Ontario, Canada
1983

UMI Number: EC54762

INFORMATION TO USERS

The quality of this reproduction is dependent upon the quality of the copy submitted. Broken or indistinct print, colored or poor quality illustrations and photographs, print bleed-through, substandard margins, and improper alignment can adversely affect reproduction.

In the unlikely event that the author did not send a complete manuscript and there are missing pages, these will be noted. Also, if unauthorized copyright material had to be removed, a note will indicate the deletion.

UMI[®]

UMI Microform EC54762
Copyright 2010 by ProQuest LLC
All rights reserved. This microform edition is protected against
unauthorized copying under Title 17, United States Code.

ProQuest LLC
789 East Eisenhower Parkway
P.O. Box 1346
Ann Arbor, MI 48106-1346

© M. P. Attanayake 1983
All rights reserved

787685

This work is dedicated to my mother
in appreciation of her love and encouragement
throughout my life.

ACKNOWLEDGEMENTS

I wish to express my sincere gratitude to my thesis supervisor, Dr. M. Sklash for his unselfish guidance and encouragement throughout the preparation of this work. Dr. Sklash also suggested the research topic and financed it from his NSERC grant.

Special thanks go to Dr. W. Findlay, Agriculture Canada, Research Station, Harrow, Ontario, who gave useful suggestions and technical assistance.

Thanks are also extended to all the staff of Agriculture Canada, Research Station, Harrow, Ontario, for various assistance.

I am deeply indebted to my friends, Charles Kamidi, Mitch Obradovic, Ja'afar Ali, Francis Achampong, K. G. Jinadasa, Ranjith Gunethilake, and Ravi Wickramasinghe who painstakingly helped me in the field work.

Thanks also go to Miss Annette Bacon for the typing of this thesis.

Last, but not least, I would like to thank my wife Sununda, without whose moral support and patience, this work could not have been completed.

ABSTRACT

A small experimental plot located at the Agriculture Canada Research station at Harrow, Ontario, was instrumented for a field investigation of the groundwater ridging hypothesis proposed by Sklash and Farvolden (1979).

The first stage of the investigation consisted of a refraction seismic and electrical resistivity survey, which revealed a three layered structure in the area. A single borehole was augered and logged to calibrate the results of the geophysical survey. The results of the drilling show that the topsoil is underlain by a medium-fine sand layer. This sand layer is underlain by a sandy silt layer which gradually changes into silt at a depth of about 4.5 m. The groundwater table was encountered at a depth of 1.7 m.

The subsequent hydrogeological instrumentation installed at the site consisted of twenty-three small diameter piezometers and three observation wells; four tensiometer nests, and four neutron access tubes. A sodium chloride tracer was injected at various distances from the stream to observe how its migration might be affected by the formation of a groundwater ridge.

Results of the tracer test show that the tracer generally moved in the direction of the natural water flow. No movement against the natural hydraulic gradient was observed, however, these observations may be in part due to inappropriate timing of sampling. Data on pressure head,

soil moisture, water table elevation, and piezometric head were collected during one natural and three artificial storms. During all the storm events, a rapid water table response occurred in near-stream piezometers first and in more remote piezometers hours later. It was also observed that the water table response is a function of the depth to the water table. The data indicated an average percentage rise (rise/pre-storm depth from ground surface) of the water table near the stream of about 25% and only 2%, 20 m from the stream. The average height of the capillary fringe determined by neutron logging was about 0.24 m and it remained unchanged even in locations where a considerable water table rise occurred. Tensiometer experiments suggest that the water table rise occurred through the conversion of the tension saturated capillary fringe into phreatic water.

The results of the investigation support groundwater ridging as a possible mechanism for significant and rapid groundwater contribution to storm runoff.

III

TABLE OF CONTENTS

	Page
ACKNOWLEDGEMENTS	I
ABSTRACT	II
LIST OF FIGURES	VII
LIST OF TABLES	XI
1.0 INTRODUCTION	1
1.1 The problem	1
1.2 The importance of recognizing the groundwater contribution to storm runoff ..	3
1.3 Objectives of this study	6
2.0 REVIEW OF EXISTING THEORIES FOR STORM RUNOFF GENERATION	7
2.1 Introduction	7
2.2 Partial area overland flow	8
2.3 Variable source area overland flow	10
2.4 Variable source area subsurface flow	12
2.5 Hortonian overland flow	16
2.6 Channel interception	18
2.7 Groundwater flow	18
2.8 Groundwater ridging hypothesis	21
3.0 THE STUDY AREA	26
3.1 Location and access	26
3.2 Physiography (Richards and Caldwell 1949, Chapman and Putnam 1966).....	26
3.3 Climate (Richards and Caldwell 1949, Sanderson 1980).....	29
3.4 Geology (Richards and Caldwell 1949, Chapman and Putnam 1966, Vagners, 1972, Guiton 1978).....	29
3.5 Hydrogeology (Groundwater probability map 1971, Guiton 1978).....	35
4.0 METHOD OF STUDY	37
4.1 Introduction	37
4.2 Field instrumentation	38
4.2.1 Piezometers and wells	38
4.2.2 Neutron access tubes	43
4.2.3 Tensiometer nests	45
4.3 Field investigation	45
4.3.1 Geophysical survey	45
a) Electrical resistivity survey	47
b) Hammer seismic survey	47
4.3.2 Drilling	48

	Page
4.3.3 Topographical survey	49
4.3.4 Auger holes and test pits	49
4.3.5 Artificial and natural storm monitoring	49
4.3.6 Neutron logging	49
4.3.7 Tensiometer experiments	51
4.3.8 Tracer experiments	51
4.3.9 Testing for hydraulic conductivity	52
4.3.10 Water sampling	52
4.4 Laboratory testing	53
4.4.1 Grain size analyses	53
4.4.2 Chemical analyses for chloride ions	54
4.4.3 Electrical conductivity measurements	55
5.0 RESULTS AND DISCUSSIONS	56
5.1 Introduction	56
5.1.1 Geophysical surveys	57
5.1.2 Drilling	62
5.1.3 Topographical survey	64
5.1.4 Tests for hydraulic conductivity	64
5.1.5 Grain size analyses	64
5.1.6 Water level observations	75
5.2 Natural and artificial storm events	75
5.2.1 October 12, 1982 storm event	75
a) Water table response	75
b) Neutron logging	87
c) Tensiometer experiments	92
5.2.2 October 28, 1982 storm event	96
a) Water table response	96
b) Neutron logging	104
c) Tensiometer experiments	110
5.2.3 October 29, 1982 storm event	116
a) Water table response	116
b) Neutron logging	124
c) Tensiometer experiments	129
5.2.4 November 1 and 2, 1982 storm event ..	133
a) Water table response	133
b) Tensiometer experiments	139
5.3 Tracer experiments	142
5.4 Summary of results	148
5.5 Discussion of results	149
6.0 CONCLUSIONS AND RECOMMENDATIONS	152
6.1 Conclusions	152
6.2 Recommendations	154
LIST OF REFERENCES	155
APPENDIX I Analytical Methods	163

		Page
APPENDIX II	Results of the Investigation of the Site	168
APPENDIX III	Results of the October 12, 1982 Storm Event	179
APPENDIX IV	Results of the October 28, 1982 Storm Event	184
APPENDIX V	Results of the October 29, 1982 Storm Event	189
APPENDIX VI	Results of the November 1, 2, 1982 Storm Event	194
APPENDIX VII	Results of the Tracer Experiments ...	197

LIST OF FIGURES

	Page
Figure 1 Mechanisms of storm flow generation (after Freeze, 1974).	9
Figure 2 Block diagram and a cross-section showing the partial area overland flow concept (after Wilson, 1981).	9
Figure 3 Block diagram showing the variable source area overland flow concept (after Wilson, 1981).	14
Figure 4 Block diagram showing the variable source area subsurface flow concept (after Wilson, 1981).	14
Figure 5 The expansion of the source area and the channel system during a storm under the variable source area sub- surface flow concept (after Hewlett and Nutter, 1970).	15
Figure 6 A block diagram showing Hortonian over- land flow concept (after Wilson, 1981).	19
Figure 7 A block diagram showing channel inter- ception (after Wilson, 1981).	19
Figure 8 Formation of a near stream groundwater ridge in response to rain (after Sklash and Farvolden, 1979).	23
Figure 9 A block diagram showing the groundwater ridging hypothesis (after Wilson, 1981).	24

		Page
Figure 10a	Location map of Essex County.	27
Figure 10b	Location map of the experimental plot.	28
Figure 11	Annual mean daily temperature of Essex County (after Sanderson, 1980).	31
Figure 12	Mean annual precipitation of Essex County (after Sanderson, 1980).	31
Figure 13	Mean annual snow fall of Essex County (after Sanderson, 1980).	32
Figure 14	Surficial geology of Essex County (after Guiton, 1978).	34
Figure 15	Instrumentation of the experimental plot.	39
Figure 16a-c	Cross-sections along the lines of instrumentation.	40
Figure 17	Sketch of a typical piezometer installation.	44
Figure 18	Sketch of a typical tensiometer nest.	46
Figure 19	Interpretation of resistivity survey data.	58
Figure 20	Seismic survey travel-time curve for Line 1.	60
Figure 21	Seismic survey travel-time curve for Line 2.	61
Figure 22	Borehole log of the deep well.	63
Figure 23	Topographic map of the experimental plot.	65

VIII

		Page
Figure 24	Determination of hydraulic conductivity using Hvorslev's method.	66
Figure 25a-d	Particle size distribution curves.	71
Figure 26	Map showing the depth to the water table.	76
Figure 27	October 12, 1982 storm event. Flow net before the storm event.	80
Figure 28a-c	October 12, 1982 storm event. Cross-sections showing water table response during the storm.	81
Figure 29	October 12, 1982 storm event. Groundwater table response in selected wells and piezometers.	86
Figure 30a-d	October 12, 1982 storm event. Relationship of volumetric moisture content with depth.	88
Figure 31a-c	October 12, 1982 storm event. Relationship of pressure head with depth.	93
Figure 32	October 28, 1982 storm event. Flow net before the storm event.	98
Figure 33a-c	October 28, 1982 storm event. Cross-sections showing water table response during the storm event.	99
Figure 34	October 28, 1982 storm event. Groundwater response in selected wells and piezometers.	105
Figure 35a-d	October 28, 1982 storm event. Relationship of volumetric moisture content with depth.	106

IX

		Page
Figure 36a-c	October 28, 1982 storm event. Relationship of pressure head with depth.	111
Figure 37	October 29, 1982 storm event. Flow net before the storm event.	117
Figure 38a-c	October 29, 1982 storm event. Cross- sections showing water table response during the storm event.	118
Figure 39	October 29, 1982 storm event. Ground- water table response in selected wells and piezometers.	123
Figure 40a-d	October 29, 1982 storm event. Relation- ship of volumetric moisture content with depth.	125
Figure 41a-c	October 29, 1982 storm event. Relation- ship of pressure head with depth.	130
Figure 42	November 1 and 2, 1982 storm event. Flow net after the storm.	135
Figure 43a-c	November 1 and 2, 1982 storm event. Cross-sections showing water table response.	136
Figure 44	November 1 and 2, 1982 storm event. Relationship of pressure head with depth.	140
Figure 45a-e	Migration of the tracer, based on chemical analyses and electrical conductivity.	143

Figure 46 Migration of the tracer, based on
the resistivity profiling.

147

LIST OF TABLES

	Page
Table 1. Studies using environmental oxygen-18 and tritium to determine pre-event water contributions to storm flow (after Bernier, 1982).	2
Table 2. Seasonal distribution of mean temperature, precipitation, and snowfall in Harrow area (after Sanderson, 1980).	30
Table 3. Hydraulic head before storm events (m).	78
Table 4. October 12, 1982 storm event. Percentage rise/decline of the water table.	84
Table 5. October 12, 1982 storm event. Rise of the water table determined by different methods.	97
Table 6. October 28, 1982 storm event. Percentage rise/decline of the water table.	102
Table 7. October 28, 1982 storm event. Rise of the water table determined by different methods.	115
Table 8. October 29, 1982 storm event. Percentage rise/decline of the water table.	121
Table 9. October 29, 1982 storm event. Rise of the water table determined by different methods.	134

	Page
Table 10. November 1, 2, 1982 storm event. Decline of the water table determined by different methods.	141
Table 11. Summary Table.	150

A Field Investigation of the Groundwater Ridging Hypothesis

1.0 INTRODUCTION

1.1 The Problem

Most of the recent literature and existing theories on storm runoff generation do not consider groundwater flow as a significant component in storm runoff peaks (Betson, 1964; Dunne and Black, 1970; Freeze, 1974; Steppuhn, 1975). It is argued that, with its inherent low velocity, groundwater cannot respond rapidly enough to contribute significantly to a storm runoff peak (Ward, 1982). However, recent studies by Toler (1965), Pinder and Jones (1969), Crouzet et al. (1970), Dincer et al. (1970), Foster (1974), Martinec (1975), Sklash et al. (1976), Fritz et al. (1976), Anderson and Burt (1977), Sklash (1978), Sklash and Farvolden (1979), O'Brien (1980), Reid et al. (1981), Martinec et al. (1981), and Sklash and Wilson (1982) have demonstrated that groundwater often constitutes the major component in flood peaks. Bernier (1982) tabulated most of the available data on pre-event water contributions to storm runoff (Table 1). As is shown in Table 1 for the different areas studied, contributions of pre-event water account for 50 to 90 percent of discharge.

Pinder and Jones (1969) used analyses of total dissolved solids to determine the groundwater component in three different watersheds in Nova Scotia. In these watersheds

Table 1. Studies using environmental O^{18} and tritium to determine pre-event water contribution to storm flow (after Bernier 1982)

Study	Location	Area and land use/cover	Deposits	Range in Rainfall events (mm)	Pre-event water Contributions (%)	
					To Peak discharge	To total stormflow*
Dincer <i>et al.</i> 1970	Czechoslovakia	2.65 km ² 70% mountain meadows 30% forest	glacial deposits	snowmelt	---	major
Martinec <i>et al.</i> 1974	Switzerland	43.3 km ² 6% forest & glaciers 94% mountain meadows	glacial deposits	snowmelt	---	major
Fritz <i>et al.</i> 1974	Ontario, Canada	forest	glacial deposits	---	---	50-70
Cherry <i>et al.</i> 1975	Ontario, Canada	1.2-22 km ²	glacial deposits	50	50-60	50-90
Sklash <i>et al.</i> 1976	Ontario, Canada	73-108 km ² improved farmland	silty to coarse sand	21-28	70-75	70
Sklash and Farvolden 1979	Ontario, Canada	1 km ² intensive agriculture	coarse sand over silty clay	17-38	60-80	—
" "	Quebec, Canada	1.2 km ² forest	glacial till	6-35	65-80	---
Crouzet <i>et al.</i> 1970	France	5.7-91 km ²	—	6-31	—	54-99

*as defined in the different studies.

groundwater runoff constituted 42% of the peak discharge for the period of analysis. Sklash and Farvolden (1979) using environmental isotopes in several small watersheds in Quebec showed that groundwater constituted about 60% of the peak discharge. O'Brien (1980) used a dynamic hydrograph separation method to analyze stream runoff for two wetland controlled basins in eastern Massachusetts. As a result of this study, he concluded that groundwater was the major component of flood peaks and accounted for approximately 93% of the total annual discharge.

Although large groundwater contributions to storm runoff are now recognized by many hydrologists, no mechanism has been widely accepted to explain it. One plausible solution was formalized by Sklash and Farvolden (1979) in terms of a large and rapid increase in groundwater potential near the stream channels, reflecting the formation of a groundwater ridge.

1.2 The Importance of Recognizing the Groundwater Contribution to Storm Runoff

The prediction of storm runoff peaks and the maintenance of acceptable water quality standards in streams has a vital importance. In an agricultural area, surface and subsurface runoff constitute the primary transport vehicle for movement of agricultural chemicals. It is quite important that their flow paths be clearly identified, if pollution of streams and groundwater supplies are to be

prevented. It is also important to know the paths through which rain water reaches the streams to design watershed management schemes for more effective flood control.

The literature suggests a common inverse relation between water discharge and the concentration of several dissolved species in the stream water. It also suggests that the direct surface runoff which provides the greater part of the discharge during the floods dilute the stream water (Glover and Johnson, 1974; Hall, 1971; Pilgrim and Huff, 1979). In contrast to this concept, Sklash et al. (1978) showed that nitrate concentrations in stream runoff can increase during a storm event as a result of increased nitrate-enriched groundwater discharge. Pinder and Jones (1969) also showed that the stream runoff was less diluted during a storm, than anticipated. Following a runoff analysis by electrical conductance of water, Nakamura (1971) concluded that present dilution models failed to account for the chemical behaviour of the storm runoff. Walling and Foster (1975) wrote that in many streams individual solute species do not all exhibit a drop in the concentration associated with a rise in discharge. They showed that nitrate and potassium concentrations, in particular, often increase during flood events. As a result of research carried out in a watershed in Scotland, Reid et al. (1981) concluded that the chemistry of the stream water was controlled by processes in the soil. They also suggested that, at times of baseflow, water drains from the lower

mineral horizons and has high concentrations of cations, silicon, and bicarbonate produced by weathering. During storms, river water is mostly derived from upper organic and organo-mineral surface horizons and contains much lower concentrations of weathering products. It is, however, enriched in aluminum, iron, and manganese, so that most of the loss of these metals occur at times of high discharge. Toler (1965) showed that the decrease in concentration of dissolved solids is not proportional to the dilution of stream water during storm events. He also showed that the total amount of dissolved solids is much higher at high discharge than at low discharge. All of these observations suggest that the groundwater component in storm runoff is greater than it is generally thought to be.

Existing models for runoff generation, such as overland flow, can explain the quantitative aspects of storm runoff peaks. For example, these concepts can explain the increased discharge during storm events. But as it was shown by Pinder and Jones (1969), Nakamura (1971), Walling and Foster (1975), Reid, et al. (1981), and Toler (1965), they are unable to account for the observed stream chemistry variation during runoff events.

Sklash and Farvolden (1979), in an attempt to explain the observed increase in groundwater flow to streams during storms, introduced a new hypothesis, the groundwater ridging hypothesis. According to Sklash and Farvolden, a groundwater ridge is formed near the streams during storms.

The resulting steepened hydraulic gradient and increased groundwater discharge area would then be capable of producing large groundwater contributions to the stream channel. The groundwater ridging hypothesis, if valid, may be able to explain the observed stream chemistry variations during storm runoff.

1.3 Objectives of this Study

The primary objective of this study is to examine the validity of the groundwater ridging hypothesis. To achieve this objective, the following main points of the hypothesis are to be tested:

1. Is there a rapid groundwater table response in near stream wells and piezometers?
2. Is there a conversion of the tension saturated capillary fringe into a pressure saturated zone?
3. What is the response of the capillary fringe to storm events?

A combination of hydrometric and tracer techniques was utilized on a selected experimental plot at the Agriculture Canada Research Station at Harrow. The responses of the water table, piezometric head, soil moisture and tracer migration were recorded and analyzed to determine if the responses are compatible with the groundwater ridging hypothesis.

2.0 REVIEW OF EXISTING THEORIES FOR STORM RUNOFF GENERATION

2.1 Introduction

The relationship between precipitation and river flow can be expressed in terms of the continuous circulation of water through the hydrologic cycle (Ward, 1982). This relationship is at the very core of hydrology; the prediction of runoff from rainfall which is one of the major problems hydrologists face today (Freeze and Cherry, 1979). To solve this problem, one has to understand the watershed response to rainfall and the paths through which water reaches streams. These paths are a function of local geology, climate, topography, soils, vegetation, and land use (Freeze and Cherry, 1979). It means, that in various watersheds or even in different parts of the same watershed, various processes may generate stream flow. Until a hydrogeological theory of how water moves rapidly into stream channels is confirmed, it will not be possible to finalize models for erosion or to provide satisfactory predictions about the effect of pollution, agricultural practices, forest management techniques, or land drainage improvements upon the quality and quantity of water in landscape (Ward, 1982).

Most of the numerous theories for runoff generation were summarized into three basic mechanisms by Freeze (1974):

1. partial area overland flow,

2. variable source area subsurface flow, and
3. variable source area overland flow.

Figure 1 (after Freeze, 1974) shows the mechanisms of storm flow generation. In addition to the above mentioned theories, Hortonian overland flow, channel interception, groundwater flow, and groundwater ridging are possible mechanisms of runoff generation.

2.2 Partial Area Overland Flow

Betson (1964) developed a non-linear mathematical model to analytically equate the difference between rainfall and runoff to hydraulic variables. This equation indicated that runoff usually originates from a small, but relatively consistent, part of the watershed. Based on this observation, Betson suggested the partial area overland flow concept. Figure 2 is a block diagram and a cross-section showing the partial area overland flow concept.

According to Betson, overland flow does not commonly occur throughout a watershed, but it originates from a small but relatively consistent part of the watershed where the infiltration capacity of the soil is exceeded by the rainfall intensity. Other parts of the watershed seldom or never contribute to the overland flow. The partial areas can be located anywhere in the watershed but are usually associated with soils that have a shallow A horizon. The transfer of runoff water takes place as overland flow, consequently the amount of water that reaches the stream is

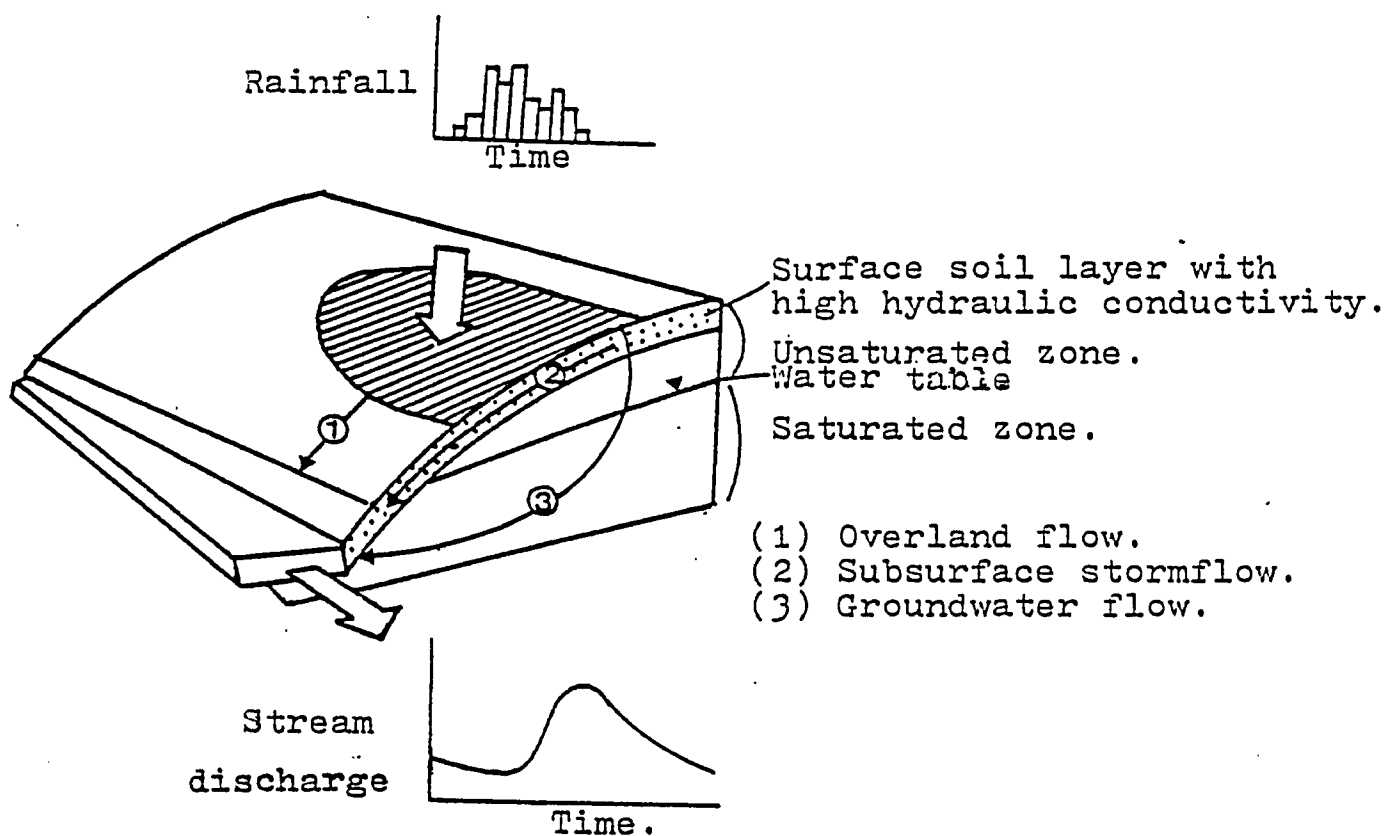


Figure 1. Mechanisms of storm flow generation (after Freeze, 1974).

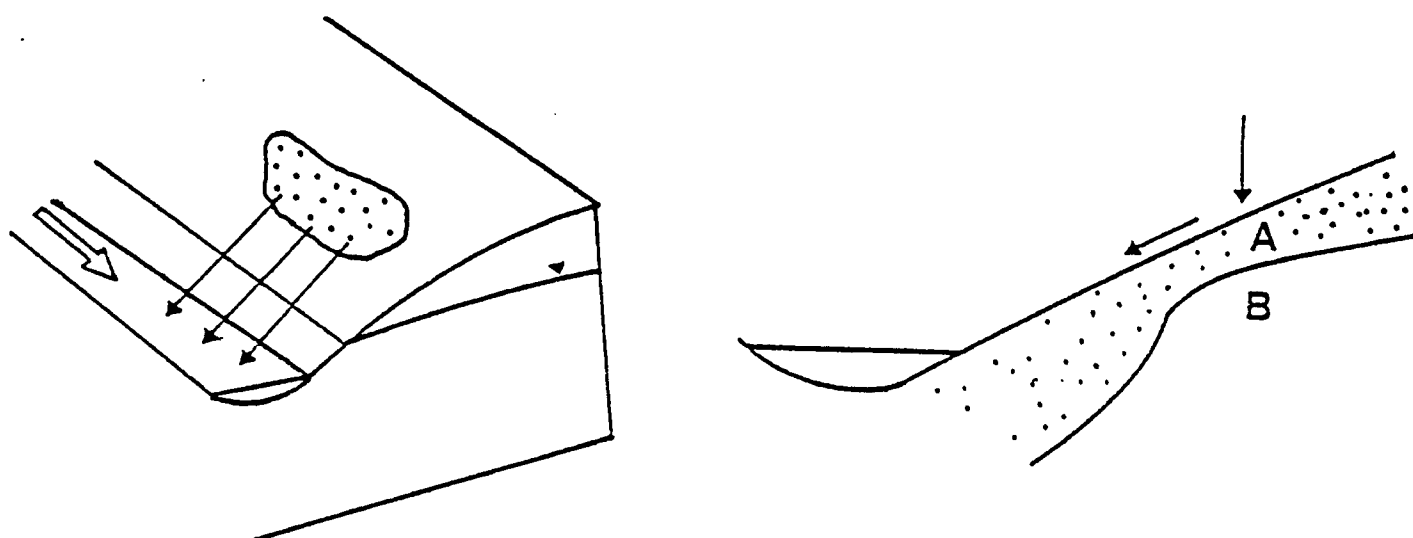


Figure 2. Block diagram and a cross sections showing the partial area overland flow concept (after Wilson, 1981).

a function of the soil type found on its route.

Further field investigation of the partial area overland flow concept was done by Betson and Marius (1969) in an agricultural watershed. The study included the use of subplots, observation wells, and piezometers. The results obtained supported the concept. Engman and Ragowski (1974) using a hydrograph model which utilized a physically based infiltration capacity distribution for computation of excess rainfall, showed that the partial area overland flow is a possible mechanism of stream flow generation.

2.3 Variable Source Area Overland Flow

Using an integrated set of surface and subsurface instrumentation, Dunne and Black (1970a, b) showed that the major portion of the storm runoff was produced as overland flow on a small proportion of the watershed. They also observed that, when the water table rose to the ground surface, overland flow was generated. Only when this overland flow occurred were significant amounts of storm flow contributed to the channel. Based on these observations, Dunne and Black (1970a,b) introduced the variable source area overland flow concept as a possible mechanism for storm runoff generation.

According to this concept, runoff is generated from watershed areas which have become saturated from below by a rising water table. These partial areas contributing quick runoff can expand or contract seasonally or during a storm.

Their position and expansion can be related to geology, topography, soils, and rainfall characteristics. A block diagram illustrating the variable source area overland flow concept is given in Figure 3.

Analyzing a series of storms, Ragan (1968) also showed that only a small portion of the watershed contributed flow to the storm hydrograph. Further research by Dunne et al. (1975) substantiated the variable source area concept. As a result of a runoff simulation for rainfall events on a hypothetical upstream area carried out with a deterministic mathematical model, Freeze (1972a, b) provided theoretical support for the variable source area overland flow concept. Furthermore, Freeze (1974) in summarizing several papers on stream flow generation, wrote that most overland flow is generated on small upland partial areas that are, more or less, fixed in size. These partial areas are controlled by the distribution of soil types on expanding and contracting 'variable source areas' that are adjacent to stream and that are controlled by the topographic and hydrogeologic configuration of the hill slopes.

Freeze (1974) pointed out that the variable source area concept differs from the partial area concept in two ways. First, the partial areas are, more or less, fixed and can be located anywhere in the watershed, while variable areas can expand and contract and are generally located near the streams. Secondly, partial areas feed streams by means of overland flow, that is, by water that accumulates as a

result of the saturation of soils at the surface from above, whereas variable areas occur due to the saturation from below by a rising water table. Since the variable source areas are generally located adjacent to the streams, rain falling on these areas flows overland to the streams. Groundwater which returns to the surface of variable source areas before reaching the stream channel (return flow) joins the overland flow and flows to the stream.

2.4 Variable Source Area Subsurface Flow

Working with a laboratory model to explain the source of stream flow, Hewlett and Hibbert (1967) observed that the soil moisture content and tension substantiated the theory that the entire unsaturated soil mass was contributing to outflow throughout their experiment. Based on these observations, Hewlett and Hibbert (1967) proposed the variable source area subsurface flow concept, as the primary source of storm flow generation.

Even before Hewlett and Hibbert, researchers like Toth (1962) and Whipkey (1965) made similar conclusions. Based on the data obtained from several small drainage basins in central Alberta, Toth (1962) showed that, during intense precipitation, water infiltrates on the upper slopes and then moves horizontally through the middle slope material and vertically upward near the base of slopes. A similar pattern was simulated by Klute et al. (1965) and further substantiated by additional research by Hewlett and Nutter

(1970) and Weyman (1970). In an experimental watershed in Ohio, Whipkey (1965) observed that subsurface stormflow is a common occurrence in forested areas. He also noted that the undisturbed forest soil is generally covered by organic litter that protects the soil surface and keeps it permeable to water infiltration. In addition, the A and B horizons of forest soils are interlaced with roots, old root holes, animal burrows, and structural channels that provide a highly permeable medium for the rapid movement of water in all directions.

According to the variable source area subsurface flow concept, all precipitation infiltrates the soil surface. Then, as a result of combined processes of infiltration and throughflow, water moves to the stream through the soil profile. When the subsurface flow of water exceeds the capacity of the soil profile to transmit it, the water comes to the surface and channel length grows. Figures 4 and 5 illustrate the variable source area subsurface flow concept.

The basic requirement for subsurface flow is a highly permeable shallow soil horizon. There is considerable evidence to support the common occurrence of such a layer in the form of the A soil horizon of agriculturally tilled soil or forest litter (Freeze, 1972b).

On the basis of simulations with a mathematical model, Freeze (1972b) showed that subsurface stormflow is significant in runoff generation only on hillslopes that

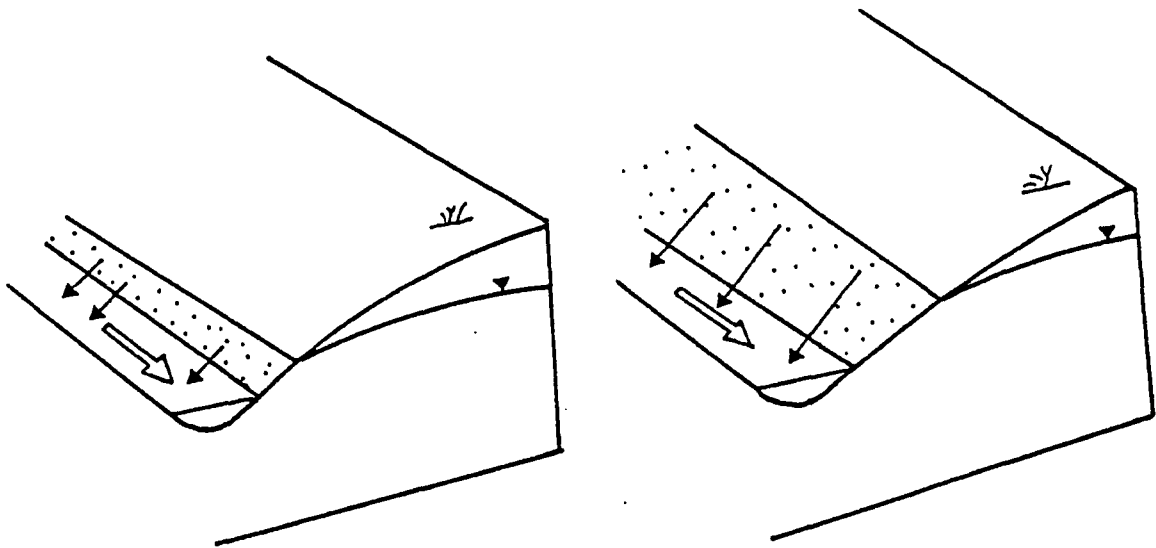


Figure 3. Block diagram showing the variable source area overland flow concept (after Wilson, 1981.).

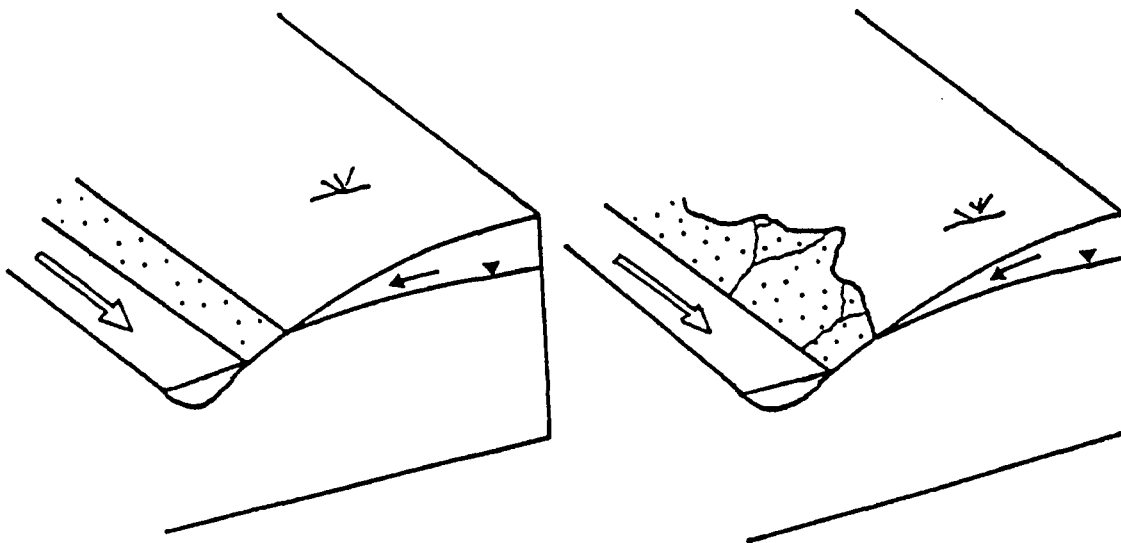


Figure 4. Block diagram showing the variable source area subsurface flow concept (after Wilson, 1981.).

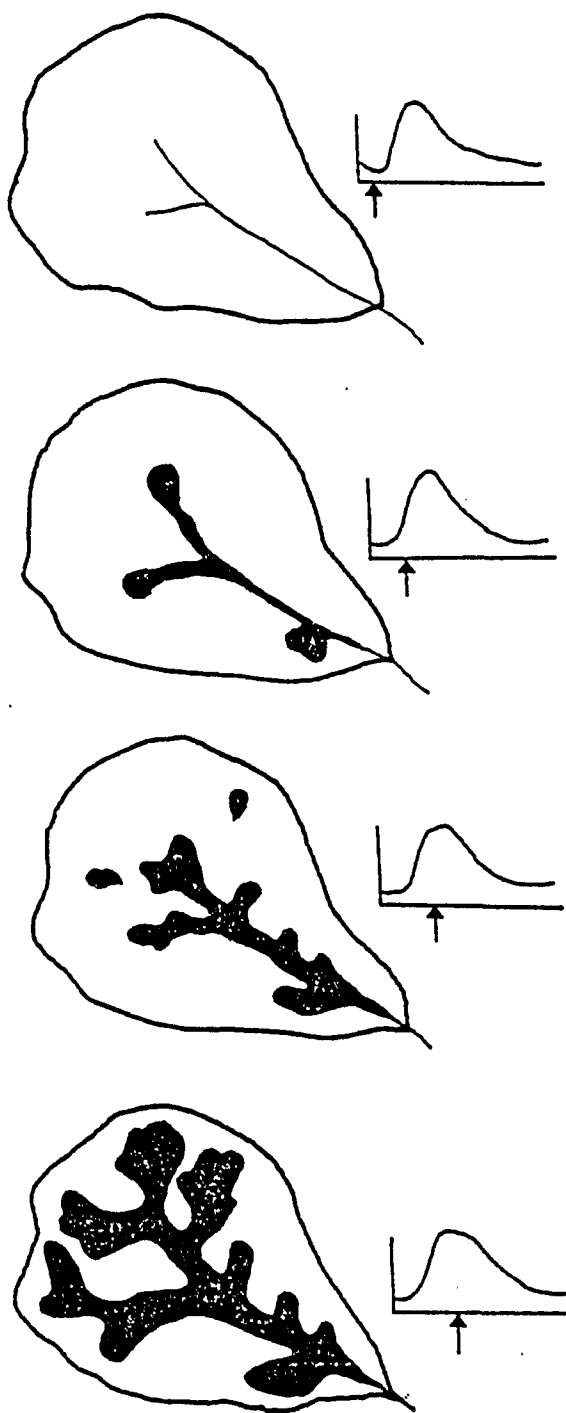


Figure 5. The expansion of the source area and the channel system during a storm under the variable source area subsurface flow concept (after Hewlett and Nutter, 1970).

feed deeply incised channels and then only when the permeability of the soils on the hillslopes is very high. However, there is considerable doubt as to the ability of this mechanism to generate a significant amount of runoff quickly enough to produce observed storm hydrographs (Freeze, 1974). Ragan (1968) also observed subsurface stormflow in the hillside forest litter, but found it to be quantitatively unimportant as a contributor to storm runoff. Based on their observations in an experimental plot, Dunne and Black (1970a,b) wrote: "Although soils and topography were those generally thought to be conducive to subsurface stormflow, the runoff produced by this mechanism was too small, too late, and too insensitive to fluctuations of rainfall intensity to add significantly to stormflow in the channel at the base of the hillside."

2.5 Hortonian Overland Flow

The overland flow concept introduced by Horton (1933) is based on the assumption that the infiltration rate of the rain water to the surface soils declines with time. The infiltration rate eventually reaches a steady state as the soil pores become filled. If the rainfall exceeds this steady state rate, excess water will pond on the surface and cause overland flow. According to Hortonian theory, most storm events exceed the steady state infiltration rate and produce widespread overland flow. Figure 6 is a block diagram showing the Hortonian overland flow concept.

Hortonian overland flow can be observed frequently in paved areas in urban centres and in poorly vegetated areas such as ploughed fields and arid environments. It can also occur under snowpack areas where the infiltration capacity is lowered by the presence of concrete frost in the soil (Dunne et al., 1975).

Betson (1964), using a non-linear mathematical model, showed that storm runoff usually occurs from only a small part of the watershed and that the infiltration capacity of a greater part of the watershed is seldom exceeded during normal storms. During their field experiments, Dunne and Black (1970a,b) observed no overland flow generated by the mechanisms described by Horton, although the rainfall intensity exceeded the infiltration capacity.

Freeze (1974) in summarizing several papers on the infiltration process, concluded that the infiltration capacity of a soil after some time approached its saturated hydraulic conductivity and that overland flow could be generated only in cases where both the rainfall rate is greater than the saturated hydraulic conductivity of the surficial material and the rainfall duration is sufficient to produce surface saturation. After relating the rainfall intensities most commonly recorded to the saturated hydraulic conductivity of soils, Freeze (1972b) showed that very few rain events are capable of producing overland flow. Hills (1971) in a similar attempt to relate infiltration measurements to local rainfall rates in sites with various

soils and slopes showed that on many sites fewer than 10% of rainfalls can produce overland flow.

Analyzing runoff producing mechanisms, Ward (1982) concluded that Horton's explanation of river response to precipitation was based on a number of false premises.

2.6 Channel Interception

Channel interception is a runoff producing mechanism which is characterized by rain falling directly onto the stream surface. Although it takes place in all storm events, channel interception is normally a minor contributor to storm runoff because the surface area of the stream is comparatively small relative to the watershed area. A block diagram showing channel interception is given in Figure 7.

Channel interception may be important during brief storms following long periods of draught, when other mechanisms are not likely to be operative (Sklash, 1978).

2.7 Groundwater Flow

Water that flows into streams from the permanent groundwater flow systems is called groundwater flow. Groundwater can be discharged into streams in three different ways: through near stream springs or seeps, through the seepage face, and directly through the stream bed.

In most studies, groundwater flow was not considered as a major contributor to runoff during storms (Betson, 1964;

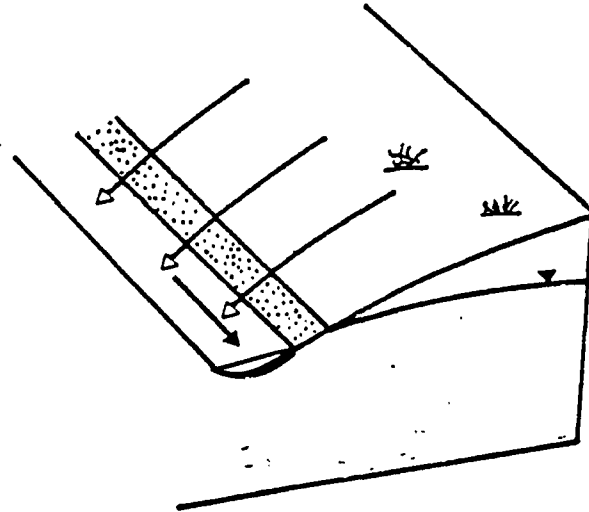


Figure 6. Block diagram showing Hortonian overland flow concept (after Wilson, 1981).

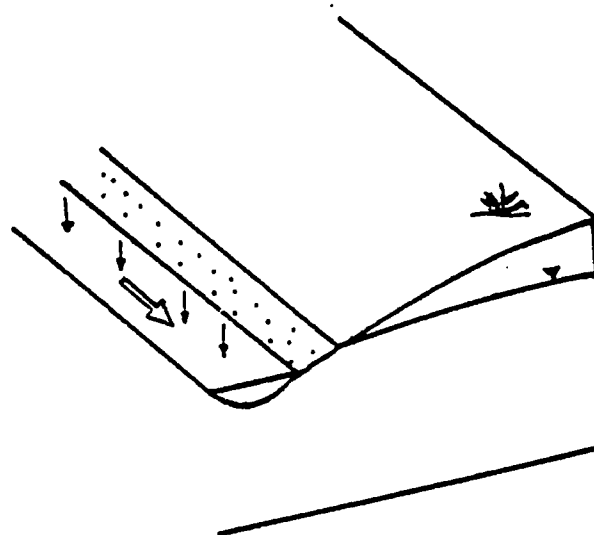


Figure 7 Block diagram showing channel interception (after Wilson, 1981).

Dunne and Black, 1970; Freeze, 1974; Steppuhn, 1975; and others). Freeze (1974) stated that the primary role of groundwater is to sustain baseflow during low-flow periods between storms. He also suggests that baseflow contributions to runoff can be increased only if and when the infiltrating rain produces a widespread rise in the watertable (Freeze, 1971).

Recent studies using chemical and isotopic mass balance and hydrometric techniques suggest that groundwater is an active and major contributor to storm and snowmelt runoff. In highly permeable catchments such as the River Hull, groundwater has long been accepted as the major component of streamflow (Foster, 1974). Toler (1965) concluded from field evidence that groundwater flow to streams is increased in areas where groundwater levels respond rapidly to rainfall. Using chemical mass balance equations, Pinder and Jones (1969) showed that in three small watersheds in Nova Scotia, groundwater runoff constituted about 42% of peak discharge. Following measurements of oxygen-18 and tritium concentrations in precipitation, snowpack and runoff in several watersheds in Northern France, Dincer et al. (1970) concluded that groundwater constituted a major part of the runoff. Crouzet et al. (1970) also used tritium concentrations to show the dominant role of groundwater in storm runoff. Using the oxygen-18 technique in several watersheds in Quebec, Sklash et al. (1978) showed that groundwater was the major component of storm runoff, providing more than 50% of the peak discharge. O'Brien

(1980) concluded from hydrometric field evidence that groundwater accounted for 93 percent of the total annual discharge from two small wetland catchments in Massachusetts. Based on tracer and piezometric measurements, Sklash and Farvolden (1979) showed the responsive and significant role of groundwater in storm runoff. Following a study on chemistry of precipitation and river water, Reid et al. (1981) concluded that all the river water originates from soil. All these observations confirm the active role played by groundwater during storm and snowmelt events.

2.8 Groundwater Ridging Hypothesis

Although the exact means by which groundwater reaches the stream so rapidly during storm and snowmelt runoff is not clearly understood, considerable evidence can be found in literature to support the large groundwater contributions to storm runoff. Sklash and Farvolden (1979) proposed the groundwater ridging hypothesis as a possible explanation of how groundwater reaches the stream so rapidly during high runoff events.

According to the groundwater ridging hypothesis, for a larger discharge of groundwater to the stream, one or more of the following criteria must be met: an increase in the hydraulic gradient, an increase in the discharge area, or an increase in hydraulic conductivity. Sklash and Farvolden (1979) argue that the hydraulic conductivity of a particular soil is not likely to change during a storm, therefore the

first two criteria may be responsible for increased groundwater discharge.

Based on their hydrometric and isotopic observations, Sklash and Farvolden (1979) showed how the hydraulic gradient and/or discharge area might increase rapidly. Sklash and Farvolden suggest that along the perimeter of perennial and transient discharge areas, the water table and its associated capillary fringe lie very close to the surface. Soon after a rain or snowmelt event begins, infiltrating water readily converts the near-surface tension saturated capillary fringe into a pressure saturated zone or groundwater ridge (Figure 8). The authors of the groundwater ridging hypothesis have used mathematical simulations of four watersheds with different near stream relief and basin width combinations to support their hypothesis. According to the groundwater ridging hypothesis, the ridge eventually becomes less pronounced as the other parts of the basin start to respond to the storm. Figure 9 is a block diagram showing the groundwater ridging hypothesis.

The variable source area overland flow concept can be considered as one particular case of the groundwater ridging hypothesis, where the ridge emerges at the ground surface to produce overland flow. The rise of the water table in the variable source area concept is equivalent to the groundwater ridge forming, however, according to the groundwater ridging hypothesis, the water table does not

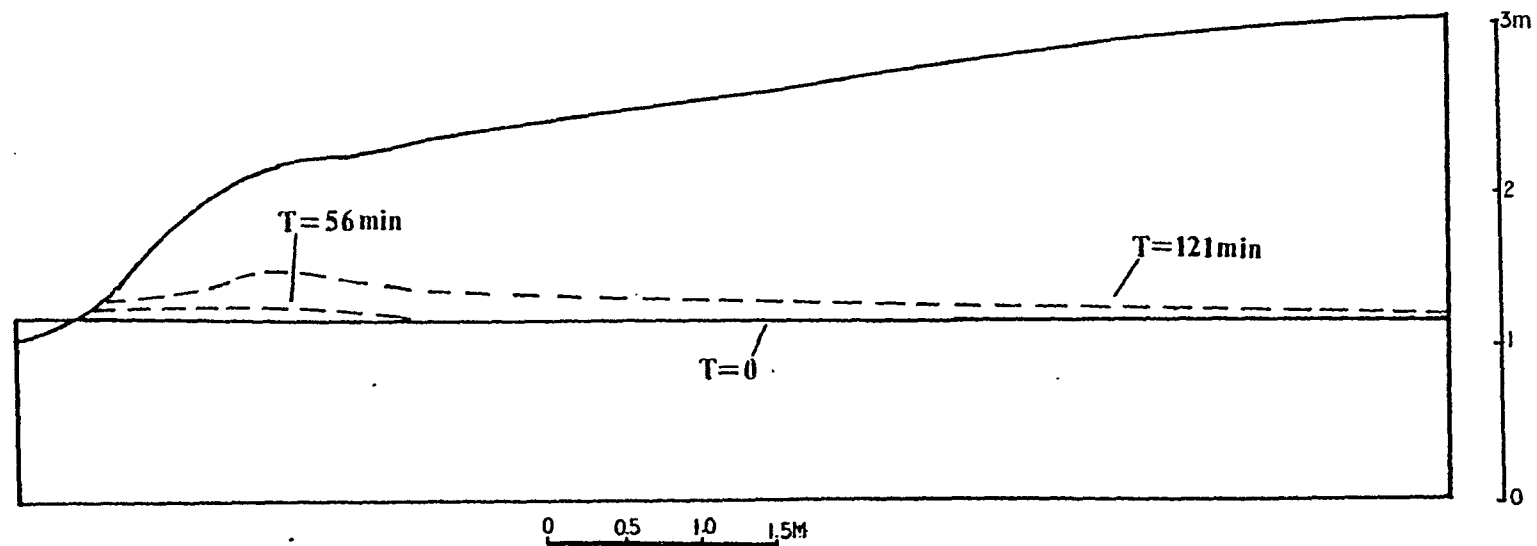


Figure 8. Formation of a near stream groundwater ridge in response to rain (after Sklash and Farvolden, 1979).

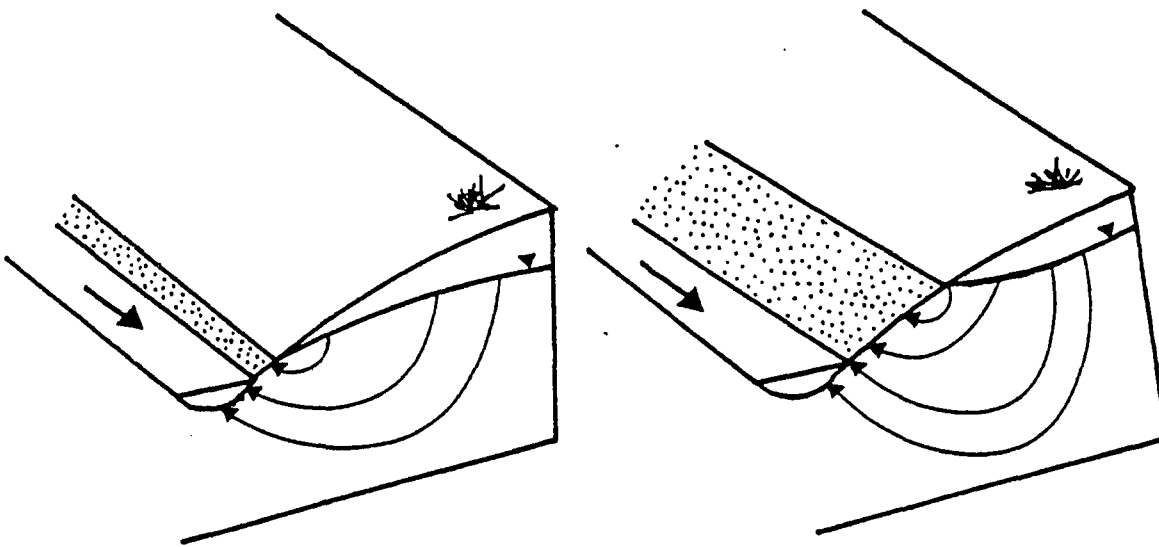


Figure 9. Block diagram showing the groundwater ridging hypothesis (after Wilson, 1981).

have to reach the ground surface before groundwater starts to discharge. As soon as the ridge starts forming, the hydraulic gradient and the discharge area increase, consequently progressively more groundwater starts flowing into the stream. Also, the variable source area overland flow concept does not specify whether the resultant overland flow is rain water or groundwater.

The groundwater ridging concept is not entirely new. For example, Hewlett (1961) offered an explanation of baseflow which visualizes the entire soil mantle as a storage aquifer feeding sustained flow. In this view, narrow groundwater bodies along the stream channels are not of themselves the source, but rather a conduit through which slowly draining soil moisture passes to enter the stream. Working in a watershed in Vermont, Ragan (1968) observed formation of a groundwater ridge along the channel. Hewlett (1969) wrote that the rise in the groundwater table near the stream channel helps to produce the storm hydrograph. Wilson (1981) witnessed a groundwater ridge forming in research watersheds in Quebec. Zaslavsky and Sinai (1981) showed the possibility of high groundwater discharge as a result of rapid increase in hydraulic gradient.

3.0 STUDY AREA

3.1 Location and Access

The study area is located at the Agriculture Canada Research Station near the town of Harrow, Ontario (42 02'N, 82 54'W) which is about 30 km S.E. of Windsor, Ontario, Canada (Figure 10a, b). Essex County is bounded by Lake St. Clair to the north, Lake Erie to the south, and Kent County to the east. The western boundary is the Detroit River.

Essex County is well serviced with a good network of paved roads at about 3 km intervals. The site is reached from Windsor by Highway 3, Walker Road, and Highway 18.

3.2 Physiography (Richards and Caldwell, 1949; Chapman and Putnam, 1966)

Other than a few scattered sand and gravel ridges and hillocks, Essex County is predominantly a smooth clay plain. Lake Erie to the south has an altitude of 187.6 m above sea level and Lake St. Clair to the north, 188.9 m. Only one hill, located in the Leamington-Ruthven area, rises more than 30 m above the surrounding plains.

Drainage water flows into Lakes St. Clair and Erie and the Detroit River through numerous small streams (Figure 10a). The streams flowing into Lake Erie are comparatively short. The Ruscom and Belle Rivers are the largest rivers in the county. Most of the Essex plain has such imperfect drainage that dredged ditches and tile underdrains have had

Figure 10a. Location map of Essex County.

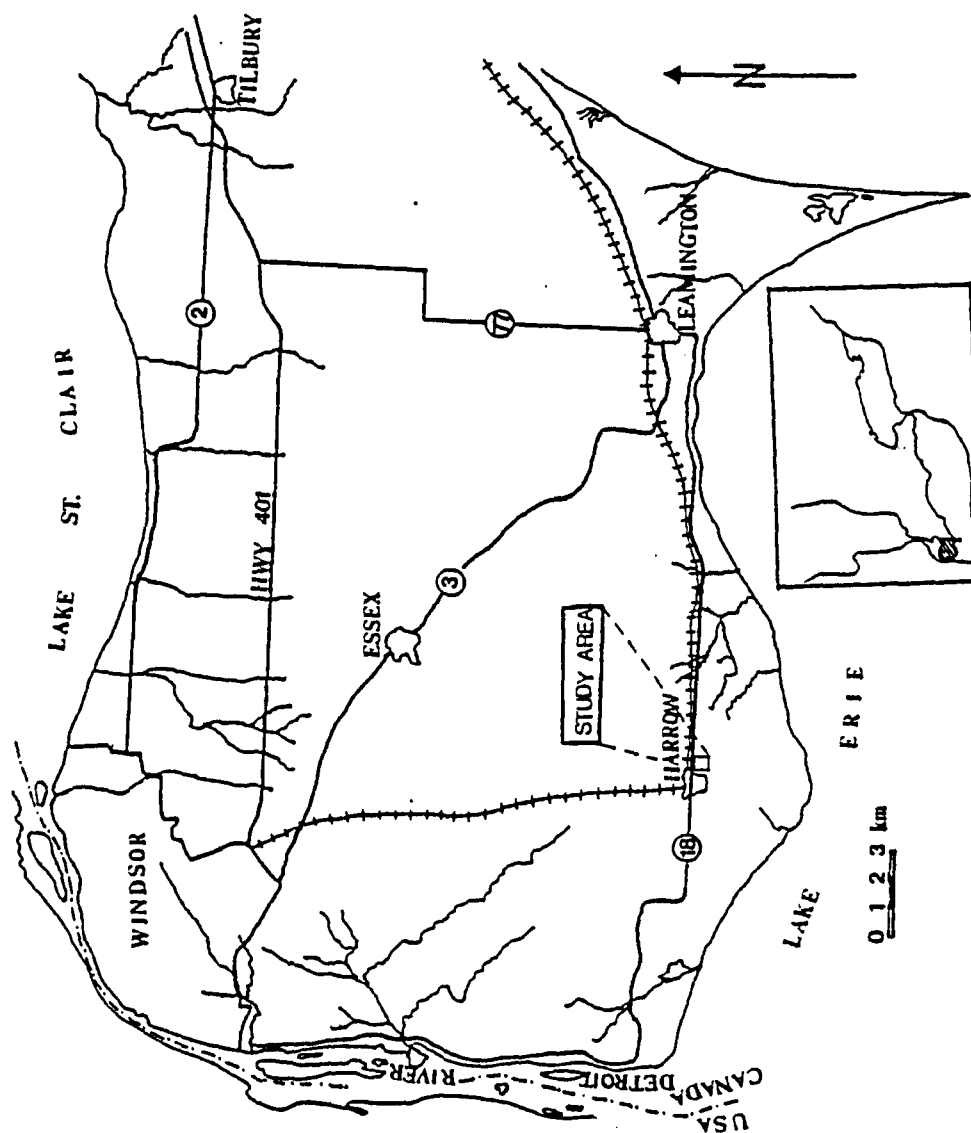
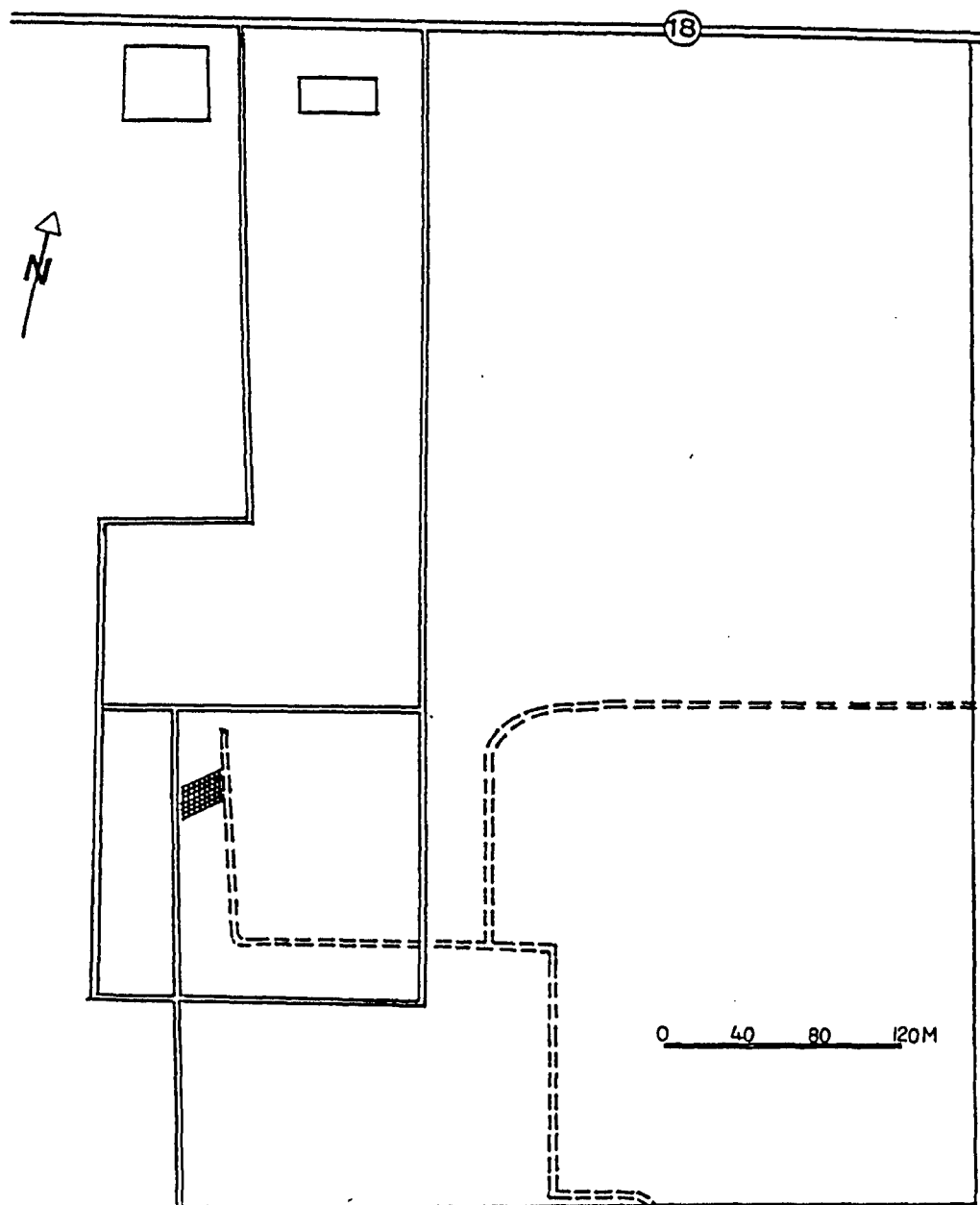

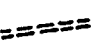




Figure 10b. Location map of the experimental plot.



LEGEND

-  Buildings.
-  Drainage.
-  Roads.
-  Experimental plot.

to be installed in order to provide satisfactory conditions for crop cultivation.

The prevailing soil type is clay loam, a dark surfaced soil developed under a swamp forest of elm, black and white ash, silver maple and other moisture-loving trees (Chapman and Putnam, 1966). There are also numerous undrained areas where peat and muck have accumulated.

3.3 Climate (Richards and Caldwell, 1949; Sanderson, 1980)

Essex County is the warmest part of Ontario and one of the warmest areas in Canada. There is a considerable variation of climate within the county (Sanderson, 1980). Because of the prevailing high summer temperatures, the effectiveness of the precipitation is usually low. The mean annual temperature is 9.4°C . The average precipitation varies from 700 mm to 800 mm per annum. Snowfall averages about 100 mm. Figures 11, 12, and 13 illustrate the annual mean daily temperature, mean annual precipitation, and mean annual snowfall, respectively for Essex County. Seasonal distributions of temperature, precipitation, and snowfall in the Harrow area are given in Table 2.

3.4 Geology (Richards and Caldwell, 1949; Chapman and Putnam, 1966; Vagners, 1972; Guïton, 1978)

The basement underlying Essex County is composed of Precambrian rocks of the Grenville geologic province. Four flat lying Devonian formations overlies the basement complex.

Table 2, Seasonal distribution of mean temperature, precipitation and snow fall in Harrow area. (after Sanderson, 1980)

	J	F	M	A	M	J	J	A	S	O	N	D
Temperature(°C)	-3.9	-3.1	1.4	8.3	14.3	20.1	22.3	21.4	17.8	12.0	4.7	-1.7
Precipitation(mm)	59.9	50.3	64.8	75.7	77.7	77.7	71.9	54.6	58.9	61.0	61.5	63.2
Snow fall (mm)	244	216	191	35	0	0	0	0	0	T*	87	221

T* Trace.

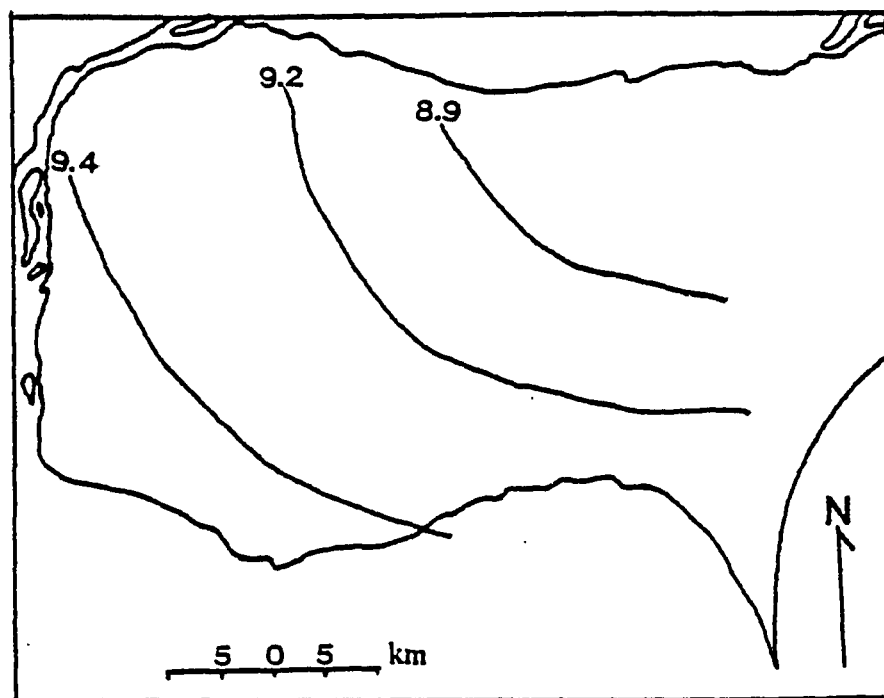


Figure 11. Annual mean daily temperature of Essex County($^{\circ}\text{C}$) (after Sanderson, 1980).

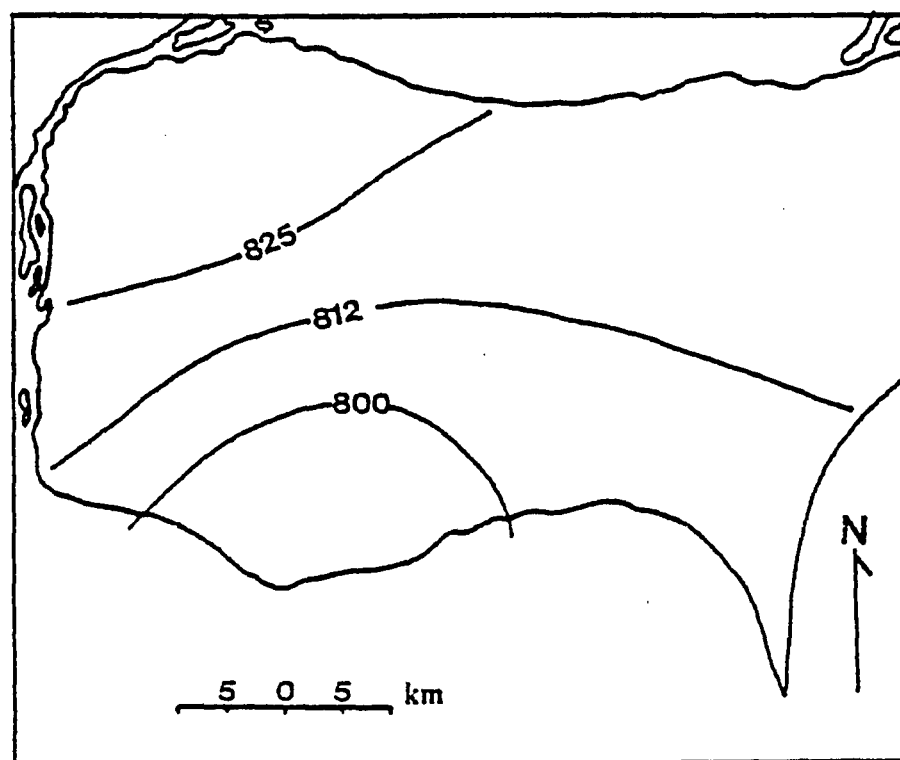


Figure 12. Mean annual precipitation of Essex County(mm) (after Sanderson, 1980).

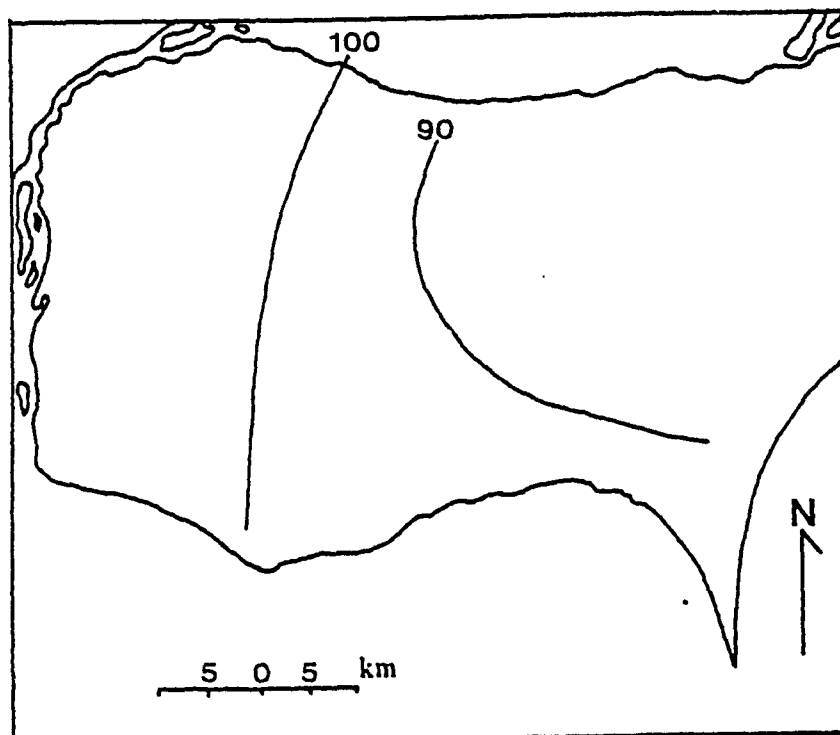


Figure 13. Mean annual snow fall of Essex county(mm)
(after Sanderson, 1980).

The Devonian formations are the:

- 1) Detroit River Formation composed of limestone, dolomite, and sandstone,
- 2) Columbus Formation composed of sandy limestone and dolomite,
- 3) Delaware Formation consisting of brown limestone,
- 4) Hamilton Formation composed of grey shale and argillaceous limestone.

Soils that overlies the bedrock reflect the profound effect of glaciation. The oldest Quaternary deposits found in the area of Essex County are tills formed by glacial action during the Wisconsin stage of glaciation (Vagners, 1972). The glaciers had deposited large amounts of glacial drift consisting of medium- to coarse-grained material. After the retreat of the Wisconsin ice sheet, the area of Essex County was under the influence of several glacial lakes ponded between high ground to the south and west and glacial ice to the north and east (Guiton, 1978).

Figure 14 is the surficial geology map of Essex County. Essex County itself is essentially a till plain smoothed by shallow deposits of lacustrine silt and clay which settled in depressions while the knolls were being lowered by wave action. Small irregular stony ridges that occur along Lake Erie indicate the morainic influence in Essex County. In Harrow, a morainic soil occurs where the mixture of stones, silts, clay, and sand has been little changed.

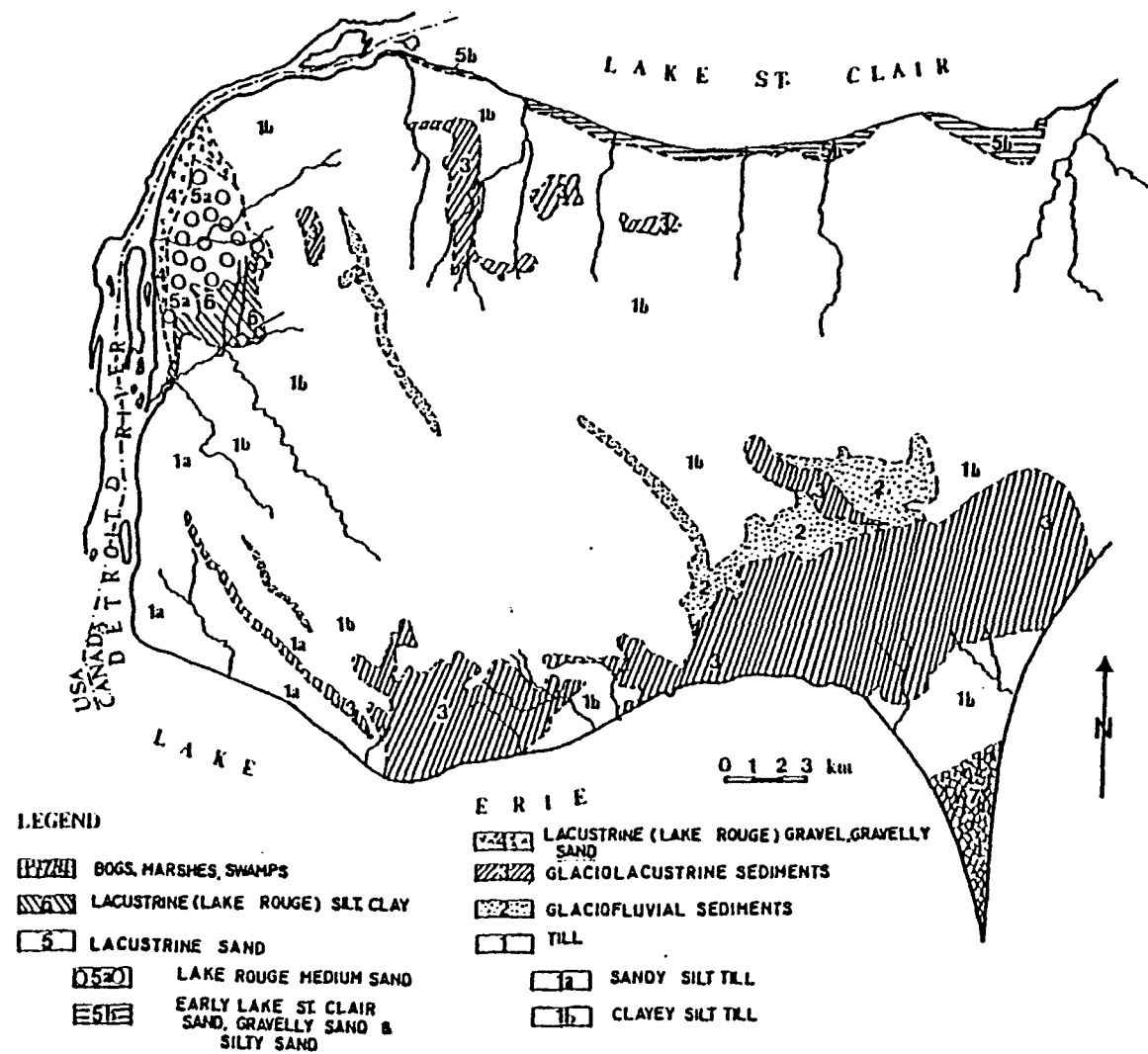


Figure 14. Surficial geology of Essex County. (after Gupton, 1978).

3.5 Hydrogeology (Ontario Water Resources Commission, 1971; Guiton, 1978)

Three main hydrogeologic units can be delineated in Essex County: a bedrock unit, a clayey silt till unit, and a lacustrine unit.

Flow systems encountered in the bedrock unit are considered to be regional (Guiton, 1978). Recharge areas for the bedrock unit lie around the Upper Great Lakes area and it discharges toward Lake Erie (Guiton, 1978). Overlying the bedrock is the extensive clayey silt till which has an average thickness of about 25 m in the Essex County area (Vagners, 1972). This till behaves as an aquitard producing the artesian groundwater conditions of the regional flow system. The lacustrine unit overlies the relatively impervious clayey silt till and forms local unconfined groundwater flow systems.

In general, groundwater is available in sufficient quantity in most parts of the county, but the chemical quality in many cases is poorer than that recommended for drinking water. According to Ontario Water Resources Commission records, the water was found to be very hard in 89 percent of wells (Ontario Water Resources Commission, 1971). The nature of the hardness is Mg/Ca. The quality of water found in sands and gravels overlying the bedrock is generally similar to that of water encountered in the bedrock. Intermediate overburden aquifers can have harder water than water from the bedrock. The water from the

surficial sands is generally hard, but otherwise of good quality. Records for 3330 wells were on file in 1970 for the whole county. Seventy-three percent of the wells were reported to yield fresh water, twenty-one percent sulfurous water, three percent mineral water, and three percent were dry (Ontario Water Resources Commission, 1971).

About 80 percent of the recorded wells in Essex County terminate in the bedrock. The majority of these wells obtain water from the upper few metres of the bedrock, but in the Harrow-Leamington area, wells penetrate deep into the bedrock and yield plentiful supplies for irrigation (Ontario Water Resources Commission, 1971). Shallow dug wells are common in the northern part of the county. Other areas where shallow wells are common are Harrow and Leamington.

4.0 METHOD OF STUDY

4.1 Introduction

To accomplish the objectives of the present study, namely observe the near-stream water table, the interaction between tension saturated and pressure saturated zones, and the response of the capillary fringe during storm events; both field and laboratory investigations were carried out during the period of July 1982 to February 1983.

The first step of the program was to investigate the subsurface geology of the experimental plot using geophysical methods and drilling. This preliminary step was followed by a topographic survey from which the locations for piezometers and wells were selected. After installation, each well and piezometer was tested for hydraulic conductivity. Four holes up to about 1.5 m were hand augered and representative soil samples were collected for grain size analyses. Four test pits were dug using a backhoe for visual examination of the soil profile. Four tensiometer nests and neutron access tubes were installed to study the unsaturated zone. An irrigation grid was set-up to simulate rains. Background measurements of depth to the water table, pressure head, volumetric moisture content, and chloride ion concentration were taken before the testing procedure began. A sodium chloride tracer was applied to three locations with different depths to the water table. Three rain events with different durations and intensities

were simulated and the system response was monitored.

4.2 Field Instrumentation

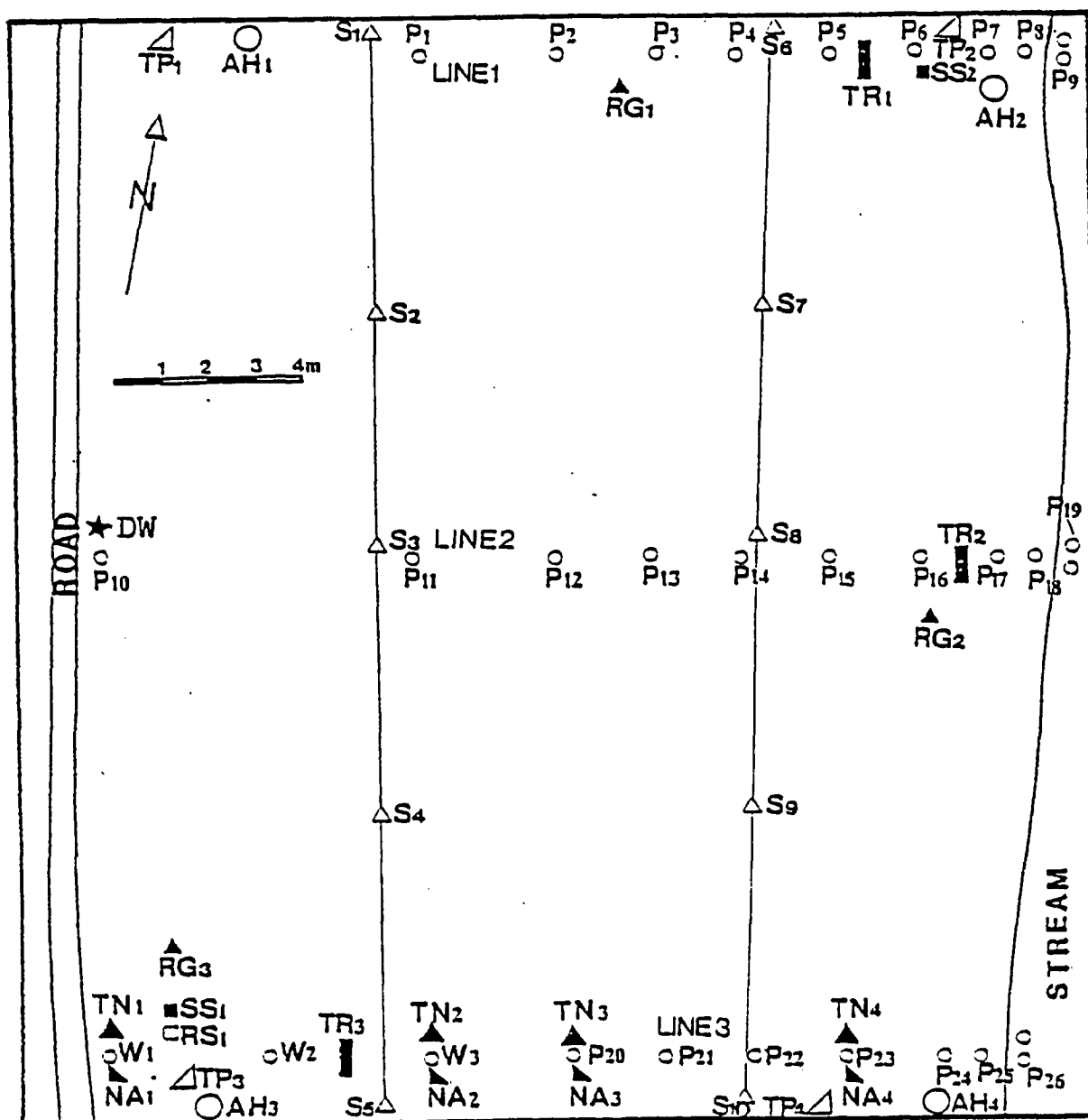
The instrumentation installed within the study plot consisted of three observation wells, twenty-three piezometers, three piezometer nests, four neutron access tubes, and four tensiometer nests. Figure 15 is a map showing the location of the instrumentation on the plot. Figures 16a, b, c are cross-sections along lines of instrumentation.

4.2.1 Piezometers and Wells

The purpose of the piezometers and wells was to observe the response of the groundwater table to natural and artificial rain events and to carry out water sampling.

Piezometers and wells can be hand dug, driven, jetted, or bored. The basic difference between wells and piezometers is the length of the intake zone. A piezometer essentially gives a point measurement, a well averages a vertical section. Access for the water to the well can be provided by a set of perforations or hand-sawn slots in the casing. The well yield can be significantly increased by using a properly designed well screen (Freeze and Cherry, 1979).

In this study, 0.025 m diameter steel pipes were used as casing. The pipes were cut into 1.5 m sections and



LEGEND

○ P_i Piezometer

○ W_i Well

▲ T_{Ni} Tensiometer nest

▴ N_{Ai} Neutron access tube

▬ T_{Ri} Tracer application

○ A_{H3} Auger holes

■ S_{S2} Seismic station

□ R_{S1} Resistivity station

△ T_{P2} Test pit

▲ R_{G1} Rain gauge

△ S₂ Sprinkler

★ DW Deep well.

Figure 15. Instrumentation of the experimental plot.

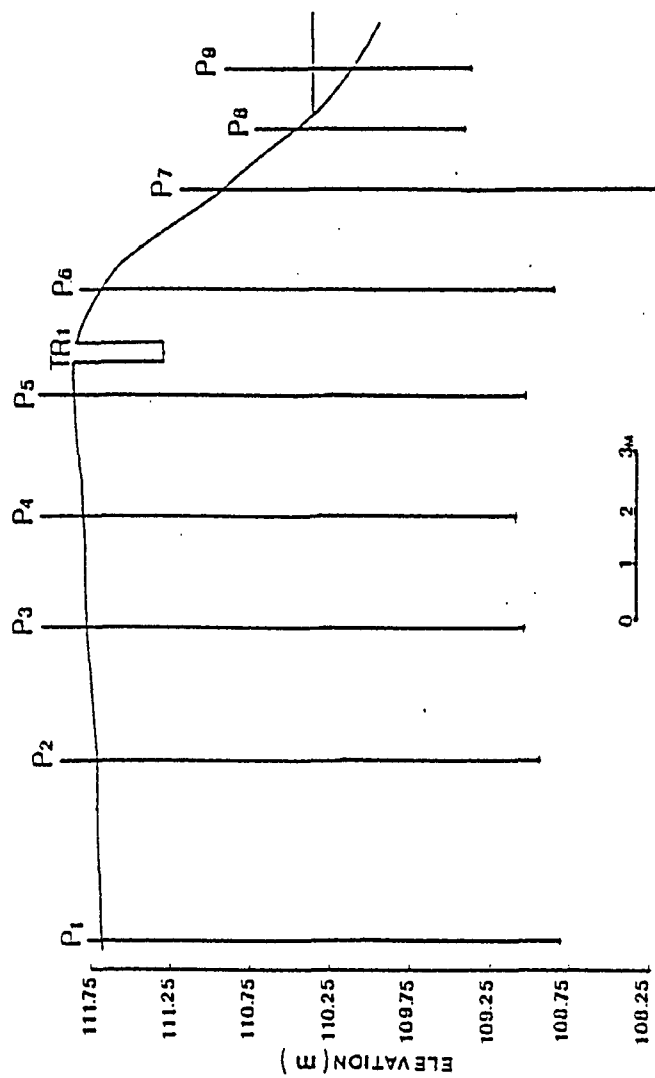


Figure 16a. Cross section along the line No.1 of instrumentation.

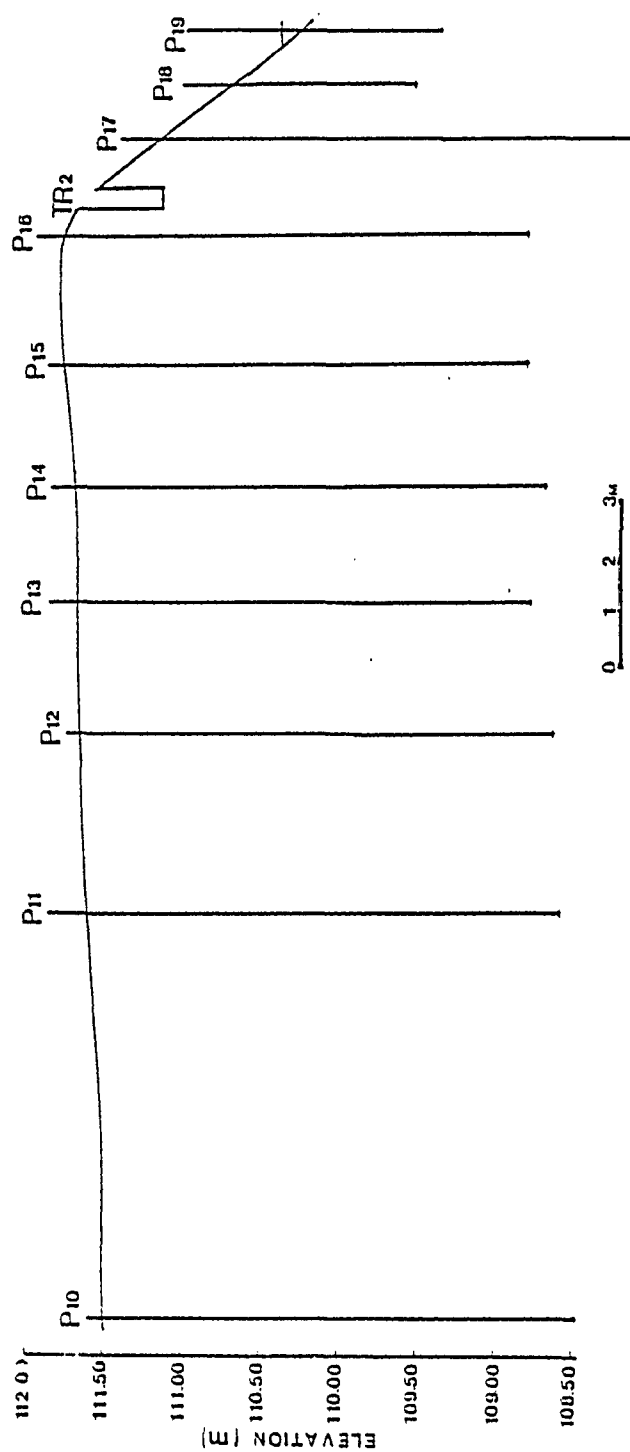


Figure 16b. Cross section along the line No.2 of instrumentation.

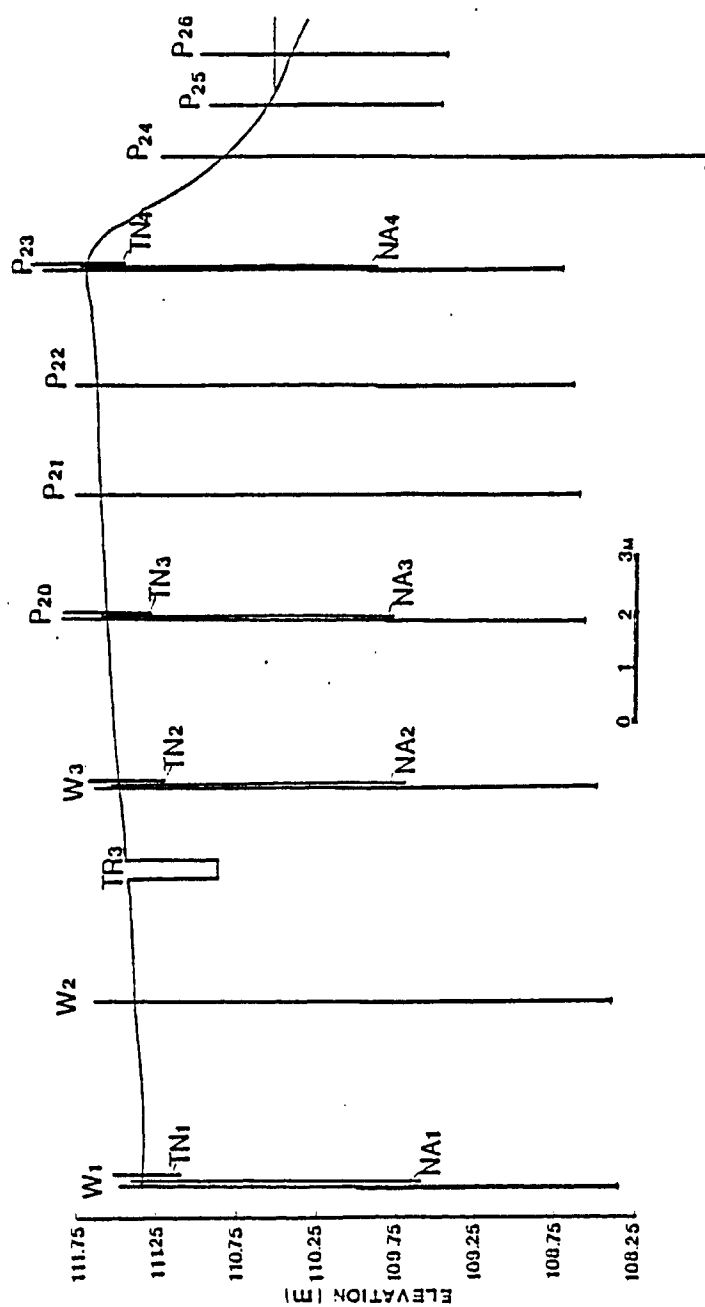


Figure 16c. Cross section along the line No. 3 of instrumentation.

threaded. A set of 3×10^{-3} m diameter perforations separated by 0.05 m were drilled to serve as the intake zone. The lengths of the intake zone for the wells and piezometers are 1.5 and 1 m respectively. Fibre glass tape was wrapped around the slotted area to prevent soil from entering the pipes. Figure 17 is a sketch of a typical piezometer installed at the experimental plot.

All of the wells and piezometers were driven into the ground to about 2.7 m using a mobile drilling rig. The drilling rig, which was assembled at the Agriculture Canada Research Station in Harrow, is essentially a tractor mounted pile driving system. All of the wells and piezometers were cemented at the ground surface to avoid direct rain water entry along the pipe to the water table.

Three piezometer nests were installed in the stream to determine the groundwater-stream water interaction. These piezometers were of the same design as the ones on the ground.

4.2.2 Neutron Access Tubes

The objective of the neutron logging was to study the changes in moisture content in the unsaturated zone during storm events. The aluminum access tubes serve as safe passage for the delicate neutron probe.

In this study, aluminum access tubes recommended by Pacific Nuclear Corporation were utilized. Four Model WWI 700/6, 1.8 m long and 0.075 m diameter tubes were carefully driven into preaugered holes.

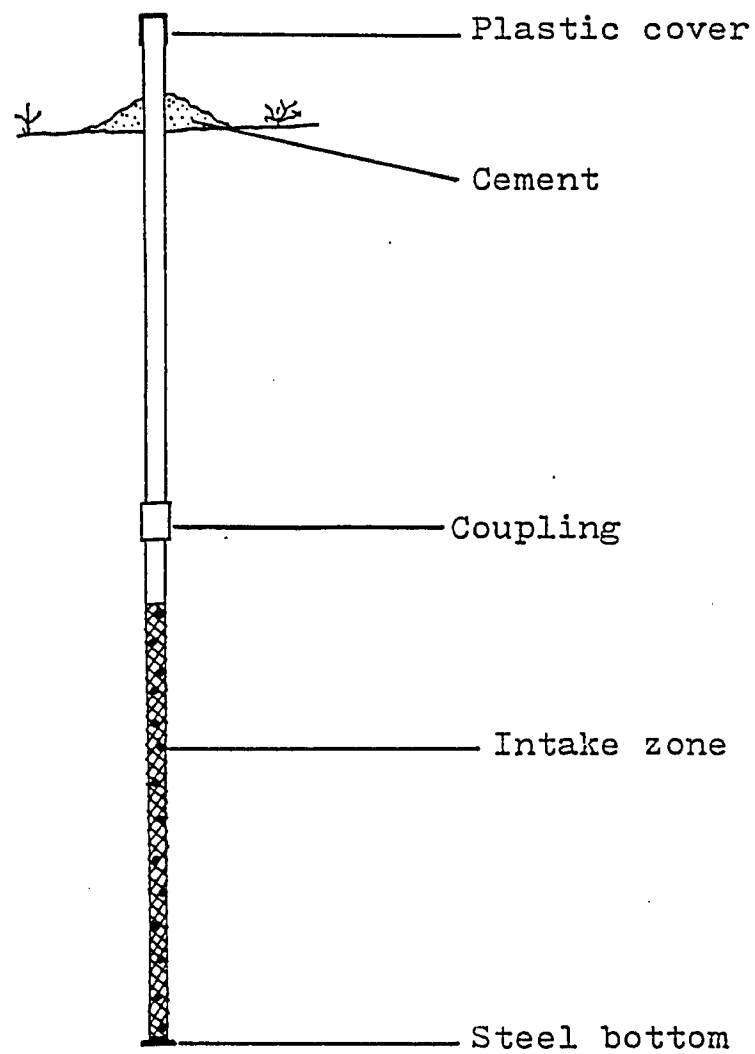


Figure 17. Sketch of a typical piezometer installation.

The neutron logging equipment Model 501 which was utilized in this study consists of a probe that goes into the ground and a receiver on the ground surface. The probe has a source of neutrons and a recorder. The recorder sends electric signals to the receiver on the ground surface, which converts them to a digital reading.

4.2.3 Tensiometer Nests

Four tensiometer nests were installed adjacent to the neutron access tubes to study the changes in the pressure in the unsaturated zone during storm events. The tensiometers, Model 2325, used in this study are products of Soilmoisture Equipment Corporation, Santa Barbara, California. The tensiometer nests consisted of five porous ceramic cups connected to a mercury filled bottle with plastic tubes. Figure 18 is a sketch of a typical tensiometer nest.

The system was filled with de-aired water. The ceramic cups were carefully placed in preaugered holes 0.3, 0.5, 0.7, 0.8, and 1.1 m deep.

4.3 Field Investigation

4.3.1 Geophysical Survey

An electrical resistivity survey supplemented by a hammer seismic survey of the site was initiated to examine the sequence of strata, to determine the depth to bedrock and to the watertable and to detect a salt tracer introduced at selected points on the plot.

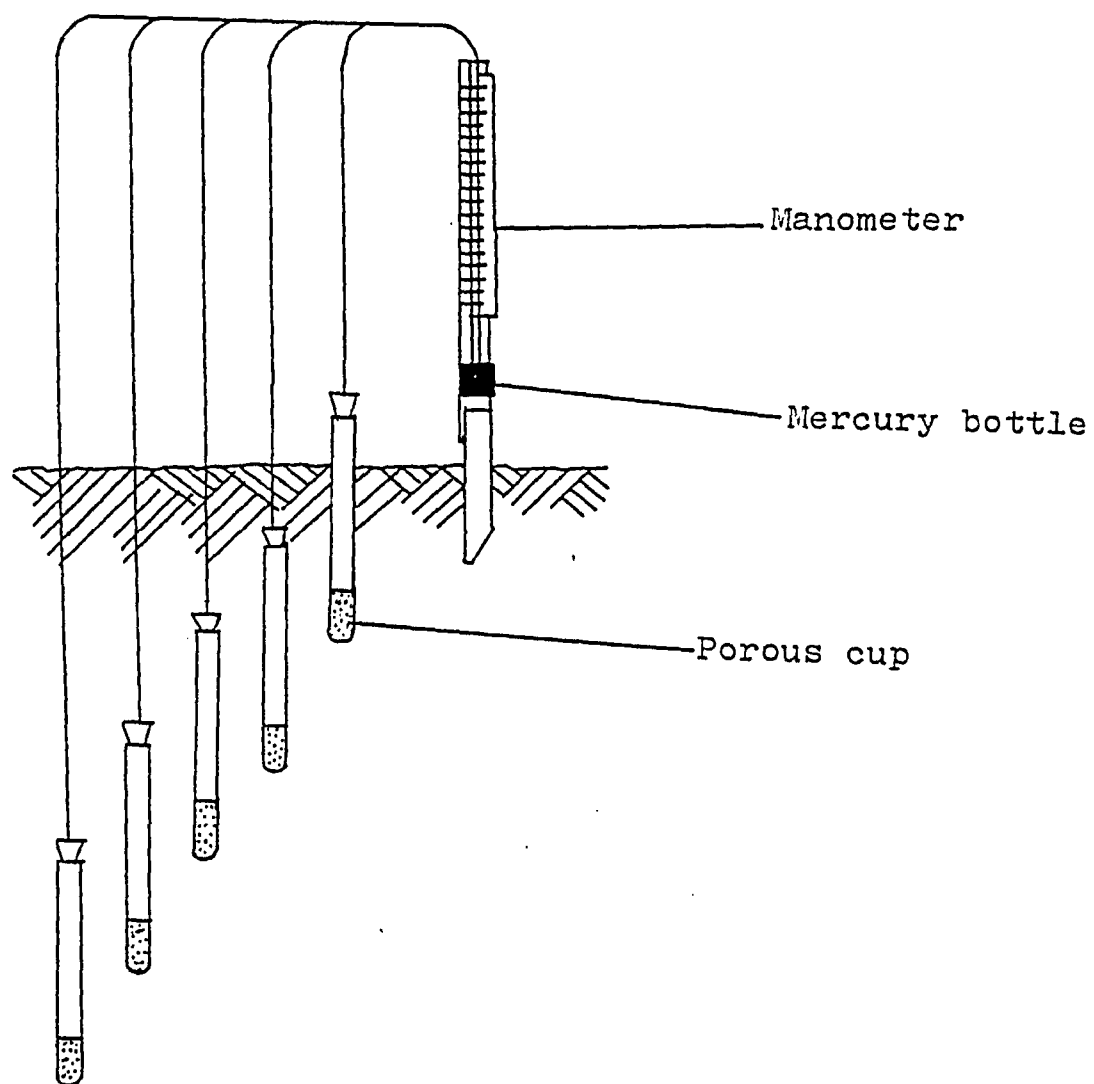


Figure 18. Sketch of a typical tensiometer nest.

a) Electrical Resistivity Survey

Resistivity of a soil is primarily related to its water content and the concentration of dissolved ions. Dry soils or solid rocks have a high resistivity, saturated granular soils have a moderate resistivity, and saturated clays have a low resistivity.

In all resistivity methods of exploration, a current is applied to the ground through electrodes while the potential is being measured between two potential electrodes.

In the present study a line perpendicular to the lines of instrumentation with a length of 195 m was surveyed. A Soiltest R-50 DC resistivity meter was utilized. Electrodes were spaced according to the Wenner configuration. Initially the spacing was 0.6 m and it gradually increased to 65 m at the last reading.

b) Hammer Seismic Survey

Seismic velocity is a useful indicator of rigidity of the material through which the seismic waves travel. From the theory of elasticity, the velocity of a compression wave in a solid is shown to be a function of mass, modulus of elasticity and Poisson's ratio. The most important of these is the modulus of elasticity which is very sensitive to grain-to-grain contact (Dobrin, 1976).

The basic technique of the seismic method is to generate seismic waves and measure the time required for them to travel from the source to the geophone, through the

explored material. By plotting arrival time against the distance between the source and the geophones, one can determine the depth to discontinuities in the subsurface material.

In the present study, seismic waves were introduced by striking a steel plate on the ground with a specially designed sledge hammer. A Bison Model 1570C Seismic unit and one geophone were utilized to survey two lines, one perpendicular, and the other one parallel to the lines of instrumentation. The hammer was moved successively to different locations along a straight line. At each position the test was repeated to give the time-distance relationship. Then the geophone was moved to the other end of the line and the whole process was repeated to determine whether the interfaces dip in the direction of survey line.

4.3.2 Drilling

Any geophysical survey should be supplemented by drilling to confirm the geology suggested by the survey. In this study one borehole was augered to a depth of 5.5 m using a truck mounted CME-750 drilling rig. Continuous sampling was done using hollow stem augers and a split spoon. Since the recovery below the watertable was very low, a sand trap was utilized.

A 0.05 m diameter slotted ABS pipe was inserted through the hollow stem auger into the borehole so that it could be used as an observation well in future operations.

4.3.3 Topographical Survey

A standard levelling survey was carried out to map the experimental plot. Bench marks used by the Harrow Agriculture Research Station were used to evaluate the relative elevations.

4.3.4 Auger Holes and Test Pits

Four auger holes and four test pits, one at each corner of the experimental plot, were dug to a depth of about 1.5 m using a hand auger and a backhoe. Representative soil samples were collected from the auger holes at 0.40 m intervals for grain size analyses.

4.3.5 Artificial and Natural Storm Monitoring

Three storm events with different intensities and durations were simulated using the irrigation grid. One natural storm was also monitored. Three standard rain gauges were used to measure the rain distribution. Depth to the water table was measured before and during the storm events. Tensiometer and neutron logging measurements were also carried out before and throughout the storm events.

4.3.6 Neutron Logging

Nuclear logging was used to monitor the changes in moisture content in the unsaturated zone during storm events. An explanation of the process follows.

The measurement process begins when neutrons are

derived by reactions of alpha particles with beryllium in the nuclear source, as it is shown by the following equation (Corey, 1970):



The neutrons are then introduced to the environment and its effect on them are measured.

Since they carry no electric charge, the neutrons lose their energy when passing through matter only by elastic collision. Neutrons from the source pass through the walls of the aluminum access tube and are slowed down by collisions with the atomic nuclei. The most effective element in moderating neutrons is hydrogen because the nucleus of a hydrogen atom has approximately the same mass as a neutron. Neutrons lose their energy with fewer collisions with hydrogen nuclei than other elements (Corey, 1970). For this reason, the number of slow neutrons largely depends on the hydrogen content, hence the moisture content, of the soil.

A Neutron Depthprobe Model 501 produced by Pacific Nuclear Corporation was utilized together with recommended aluminium access tubes. Ten standard counts were taken when the probe was still in the cell. Then the readings representing different depths were taken while lowering the probe into the aluminium access tubes. Readings were taken at 0.2 m intervals to a depth of 1.6 m.

4.3.7 Tensiometer Experiments

In the unsaturated zone, where water is held under surface tension forces, the pressure head is negative. Therefore, no piezometer can be used to measure the hydraulic head in the unsaturated zone. The most widely used method for measuring the capillary tension is based on the suction force of the soil water. In the present research, Soilmoisture Model 2310 tensiometers were used to measure the suction force. Readings were taken before and after every storm event.

4.3.8 Tracer Experiments

A tracer is matter of energy which is used to determine the direction and velocity of the water (Elrick and Lawson, 1967). Tracers can be natural such as heat carried by geothermal waters or they can be introduced artificially.

A tracer should have some minimum requirements such as: low cost, moves at the same velocity as the water, does not change the natural direction of the water flow, and is not absorbed by the material with which it comes to contact. Isotope tracers come very close to being ideal (Elrick and Lawson, 1967). Because of their low cost and ease of detection, chloride and bromide tracers are most popular among hydrogeologists (Lee et al., 1980). These substances entirely ionize when dissolved in water increasing the electrical conductivity.

In the present study, sodium chloride was applied in three different locations. The depth to the water table was

the determining factor of these locations (Figure 15). In each location 20 kg of tracer were applied to a trench with approximate dimensions of 1 X 0.4 X 0.3 m. The tracer was then washed down with water until no solid material was present in the trench.

4.3.9 Testing for Hydraulic Conductivity

In situ hydraulic conductivity measurements were made according to the method described by Hvorslev (1951). Slugs were prepared using 0.02 m diameter PVC pipes filled with sand and sealed with paraffin wax. The slugs were lowered into the wells and piezometers and were left there until the water level stabilized. Then the slugs were taken out and the water level changes with time were recorded using an electric contact gauge.

4.3.10 Water Sampling

Periodic water sampling and analyses were carried out to trace the sodium chloride tracer. Each time before sampling, all the wells and piezometers were emptied using a hand or portable water pump. Samples were collected periodically before and after the application of the sodium chloride tracer.

4.4 Laboratory Testing

4.4.1 Grain Size Analyses (Lambe and Whitman, 1976)

There are three general procedures for grain size analysis: sieve, hydrometer, and combined analysis. Sieve analyses are performed by shaking the soil through a set of sieves with openings of known sizes. Hydrometer analyses are based on Stokes equation for the velocity of a freely falling sphere.

In hydrometer analyses, a soil sample of about 0.05 kg is mixed with distilled water to form a smooth thin paste. A deflocculating agent should be added to the paste and the suspension is mixed using a mixing machine for about 10 minutes. After mixing, the specimen is washed into a 1 litre graduated cylinder and enough distilled water is added to bring the level to the 1 litre mark. Then using a standard hydrometer, readings are taken at time intervals of 2, 5, 10, 20 minutes, etc., approximately doubling the previous time interval.

The combined analysis employs both the sieve and hydrometer tests. In combined analyses, sieve analyses are carried out first. Then a hydrometer analysis is performed on a sample of about 0.05 kg from the soil retained in the pan.

The test procedure depends on the type of the soils tested. If almost all the grains cannot pass through No. 200 sieve, then the sieve analysis is preferable. For silts and silty clays, which have a measurable amount of their

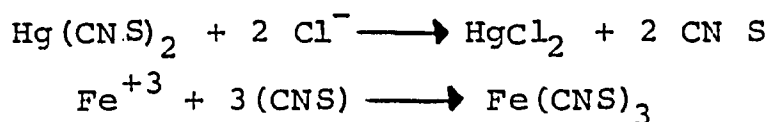
grains both coarser and finer than No. 200 sieve, a combined analyses is needed.

In this study both sieve and combined analyses were carried out. Samples collected from auger holes and the borehole were tested. Calgon was used as the deflocculating agent in the hydrometer analyses.

4.4.2 Chemical Analyses for Chloride Ions

Water samples recovered from the wells and piezometers were divided into two portions. One was analyzed for chloride ion concentration while the other one was used to determine the electrical conductivity.

The chemical analyses were run in the Agriculture Canada research laboratory in Harrow by the technicians of the station using a Technicon Autoanalyzer II. This automated procedure for the determination of chloride is based on the reaction of the chloride ions with mercuric thiocyanate. As a result of the reaction, thiocyanate ion is liberated by the formation of soluble mercuric chloride. In the presence of ferric ions, the liberated thiocyanate forms a highly coloured ferric thiocyanate proportional to the original chloride concentration (Technicon Autoanalyzer II Manual). The reaction is as follows:



4.4.3 Electrical Conductivity Measurements

In an electrolyte, the propagation of current is by ionic conduction, that is, by molecules having an excess or deficiency of electrons (Telford et al., 1976). Hence, the electrical conductivity of water varies considerably depending on the amount and conductivity of dissolved ions.

In this study, a Barnstead Conductivity Bridge Model PM-70 CB was utilized to measure the electrical conductivity of the water samples.

5.0 RESULTS AND DISCUSSIONS

5.1 Introduction

Several hydrogeological techniques were used in this study. The first several procedures deal with the hydrogeologic characteristics of the site. The later procedures are concerned with the occurrence of groundwater ridging. In summary, the work consisted of the following analyses:

1. The arrival times of seismic waves were plotted against distance between the source and the geophone to determine the subsurface geology.

2. Apparent resistivity was plotted against electrode spacing to delineate different lithologic units in the plot.

3. Results of the drilling were logged to confirm the geology suggested by the geophysical survey.

4. Results of the Hvorslev tests for hydraulic conductivity were used to calculate the hydraulic conductivity.

5. Results of grain size analyses were plotted to calculate the hydraulic conductivity using Hazen's formula.

6. Depth to the water table was used to draw cross-sections to observe the groundwater ridging effect.

7. To compare the response of the water table in different locations, the percentage rise of the groundwater table was determined using the following formula:

$$\text{Percentage rise} = \frac{\text{Rise of the water table}}{\text{Initial depth to the water table}} \times 100\%$$

Since the piezometers are shallow, they should reflect the water table conditions.

8. Volumetric moisture content, determined from neutron logging, was plotted against depth to study the capillary fringe during natural and artificial storm events.

9. Pressure head, obtained from tensiometer readings, was also plotted against depth to observe the interaction between the pressure saturated zone and the tension saturated zone, during storm events.

10. Results of the chemical analyses and electrical conductivity values were plotted to study the effects of the groundwater ridge on the movement of the sodium chloride tracer.

11. Electrical resistivity survey results were plotted to confirm the movement of the salt tracer.

5.1.1 Geophysical Surveys

Results of the resistivity survey are given in Figure 19 and Appendix II-1. The apparent resistivity was plotted against the electrode spacing after which the field curve was matched with type curves (Larzeg, 1972).

This analysis indicates that three layers are present in the study area. Two layers with a high apparent resistivity of 255 siemens lie on either side of one with a low apparent resistivity of 55 siemens. According to the

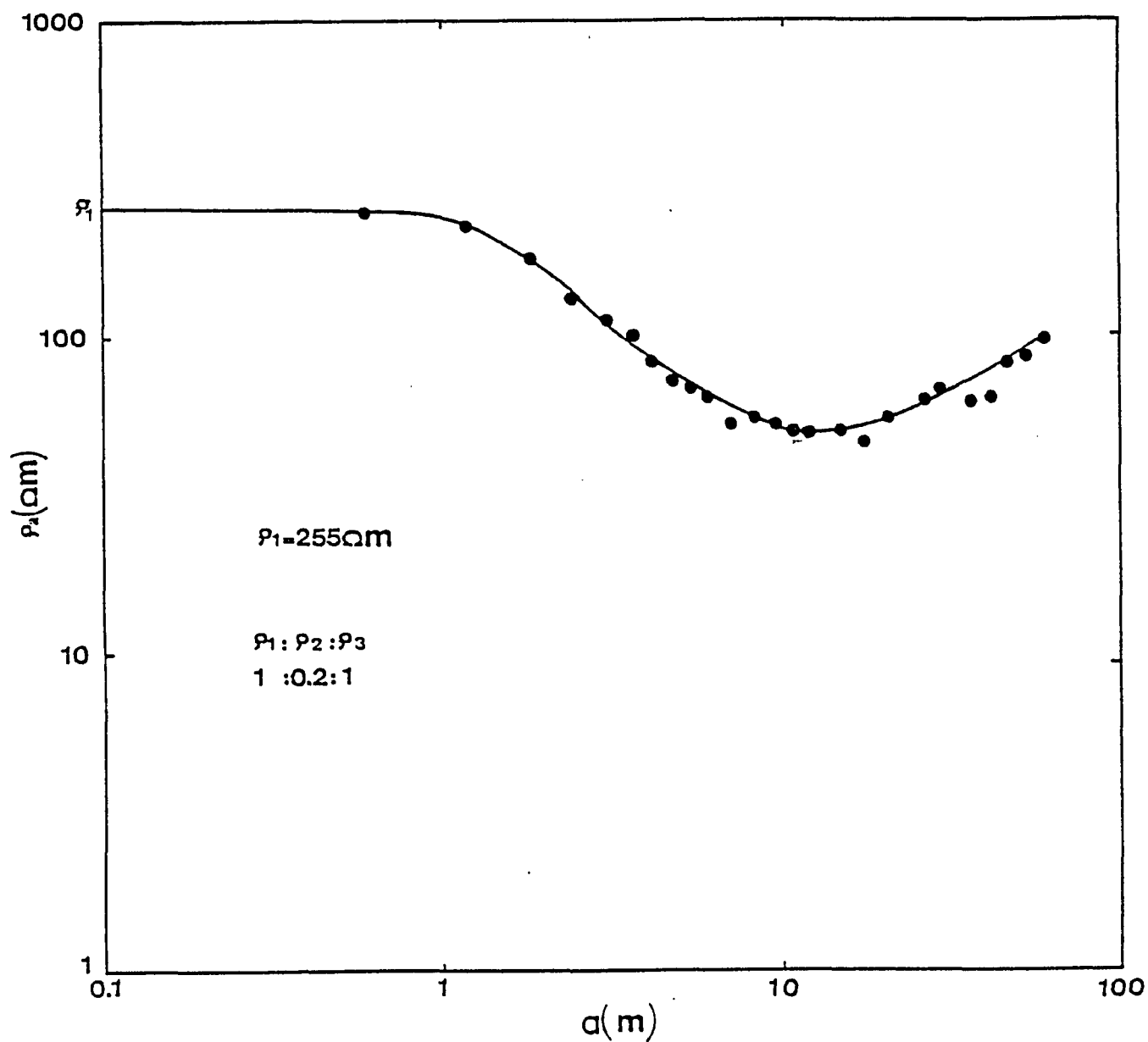


Figure 19. Interpretation of resistivity survey data.

electrical resistivity technique, the first interface is about 1.65 m below the ground surface while the other one is deeply buried at a depth of about 24.7 m. The first interface is likely to be the groundwater table and the second interface could be a boundary between two different lithologic units. Based on the geology of the area, one could expect to encounter the bedrock at that depth, however, the apparent resistivity of 255 seimens is not characteristic of limestone, which is the basic component of the bedrock found in this area. Based on the apparent resistivity values, it is likely that the material found in this plot is composed of terrestrial sand and silt (Clark, 1966).

Results of seismic survey data are given in Figures 20 and 21 and Appendix II-2 and 3.

The arrival times of seismic waves were plotted against the distance between the source and geophone. These plots revealed a three layered structure in the area. Standard formulae were used to calculate the depth to interfaces (Appendix I).

The uppermost layer has a velocity of 227 m/sec, while the middle and the lower layers have average velocities of 956 and 1333 m/sec, respectively. The low seismic velocity of the top layer suggests that it consists of sandy material. The deepest layer is likely to be fine-grained material (Clark, 1966).

The first interface is about 1.7 m below the ground

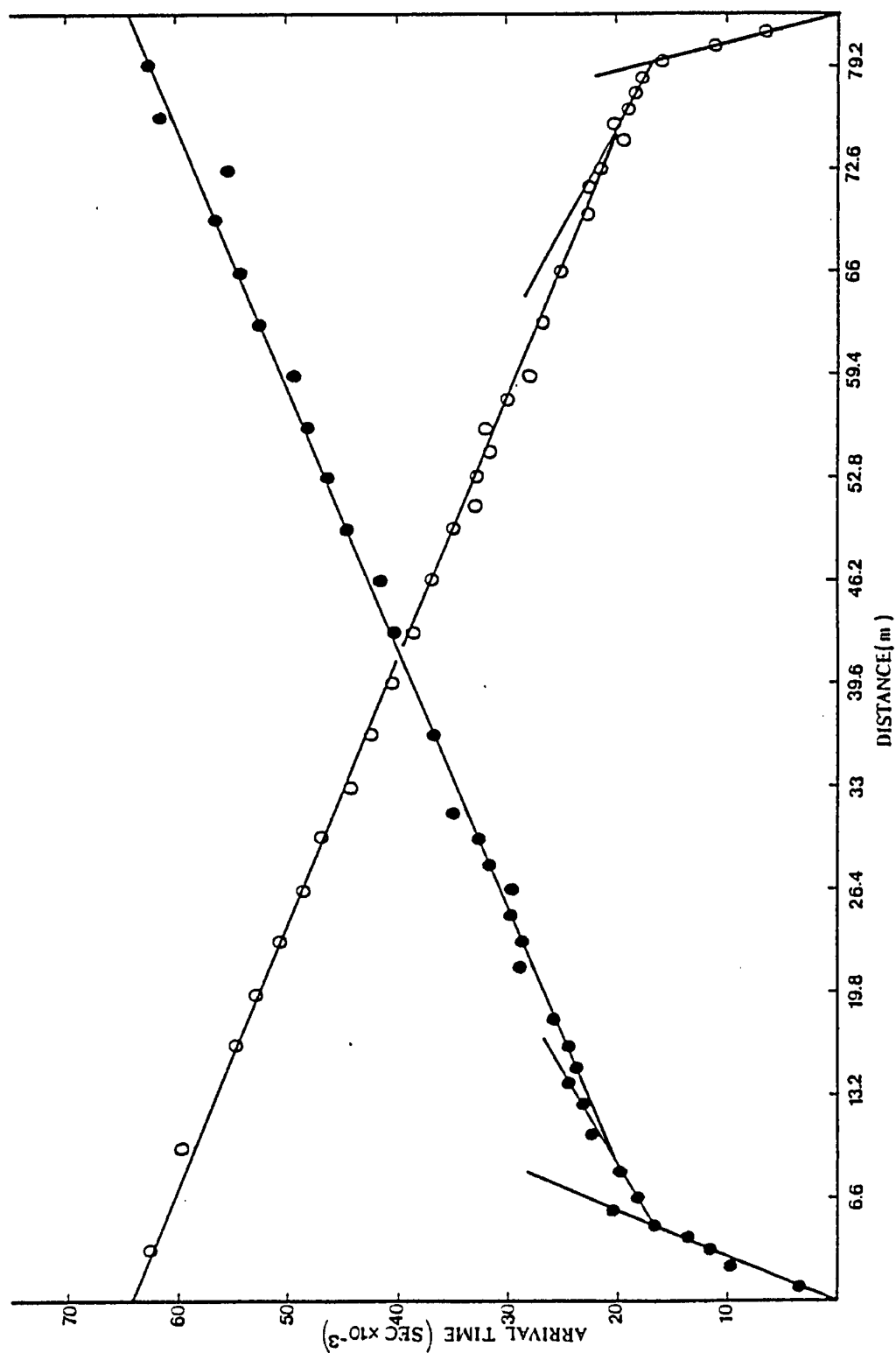


Figure 20. Seismic survey travel-time curve for line 1.

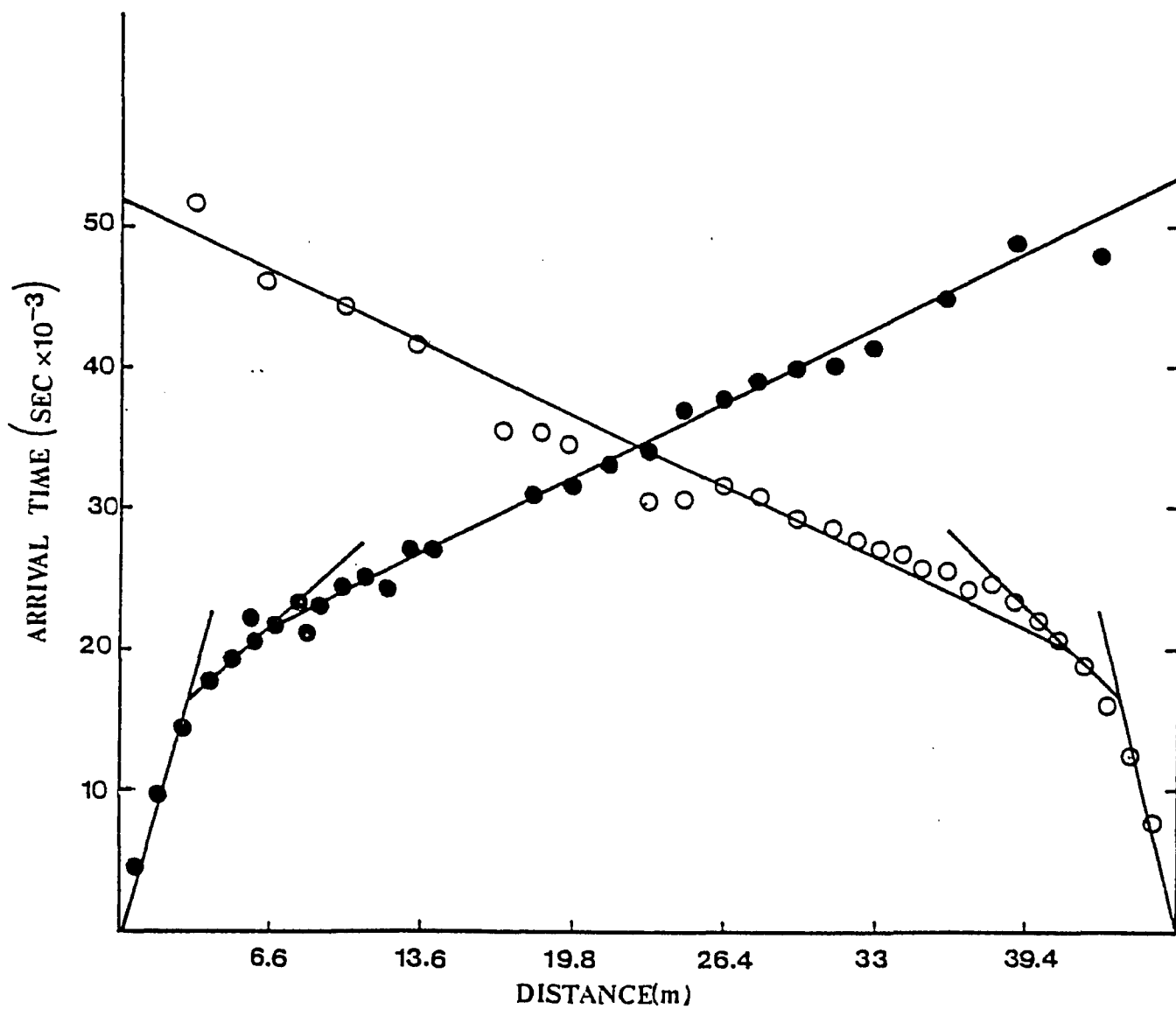


Figure 21. Seismic survey travel-time curve for line 2.

level while the second one is about 3.3 m deep. The first interface is likely to be the groundwater table. This agrees with the results obtained from the electrical resistivity survey. The second interface probably represents a boundary between two different lithologic units. The resistivity survey did not indicate this interface.

The plots for upshot and downshot along both lines of survey are fairly symmetrical. This indicates that the layers in the vicinity of the experimental plot have no significant dip (Telford et al., 1976). The undulating arrival time-distance graph suggests that the interfaces are not planar.

5.1.2 Drilling

The results of drilling are summarized in the borehole log shown in Figure 22. A 0.3 m thick organic topsoil layer is underlain by a medium to fine grained sand layer of about 2.5 m thickness. This sand layer is underlain by a sandy silt layer which gradually changes into silt at a depth of about 4.5 m. The borehole was terminated at a depth of 5.5 m. The groundwater table was encountered at a depth of 1.7 m.

The results of drilling confirm the findings of geophysical surveys. The first interface at a depth of 1.7 m was confirmed to be the groundwater table. Drilling also showed that the second interface delineated by the seismic survey, is the boundary between the medium to fine sand layer and the silty sand layer.

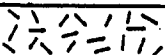
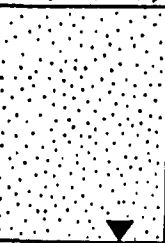
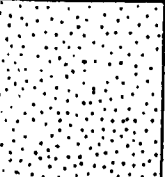
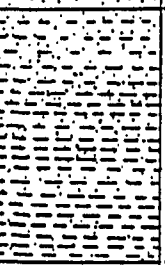
Depth(m)	Lithology	Remarks.
		Dark brown top soil
0.5		Medium-fine sand.
1.0		
1.5		
2.0		Water table
2.5		
3.0		
3.5		Silty sand
4.0		
4.5		
5.0		Silt with some fine sand
5.5		End of the borehole.

Figure 22. Borehole log for the deep well.

5.1.3 Topographical Survey

Results of the levelling survey are summarized in Appendix II-4. The relative elevations were plotted and the resulting topographical map is given in Figure 23.

5.1.4 Tests for Hydraulic Conductivity

Results obtained from Hvorslev field tests for hydraulic conductivity are plotted in Figures 24a-e. The basic time lag determined from the graphs was used to calculate the hydraulic conductivity (see Appendix I). Resulting hydraulic conductivity values are tabulated in Appendix II-5.

P-1 through P-13 have an average hydraulic conductivity of 3.5×10^{-6} m/sec, while the hydraulic conductivity is about 3.8×10^{-7} m/sec at the other sites. Although all the piezometers and wells were tested at almost the same level, the hydraulic conductivity values indicate two distinct fields in the experimental plot.

5.1.5 Grain Size Analyses

Results of the grain size analyses are plotted in Figures 25a-d. The hydraulic conductivity values were calculated using Hazen's formula ($K = Ad_{10}^2$) and the results are tabulated in Appendix II-6.

All of the samples from the auger holes and samples 1 through 9 from the deep well consist of medium to fine grained sand. Samples 10, 11, and 12 from the deep well are silt.

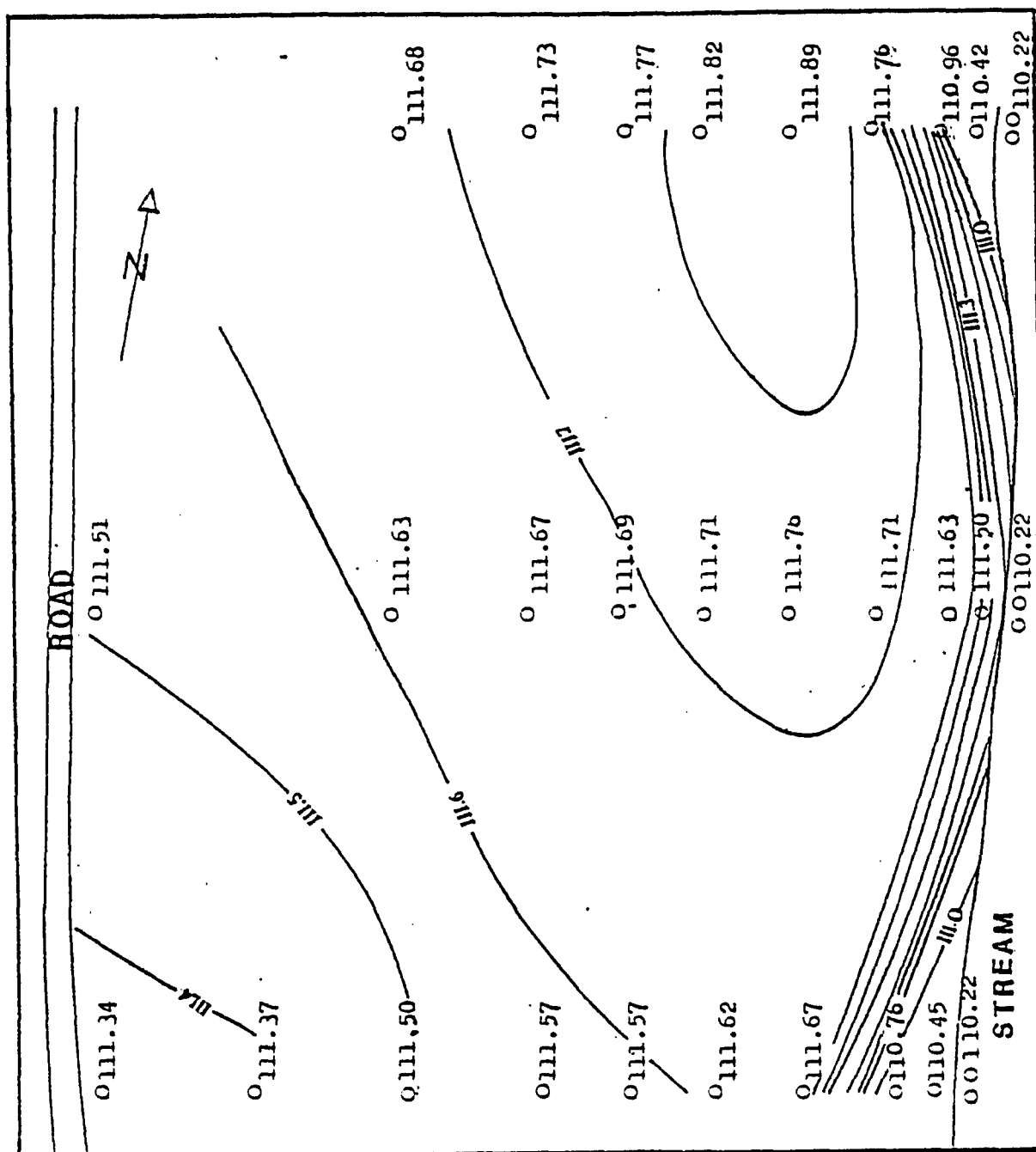


Figure 23. Topographic map of the experimental plot.

Contour interval 0.1m.

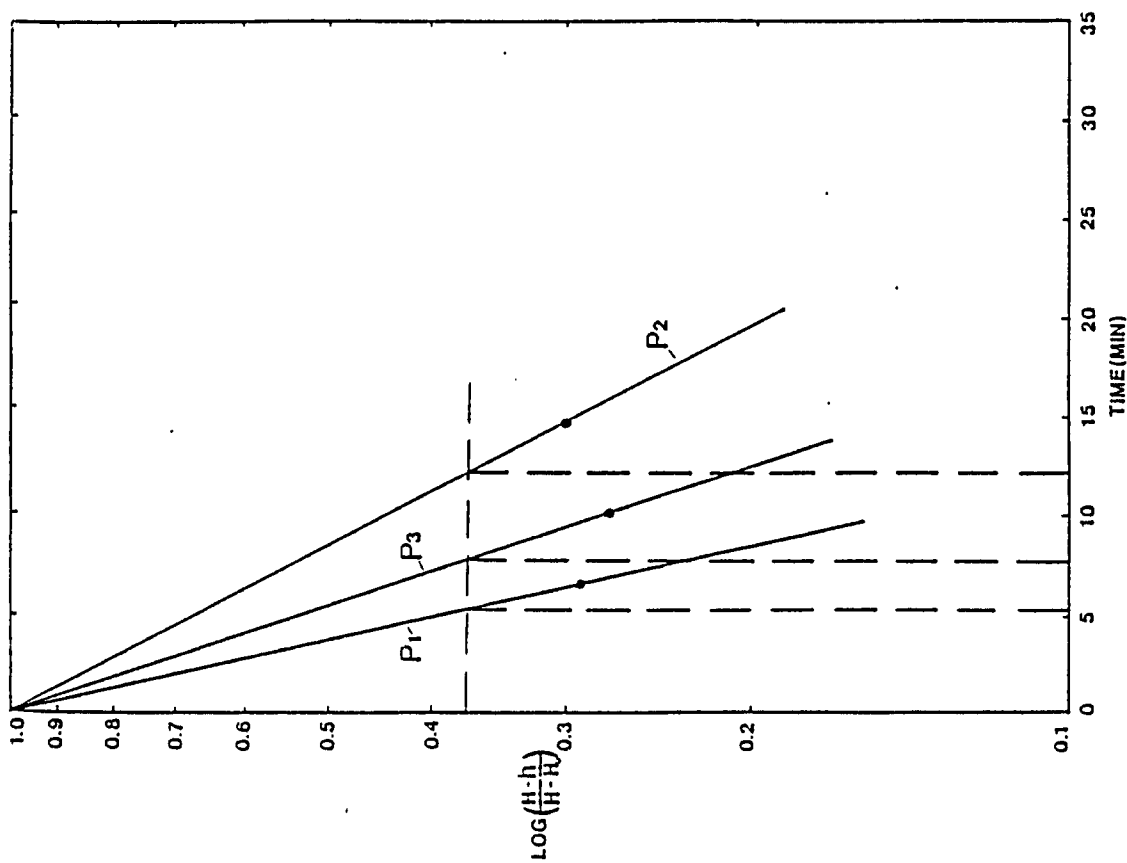
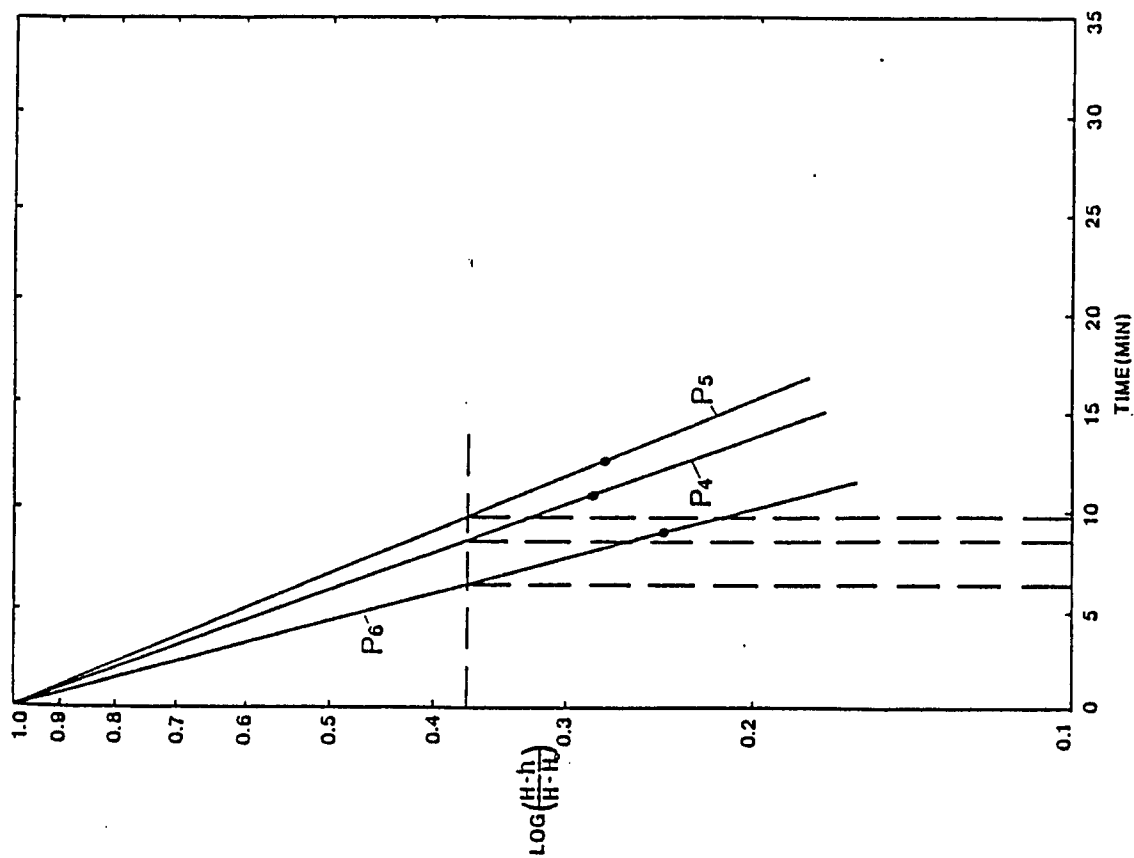


Figure 24a. Determination of hydraulic conductivity using Hvorslev's method.

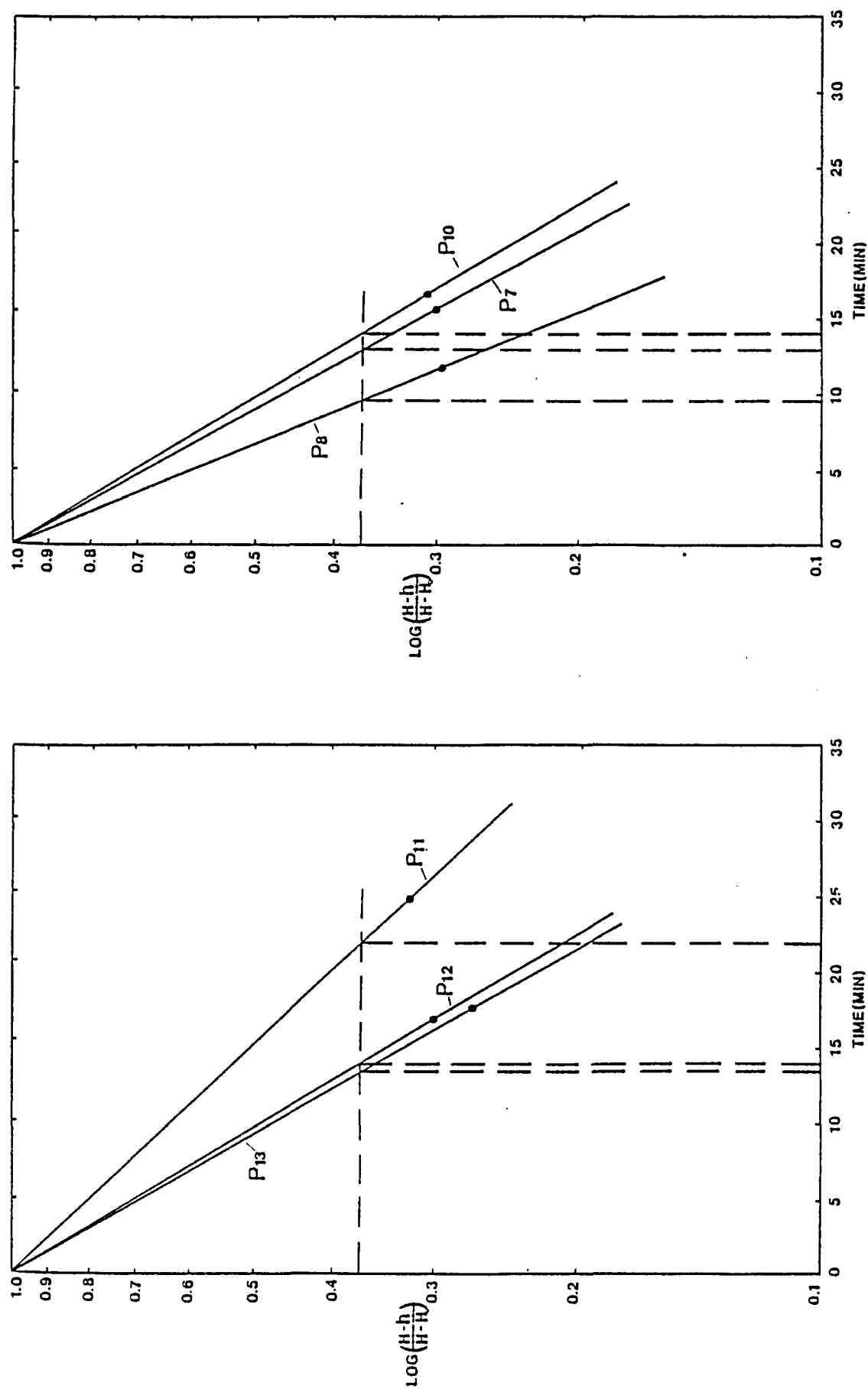


Figure 24b. Determination of hydraulic conductivity using Hvorslev's method.

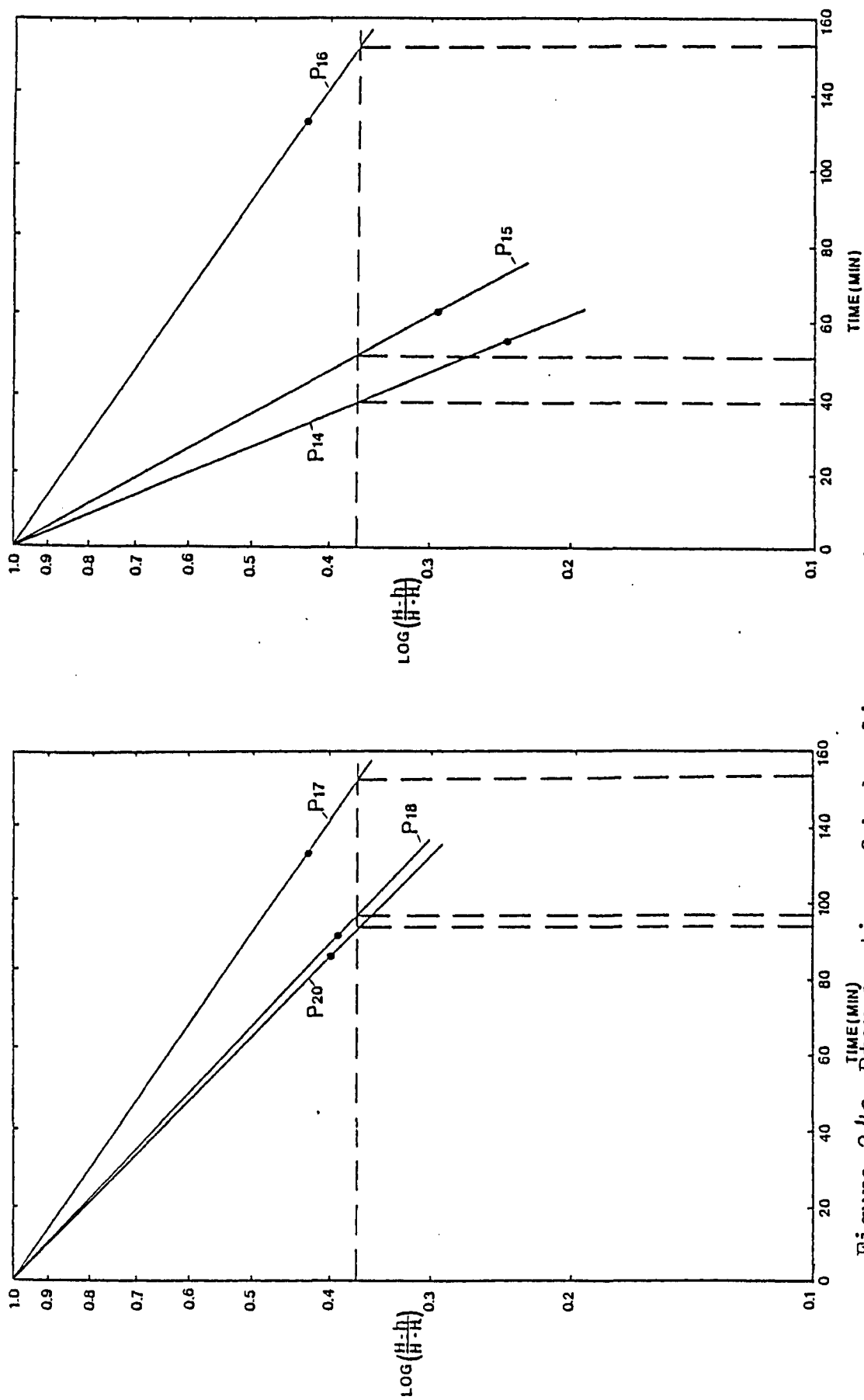


Figure 24c. Determination of hydraulic conductivity using Hvorslev's method.

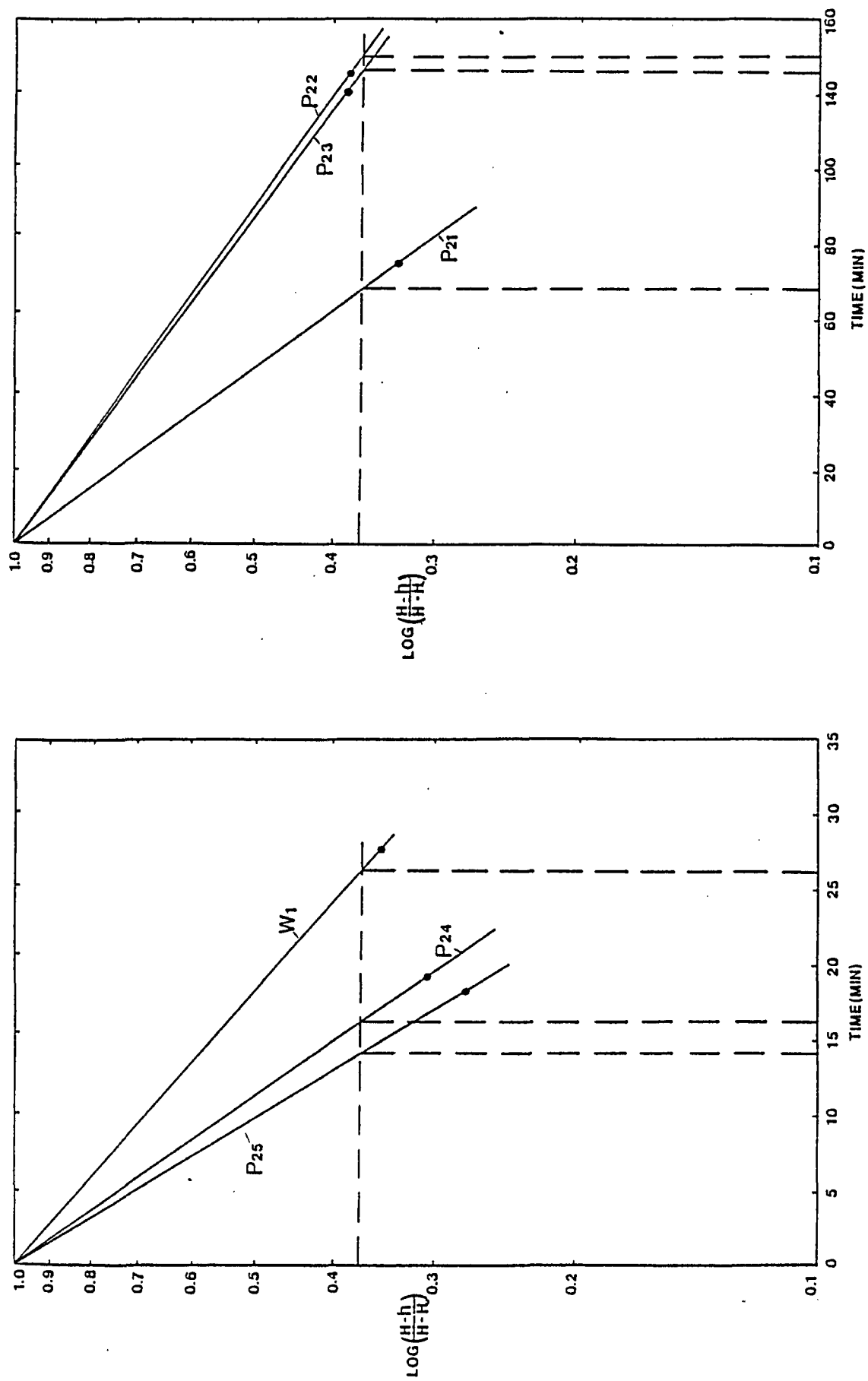


Figure 24d. Determination of hydraulic conductivity using Hvorslev's method.

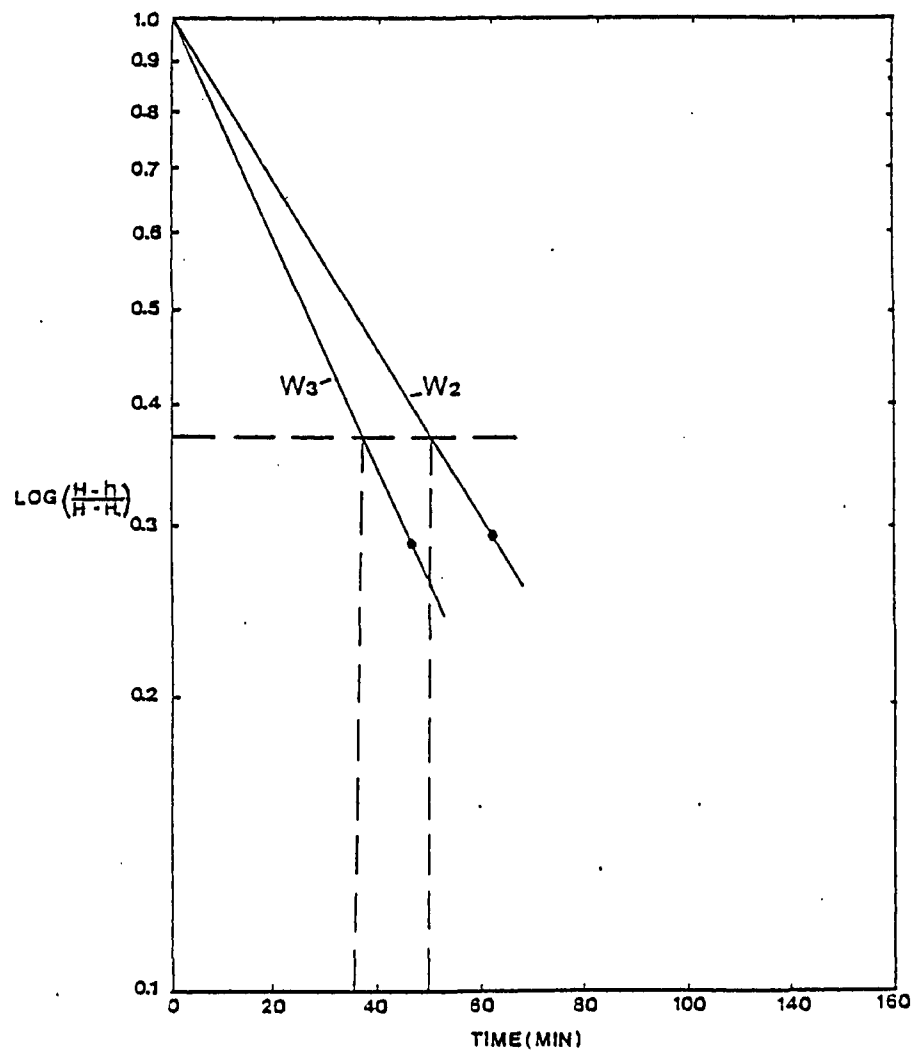
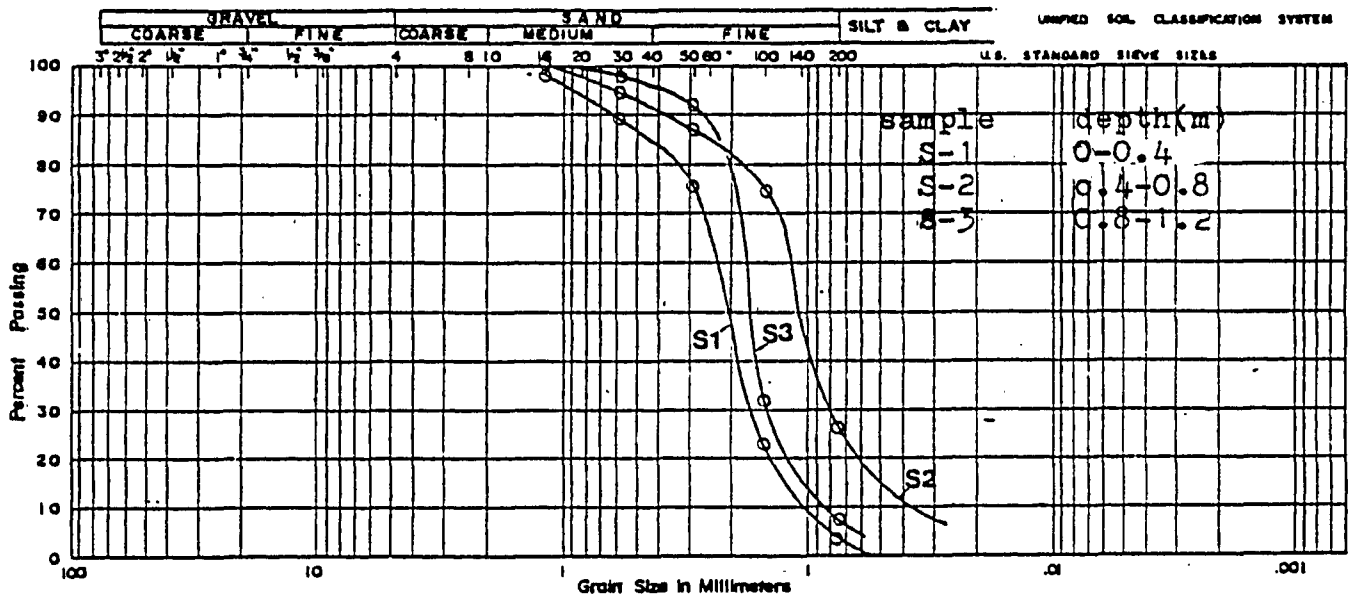


Figure 24e. Determination of hydraulic conductivity using Hvorslev's method.

Auger hole 1



Auger hole 2

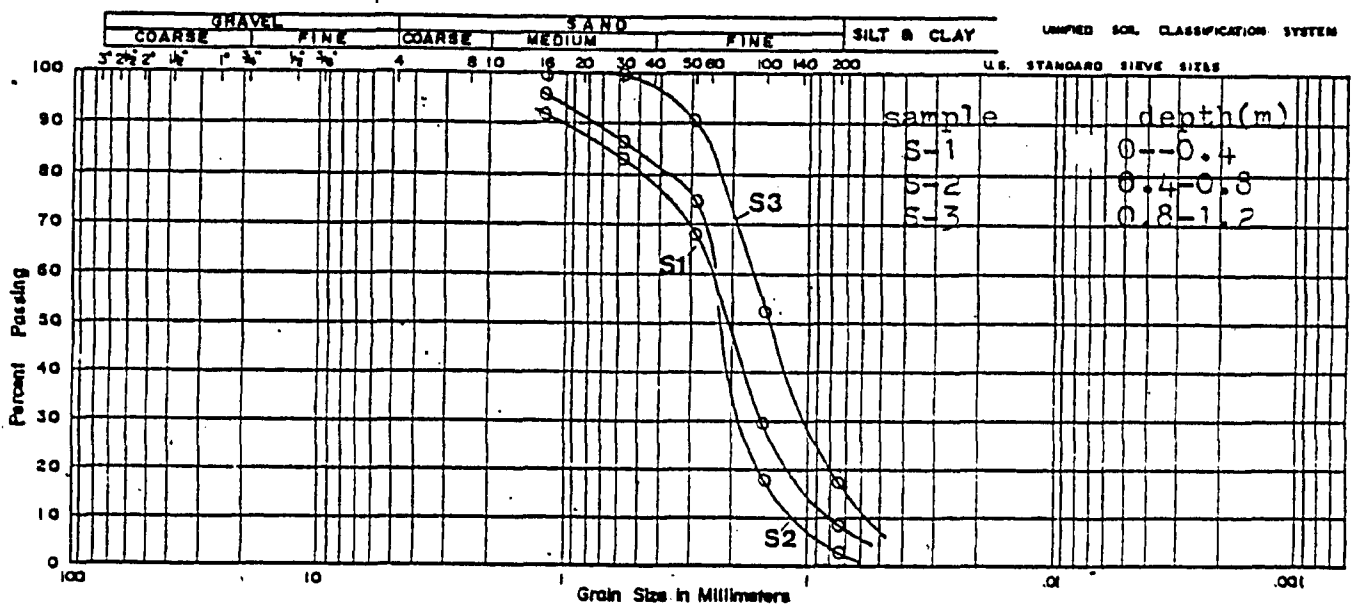
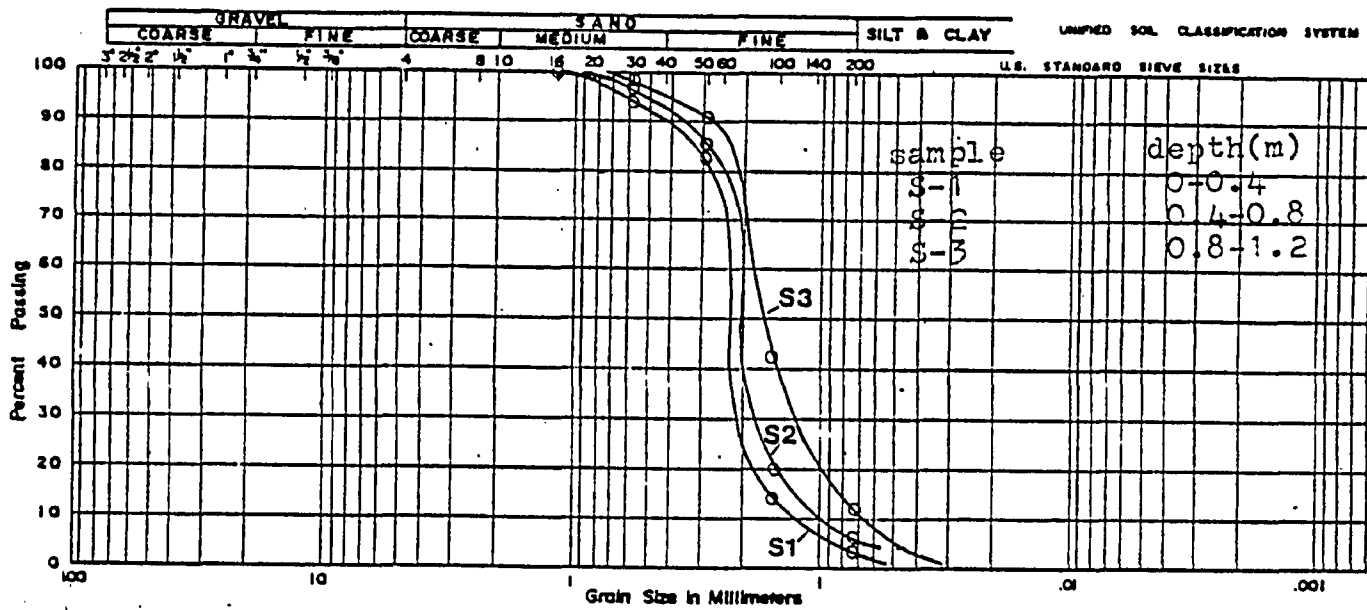


Figure 25a. Particle size distribution curves.

Auger hole 3



Auger hole 4

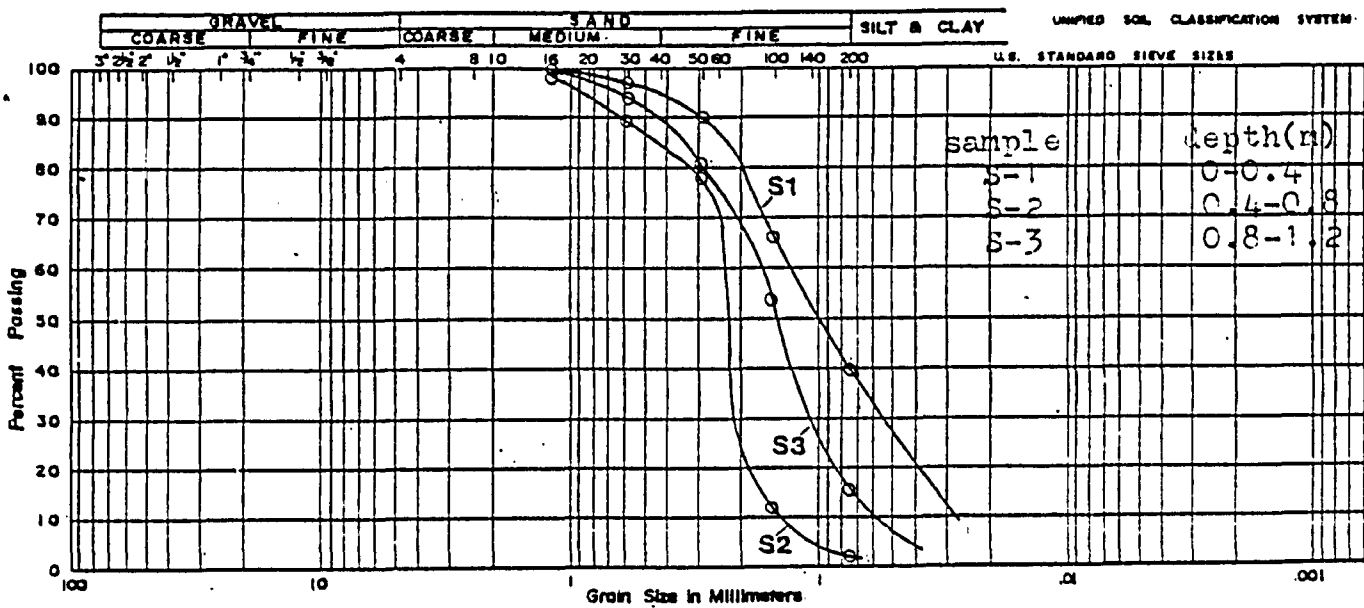
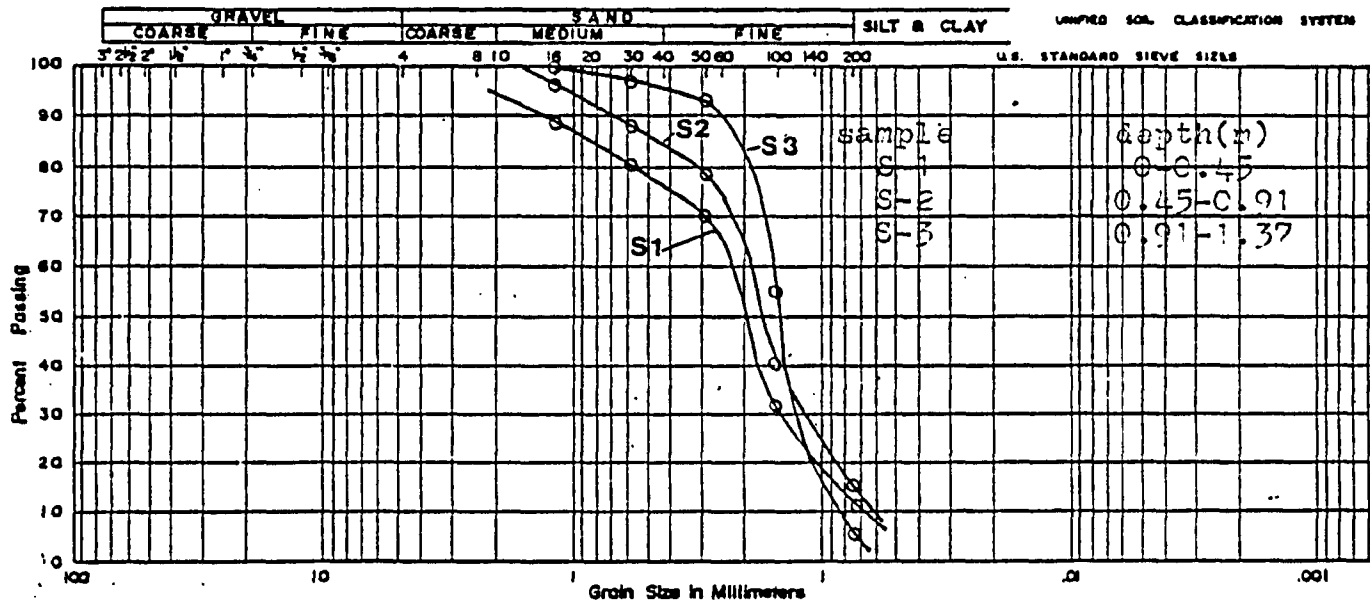


Figure 25b.. Particle size distribution curves.

Deep well.



Deep well.

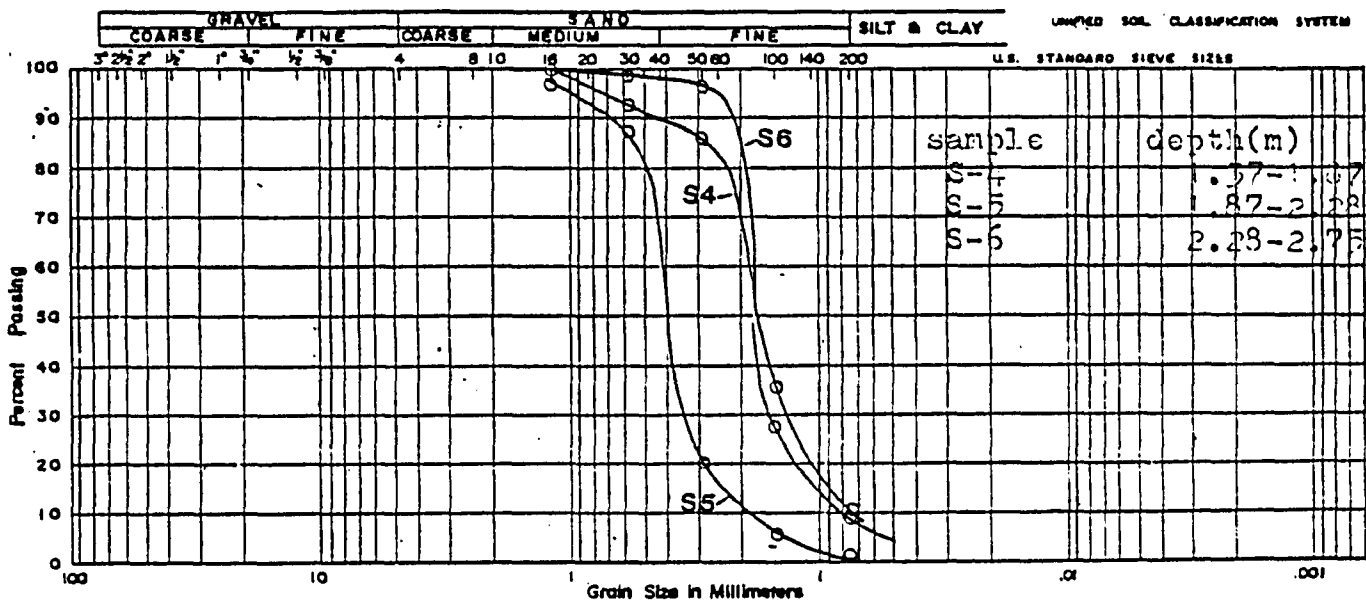
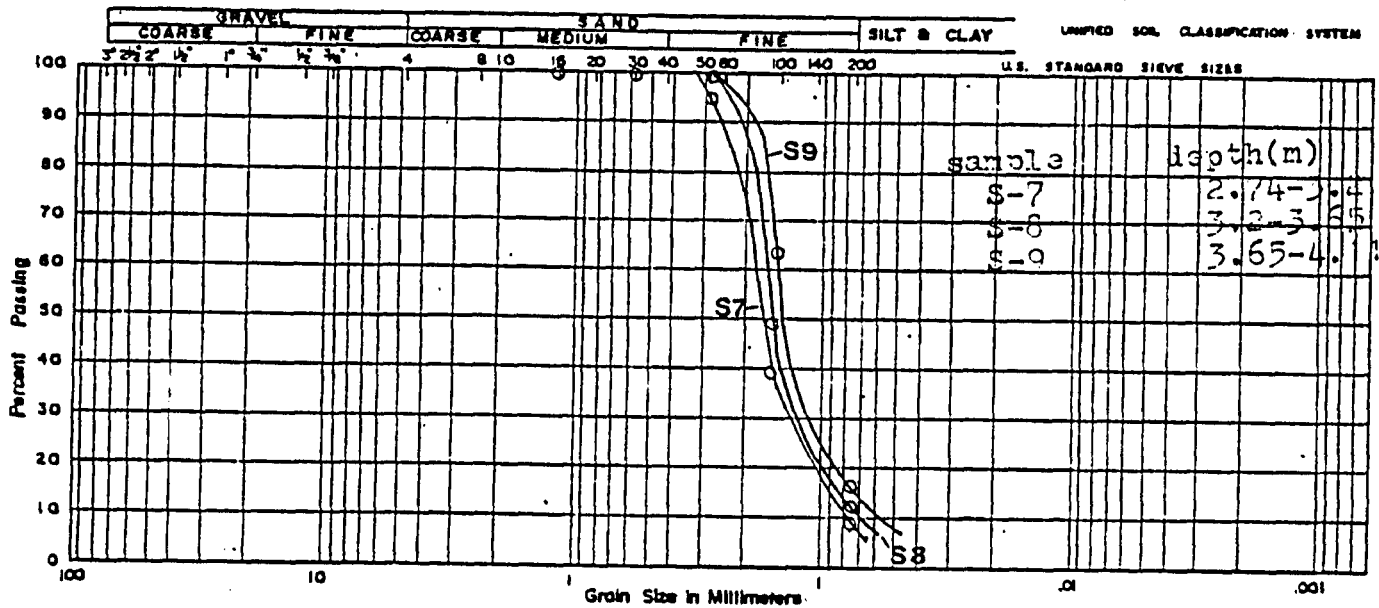


Figure 25c. Particle size distribution curves.

Deep well.



Deep well.

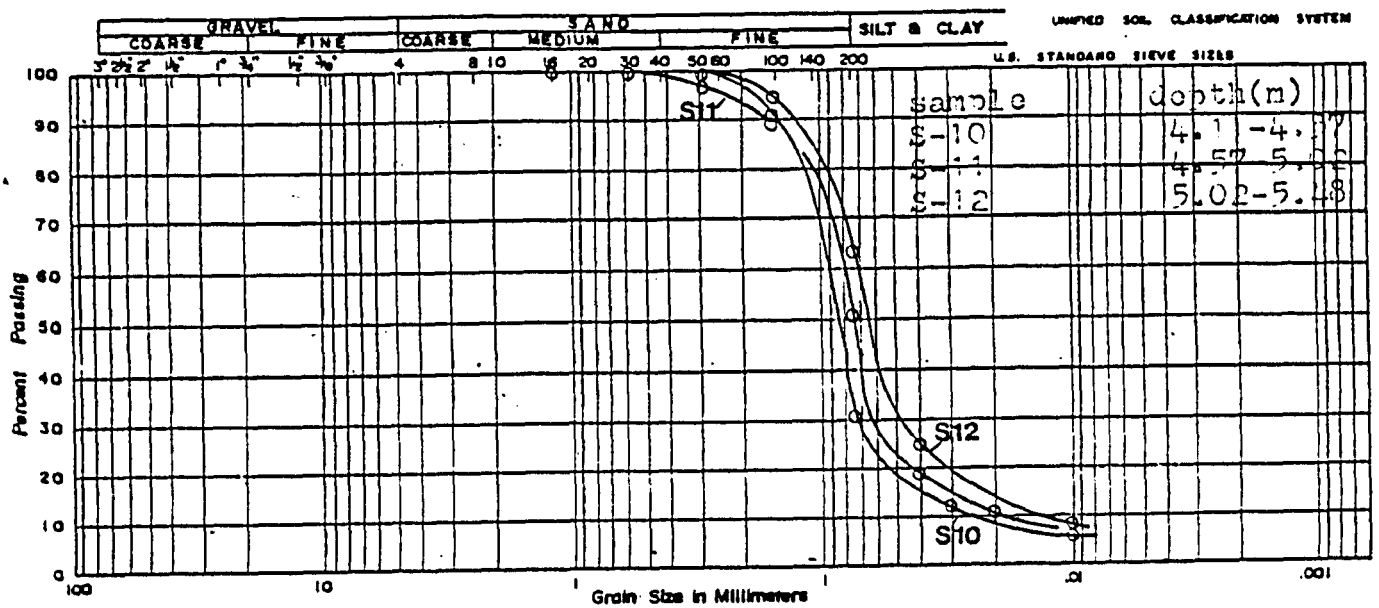


Figure 25d. Particle size distribution curves.

The hydraulic conductivity values determined for auger hole samples are consistent with the material found in the area (Clark, 1966). Hydraulic conductivity values calculated using Hazen's formula are one order greater in magnitude than the values determined from field data. For example, Sample 4 of the deep well, collected from the interval of 1.37-1.87 m gave a hydraulic conductivity value of 5.2×10^{-5} m/sec. Nearby P-10 was tested at the same depth and the hydraulic conductivity value calculated using field data is 2.3×10^{-6} m/sec. This difference is probably caused by the fact that Hazen's formula is not very reliable on fine grained soils (Freeze and Cherry, 1979).

5.1.6 Water Level Observations

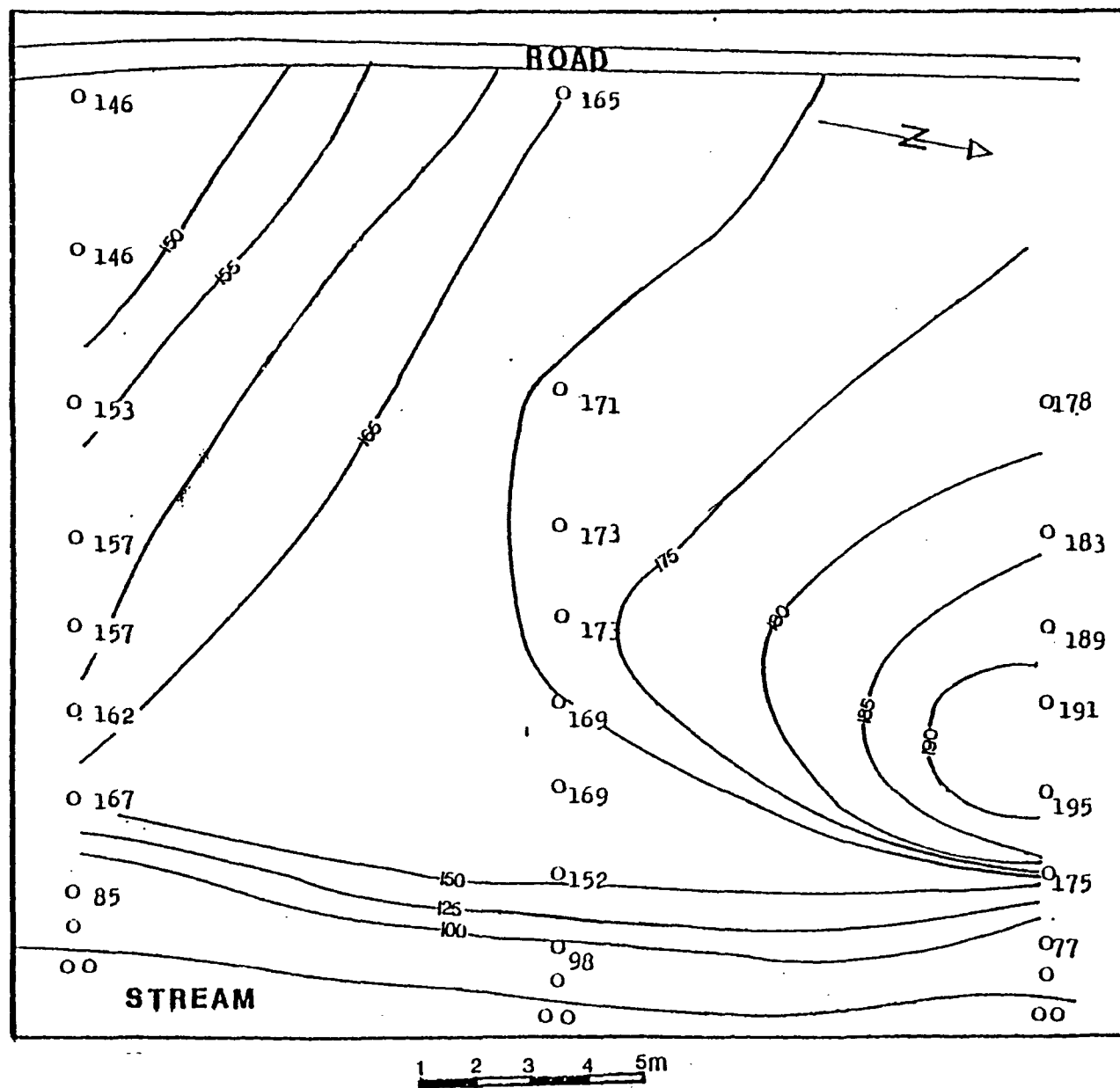
Results of the water level observations on the 7th of October, 1982 are plotted in Figure 26. The resulting water table map was used in determining the locations for tracer application.

5.2 Natural and Artificial Storm Events

5.2.1 October 12, 1982 Storm Event

a) Water Table Response

After a light rain of 8 mm on the 3rd of October, no natural rain was recorded before the artificial storm event on the 12th of October. The storm event lasted two hours with the average total rainfall of about 28 mm. The hydraulic head values before the storm event are tabulated



in Table 3. The flow net before the storm event is given in Figure 27. Prior to the storm event, the groundwater table was about 0.6 m below the surface level near the stream, while it was about 1.8 m deep near the road. The water table responses are given in Appendix III-1 and Figures 28a, b, c. The percentage rise and decline for each well and piezometer are given in Table 4.

After the first hour of rain, the water level in P-8 rose 0.15 m resulting in a percentage rise of about 25%. In P-5 an 0.03 m rise was observed which is equivalent to a 1% rise. P-1 showed no significant response after the first hour of rain. In P-18 a 21% rise (0.15 m) of the water table was recorded. P-10, which is located at the other end of the same line of instrumentation with P-18 had no response. P-13 showed a 2% (0.03 m) response while P-11 and P-12 did not respond. Along the No. 3 line of instrumentation, the largest water table response was recorded in P-25 where the rise was 28% (0.13 m). P-20 in which a 3% (0.05 m) rise occurred, was the last place on that line where a significant water table response was recorded.

Figure 29 summarizes the responses to the storm event of selected near stream piezometers and piezometers remote from the stream. No change in the stream level was observed in P-9, P-19, and P-26.

After two hours of rain, a water table rise was observed throughout the plot. The highest recorded response was closest to the stream. In P-8, P-18, and P-25, the

Table 3. Hydraulic head before storm events(m).

Well/ piezometer	Oct.12	Oct.28	Oct.29	Nov.1,2. (after the storm)
P-1	109.73	109.91	109.93	110.70
P-2	109.74	109.96	109.94	110.70
P-3	109.75	109.97	109.95	110.71
P-4	109.77	110.02	109.95	110.72
P-5	109.77	110.03	109.99	110.75
P-6	109.79	110.04	110.04	110.76
P-7	109.81	110.06	110.05	110.76
P-8	109.90	110.08	110.05	110.80
P-9	110.52	110.37	110.39	110.87
P-10	109.66	109.86	109.84	110.71
P-11	109.71	109.90	109.90	110.78
P-12	109.77	109.99	109.92	110.78
P-13	109.79	109.99	109.99	110.79
P-14	109.84	110.00	110.06	110.79
P-15	109.91	110.01	110.07	110.81
P-16	109.01	110.01	110.07	110.81
P-17	109.98	110.04	110.08	110.83
P-18	109.98	110.07	110.09	110.83
P-19	110.52	110.52	110.39	110.87
P-20	109.79	109.94	109.92	110.76
P-21	109.82	109.95	109.94	110.76
P-22	109.90	110.00	109.97	110.77
P-23	109.97	110.00	110.07	110.79

Table 3 cont'd

P-24	110.01	110.01	110.14	110.79
P-25	110.02	110.07	110.14	110.80
P-26	110.47	110.44	110.39	110.87
W-1	109.73	109.84	109.89	110.72
W-2	109.75	109.87	109.90	110.73
W-3	109.78	109.93	109.91	110.75

Relative to an arbitrary datum 100m below the ground level.

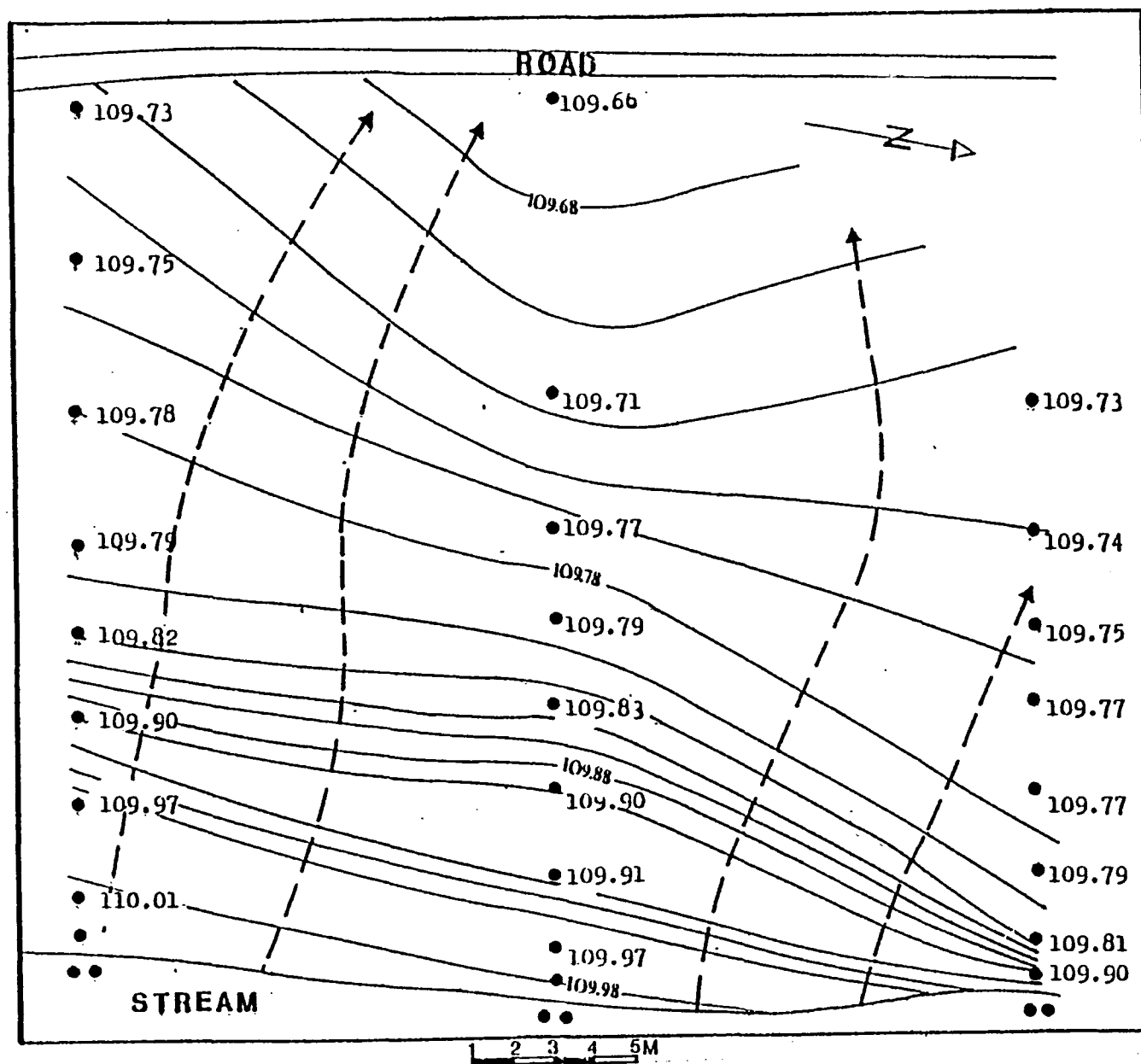


Figure 27. October 12, 1982 storm event. Flow net before the storm event.
Contour interval 0.02m

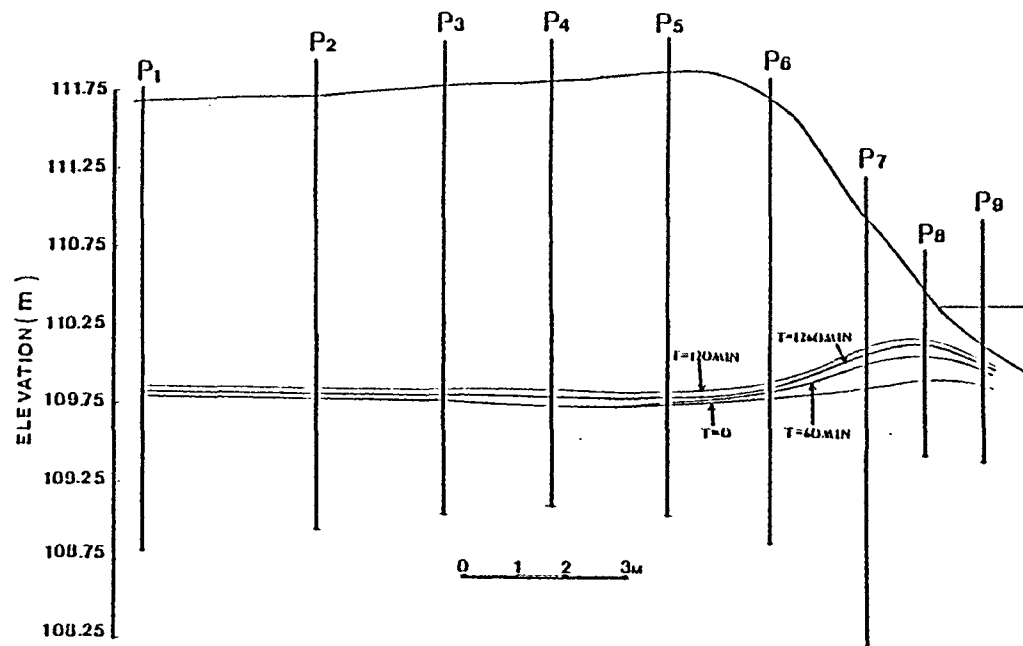


Figure 28a. October 12, 1982 storm event. Cross section 1 showing the water table response during the storm event.

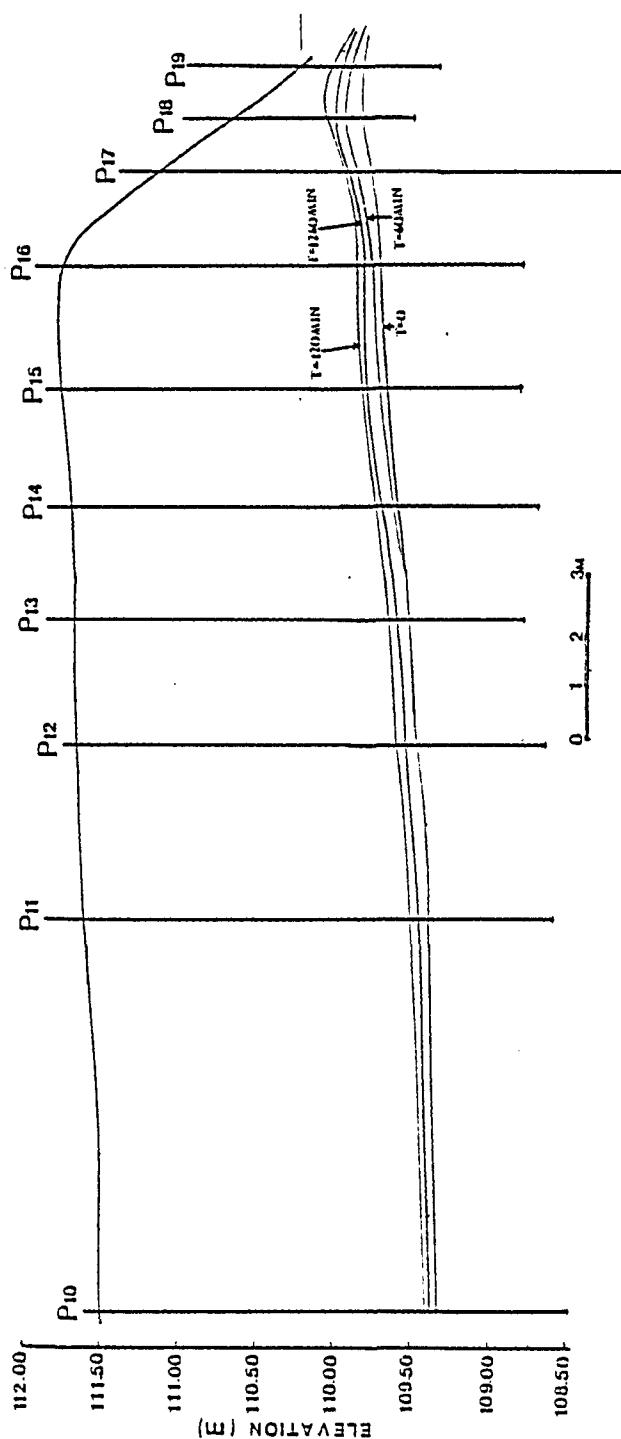


Figure 28b. October 12, 1982 storm event. Cross section 2 showing water table response during the storm event.

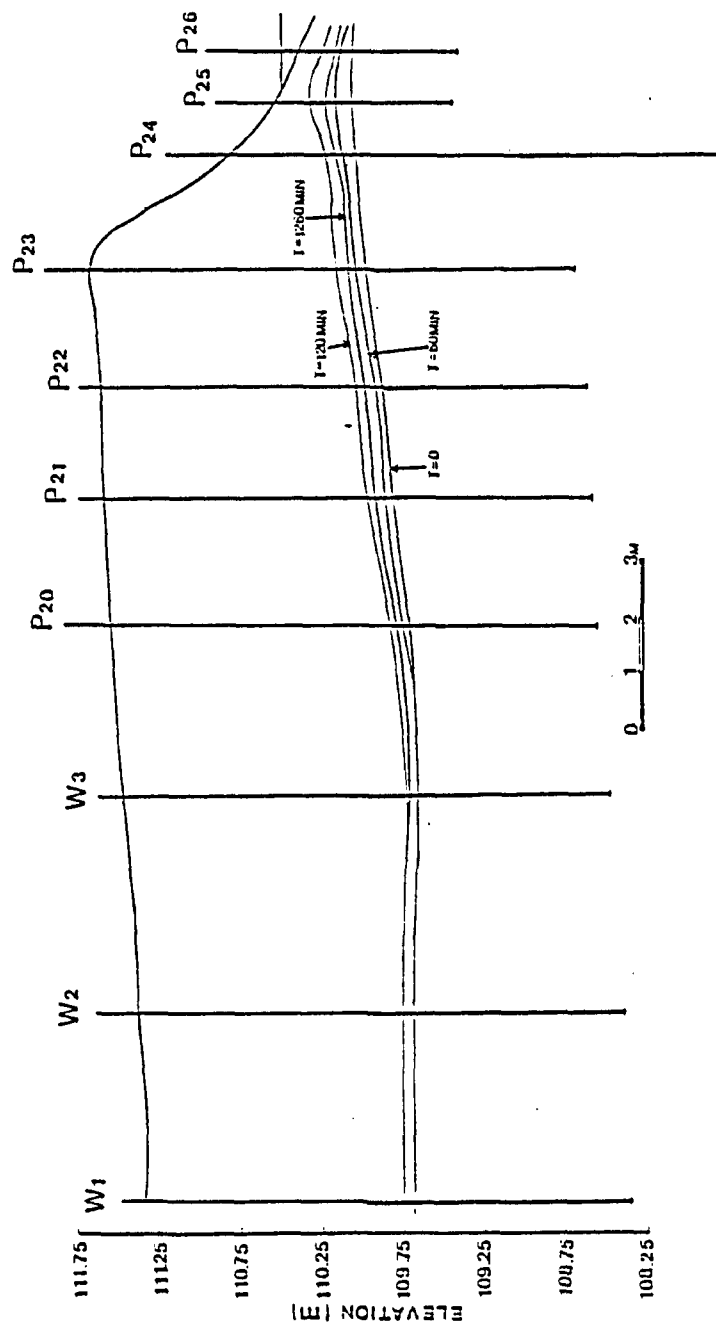


Figure 28c. October 12, 1982 storm event. Cross section 3 showing water table response during the storm event.

Table 4 . October 12,1982 storm event.Percentage rise/
decline of the water table.

Well/piezometer.	Percentage rise(%).		Percentage decline(%).
	t=60min.	t=120min.	t=1080min.
P-1	0	4.1	1.6
P-2	0	3.6	1.1
P-3	0	3.5	1.0
P-4	0	3.9	1.5
P-5	1.4	3.7	1.4
P-6	2.5	6.1	1.1
P-7	13.0	24.3	5.7
P-8	25.0	46.7	15.6
P-9	0	6.7	21.9
P-10	0	4.3	1.7
P-11	0	5.2	2.7
P-12	0	5.2	2.8
P-13	1.6	6.8	2.8
P-14	2.7	8.0	1.7
P-15	2.6	7.9	1.1
P-16	3.7	8.0	1.7
P-17	8.9	19.6	7.2
P-18	21.4	35.7	22.2
P-19	0	7.4	6.9
P-20	2.8	7.2	1.8
P-21	2.9	8.6	3.0
P-22	2.9	9.9	4.5
P-23	4.7	10.6	5.3

Table 4 cont'd

P-24	10.7	24.0	8.8
P-25	27.7	57.4	35.0
P-26	0	7.4	13.8
W-1	0	3.2	0
W-2	0	4.3	0
W-3	0	2.8	0.6

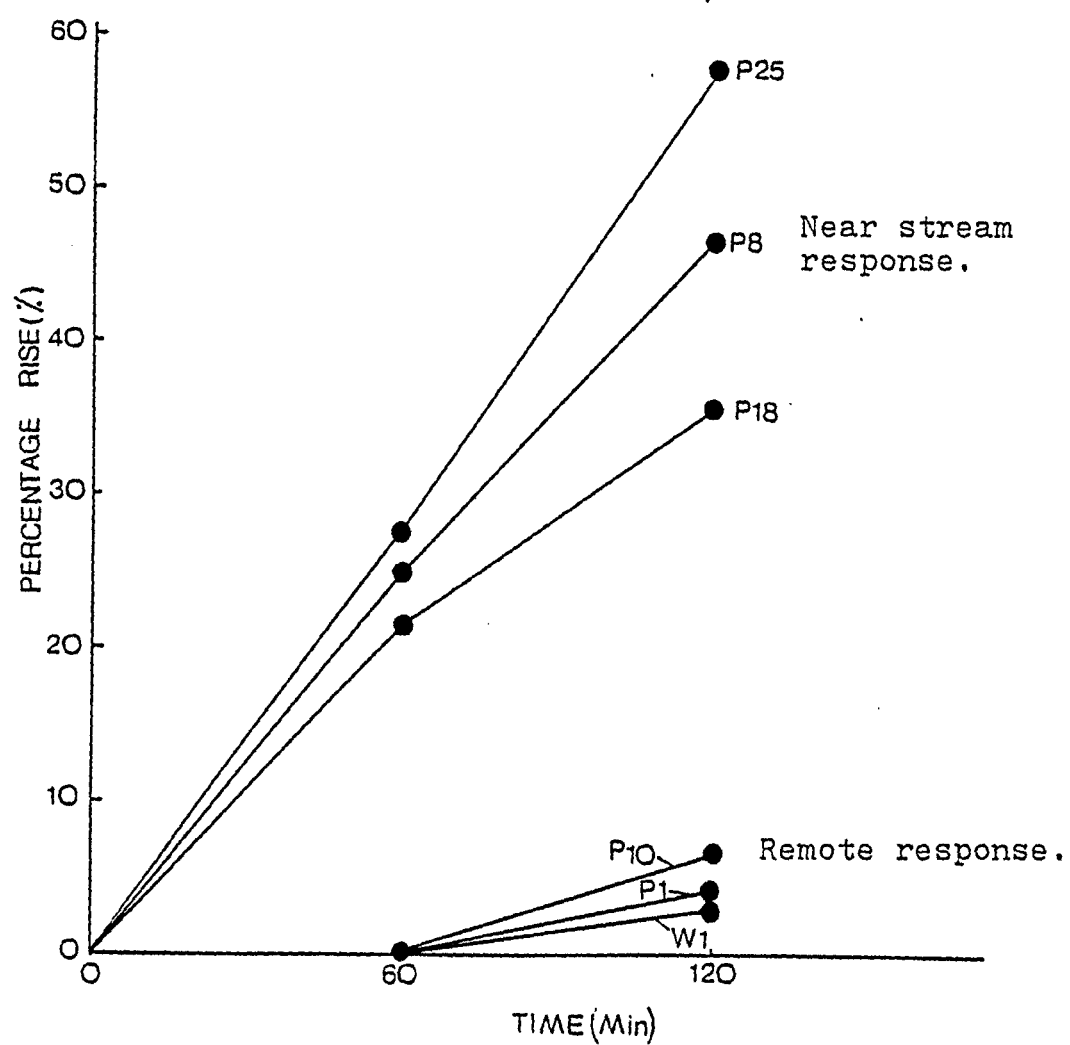


Figure 29. October 12, 1982 storm event. Groundwater table response in selected wells and piezometers.

risers were 47% (0.28 m), 36% (0.35 m), and 57% (0.27 m). The groundwater level in P-1 and P-10 rose 4% (0.08 m). W-1 had a 3% (0.05 m) rise. The stream level rose in P-9, P-19, and P-26 by 0.02 m.

After two hours the rain was terminated. Measurements taken 18 hours later showed a general decline in water level throughout the plot. The decline along the stream was far greater than in other parts of the plot. The average decline along the stream was about 24% (0.07 m), while it was 1% (0.02 m) closer to the road.

b) Neutron logging

Results of the neutron logging are presented in Figures 30a-d. Prior to the storm event the volumetric moisture content (V.M.C.) at the surface ranged from 28% at NA-1 to 26% at NA4. The VMC gradually increased with depth up to about 50% at the water table (Appendix III-2).

The first hour of rain had only a slight effect on the V.M.C. in all four locations. The average rise of the V.M.C. in all the tested areas was about 1% at the ground surface. No water level rise was observed in NA-1 and NA-2. In NA-3 and NA-4, rises of 0.05 and 0.08 m were observed.

The average height of the capillary fringe prior to the rain was about 0.25 m. After the first hour of rain, even in NA-3 and NA-4 where a considerable water level rise was observed, the height of the capillary fringe remained unchanged.

After two hours of rain, the V.M.C. had changed

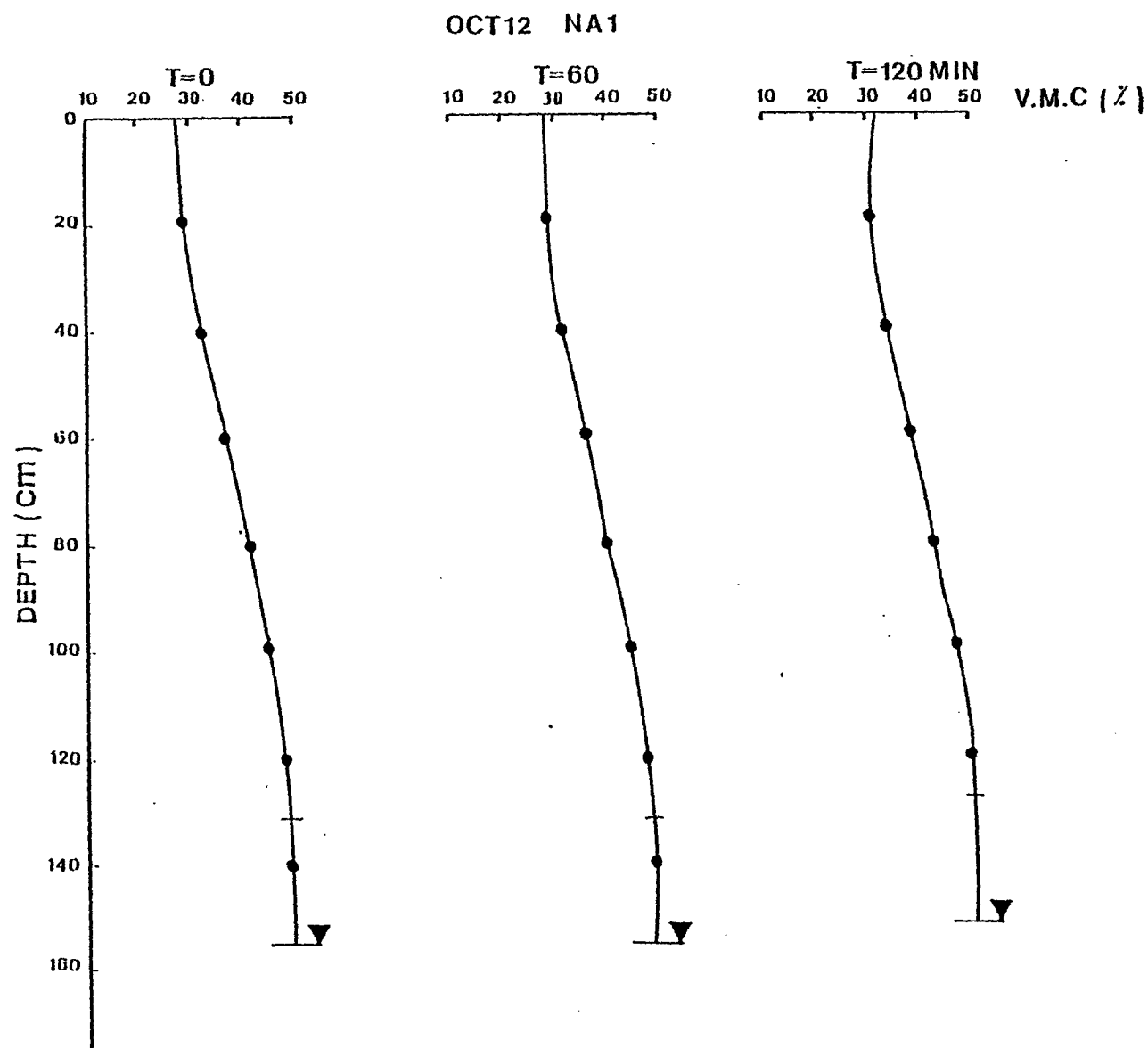


Figure 30a. October 12, 1982 storm event. Relationship of volumetric moisture content with depth.

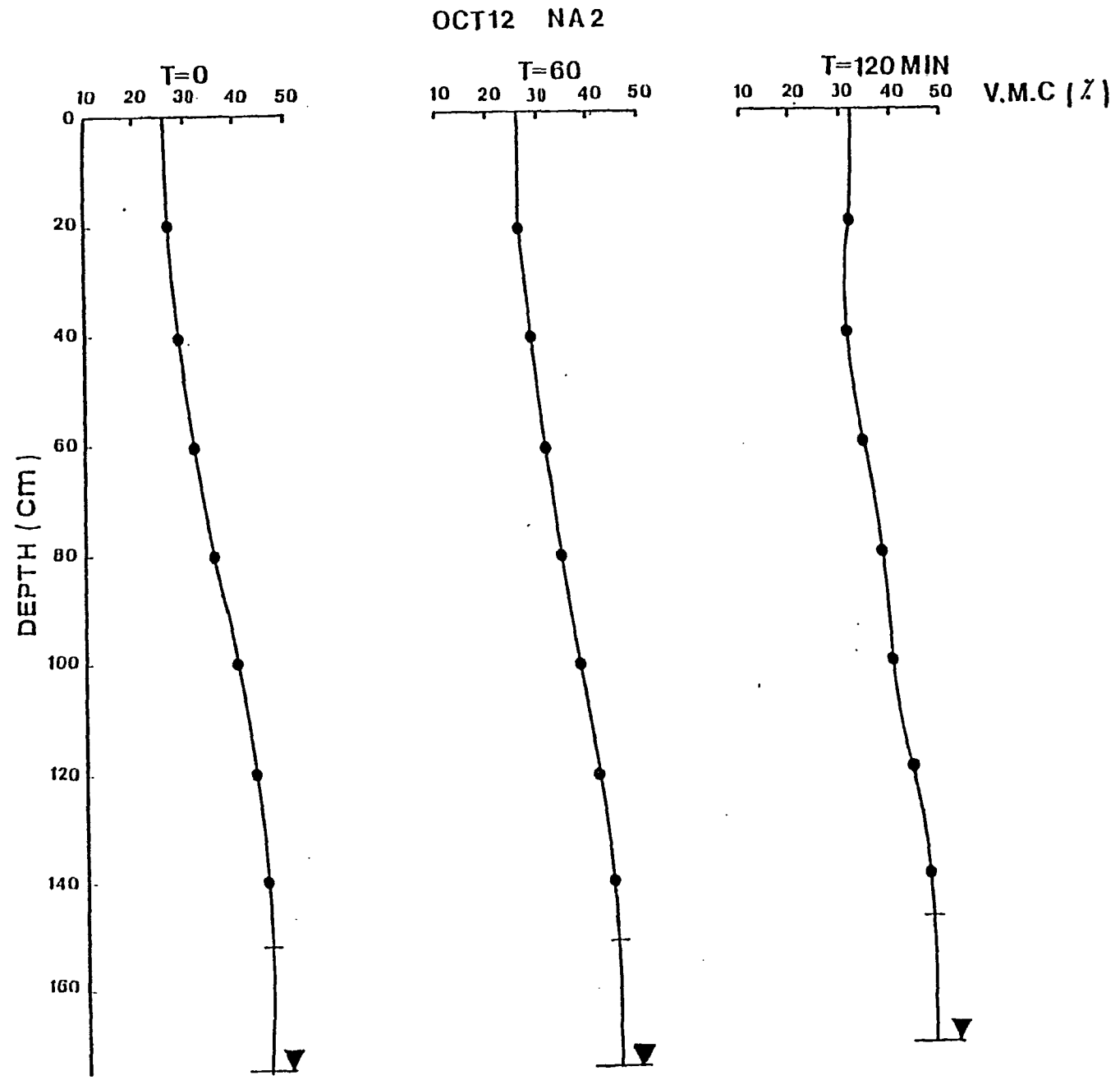


Figure 30b. October 12,1982 storm event.Relationship of volumetric moisture content with depth.

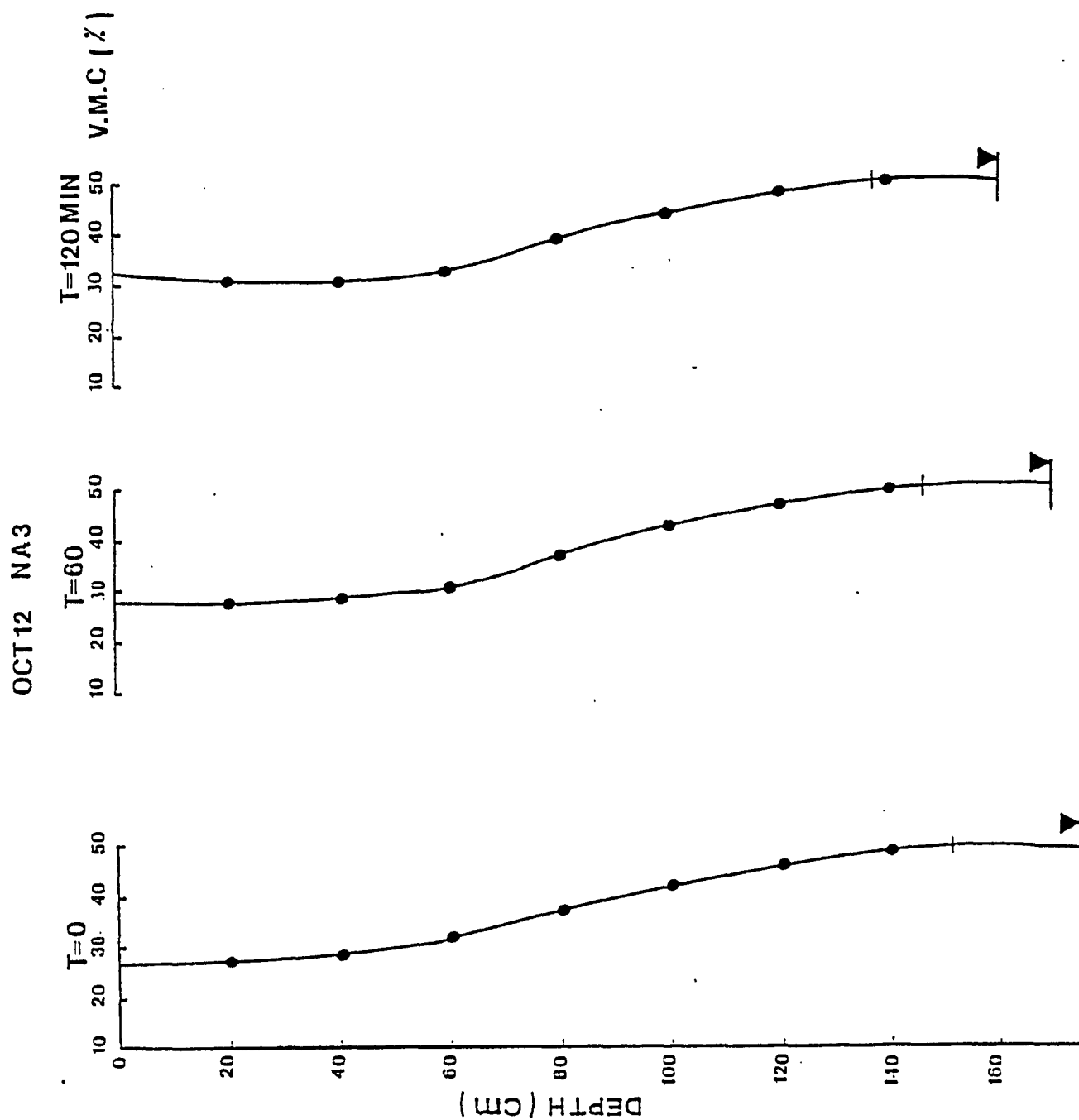


Figure 30c. October 12, 1982 storm event. Relationship of volumetric moisture content with depth.

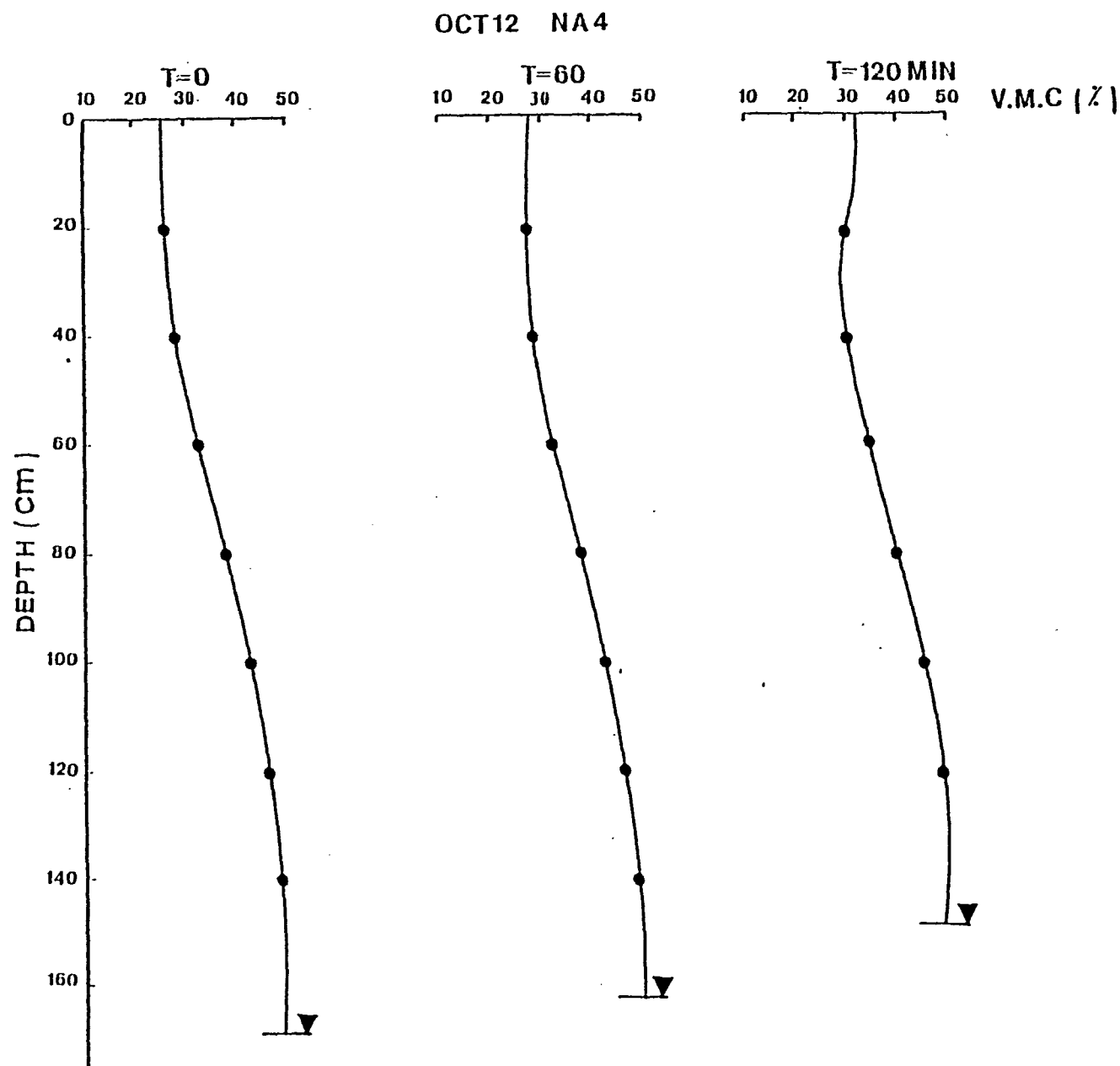


Figure 30d. October 12, 1982 storm event. Relationship of volumetric moisture content with depth.

considerably at the ground surface as well as below it. The rise in V.M.C. averaged 4% at the surface. A groundwater level rise was observed in all four locations. A maximum rise of 0.12 m occurred in NA-4 while the rise in NA-3 was 0.10 m. NA-1 and NA-2 had water table rises of about 0.04 and 0.06 m respectively.

No significant change in the height of the capillary fringe was observed in all four locations.

c) Tensiometer experiments

Interpretation of tensiometer experiment data is illustrated in Figures 31 a-c. The pressure head values are given in Appendix III-3. Prior to the storm event, the pressure head at the ground surface was -160 cm, in all three locations. It gradually increased with depth reaching zero at the water table.

After the first hour of rain the pressure head at the surface increased by about 10 cm in all three tensiometer nests, but below ground surface no significant change in pressure head was observed. After the first hour, a rise in the water table was observed only at TN-4.

The second hour of rain had an apparent effect on the pressure head at and below the ground surface, in all three tested areas. The pressure head increase at the ground surface averaged about 75 cm. At all three tensiometer nests, a considerable water table rise was observed. The maximum rise of 0.09 m occurred at TN-4 while 0.05 m and

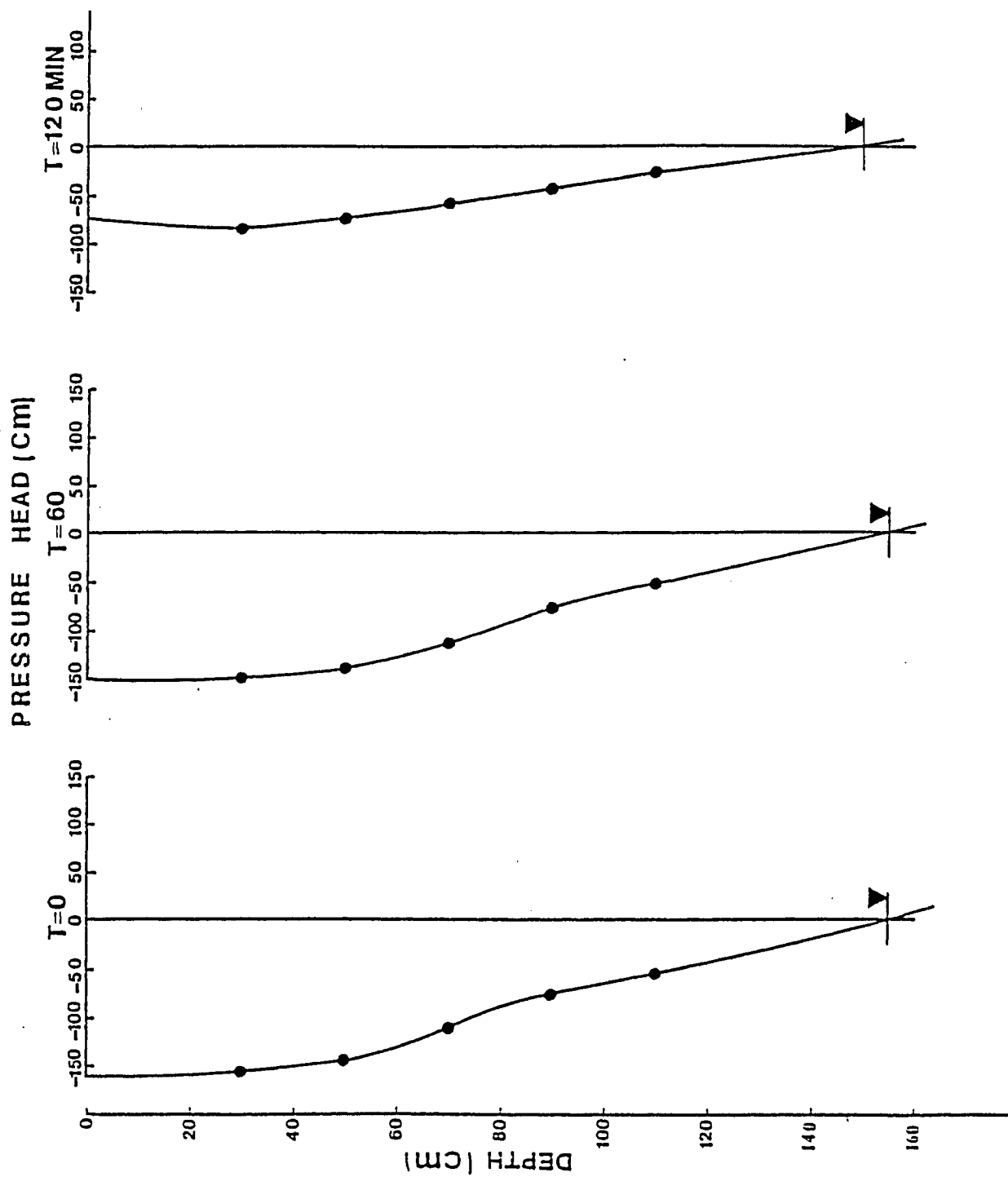


Figure 31a. October 12, 1982 storm event. Relationship of pressure head with depth. (TN1)

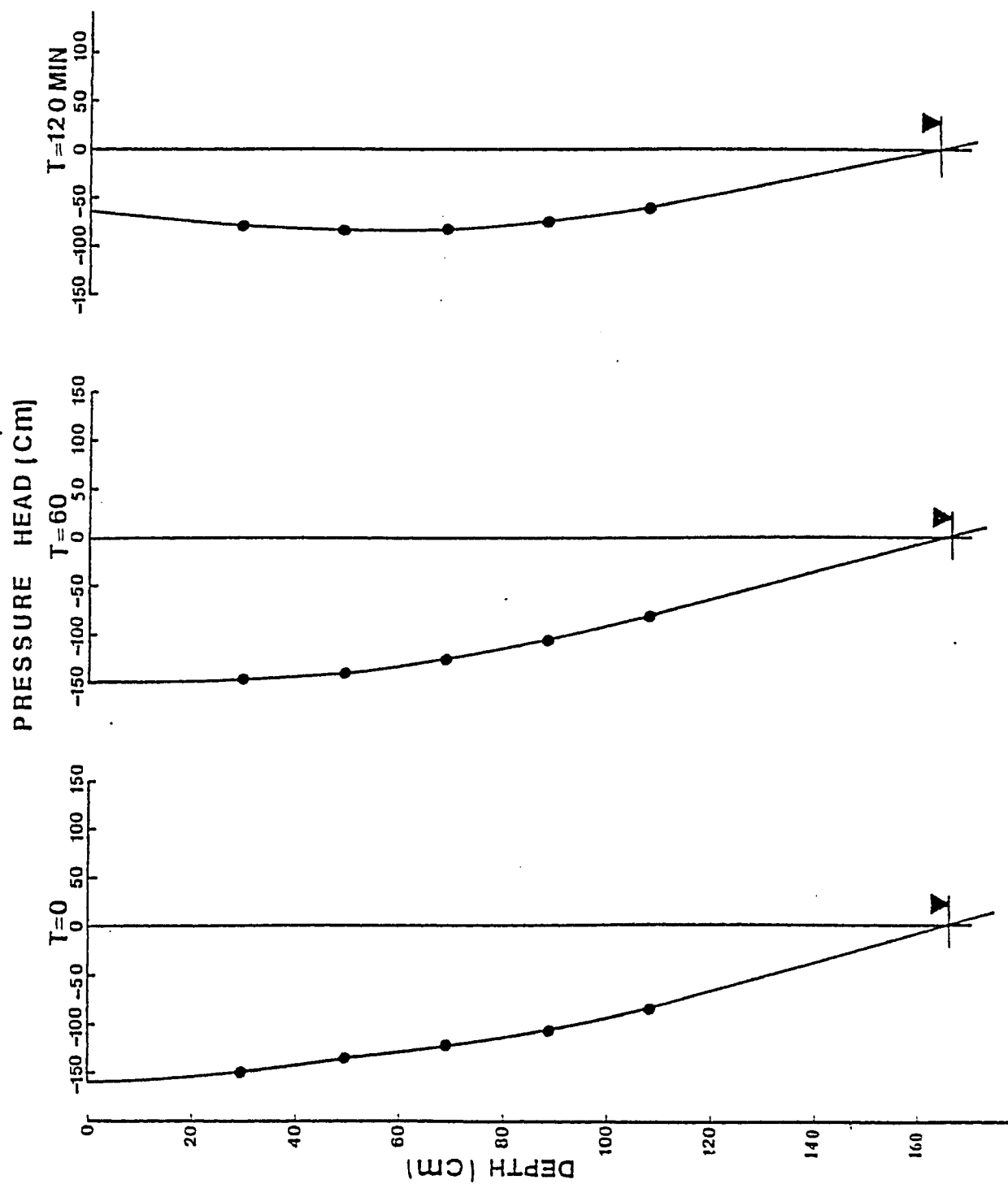


Figure 31b. October 12, 1982 storm event. Relationship of pressure head with depth. (TN2)

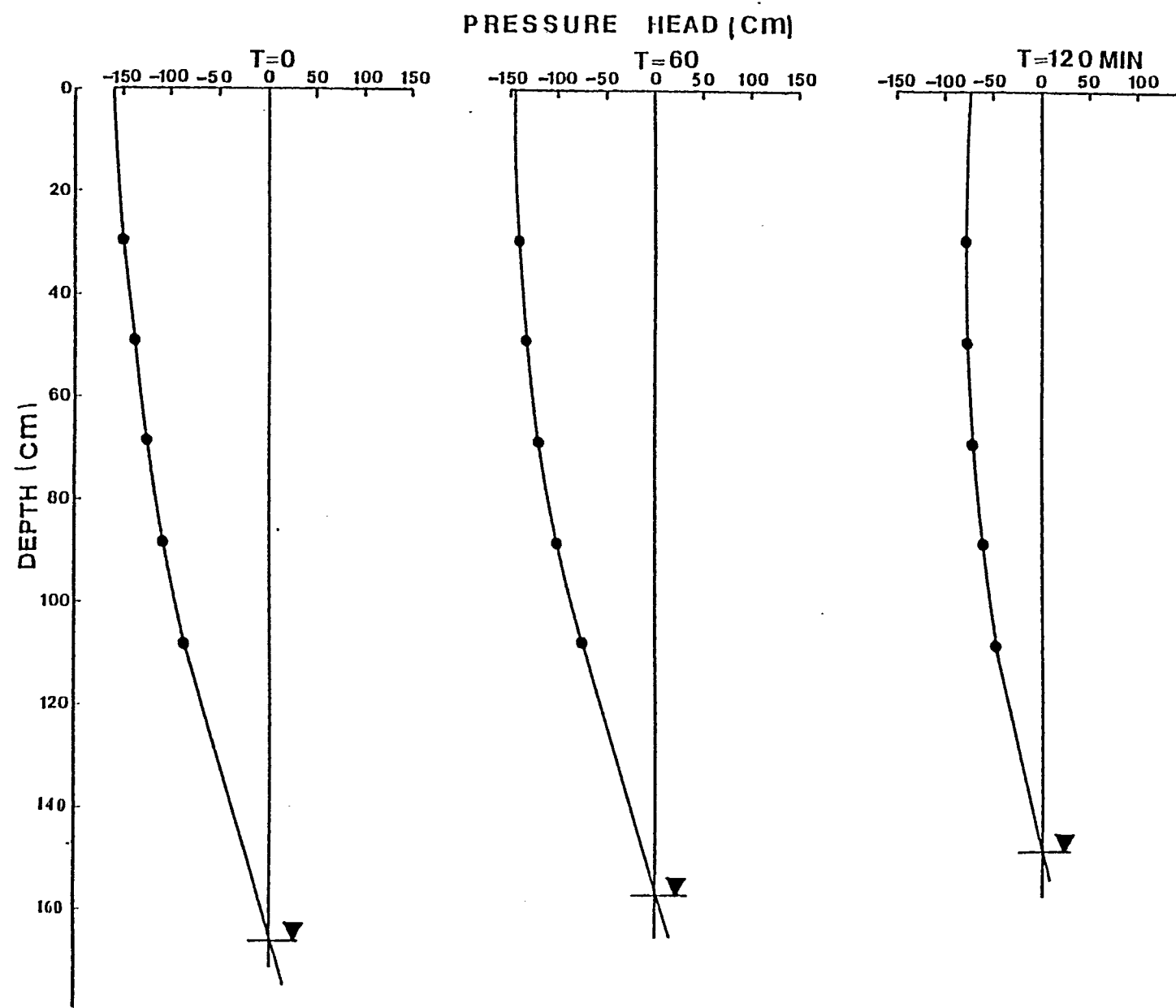


Figure 31c. October 12, 1982 storm event. Relationship of pressure head with depth. (TN4)

0.03 m rises were observed in TN-1 and TN-2 respectively.

Water level rises determined by neutron logging, tensiometer readings and direct observations are tabulated in Table 5. The water table rise obtained from different methods seem to be fairly consistent.

Results of the TN-3 were not available due to an installation error.

5.2.2 October 28, 1982 Storm Event

a) Water table response

After for the artificial rain on the 12th of October, 1982, no natural rain was recorded before the artificial storm event on the 28th of October. The storm event lasted two hours with an average rainfall of about 18 mm. The flow net before the storm event is given in Figure 32. The water table responses are given in Appendix IV-1 and Figures 33 a-c. The percentage rise and decline for each well and piezometer are given in Table 6.

Prior to the storm event, the groundwater table was about 0.4 m below the surface level near the stream, while it was about 1.6 m deep near the road.

After the first hour of rain, the water level in P-8 rose 0.1 m resulting in a percentage rise of about 21%. In P-5 a 0.01 m rise was observed which is equivalent to a 0.5% rise. P-1 showed no measurable response after the first hour of rain. In P-18, a 20% rise (0.15 m) of the water table was recorded. P-10, which is located furthest from

Table 5, October 12, 1982 storm event. Rise of the water table determined by different methods.

Location.	Distance from the stream, (m)	water table rise(m).					
		Direct observation.		Neutron logging.		Tensiometer observation.	
		t=60min	t=120min	t=60min	t=120min	t=60min	t=120min
W-1	17.5	0	0.05	0	0.04	0	0.05
W-3	11.0	0	0.05	0	0.06	0	0.03
P-20	6.5	0.05	0.13	0.05	0.10	-	-
P-23	3.0	0.08	0.18	0.08	0.12	0.07	0.09

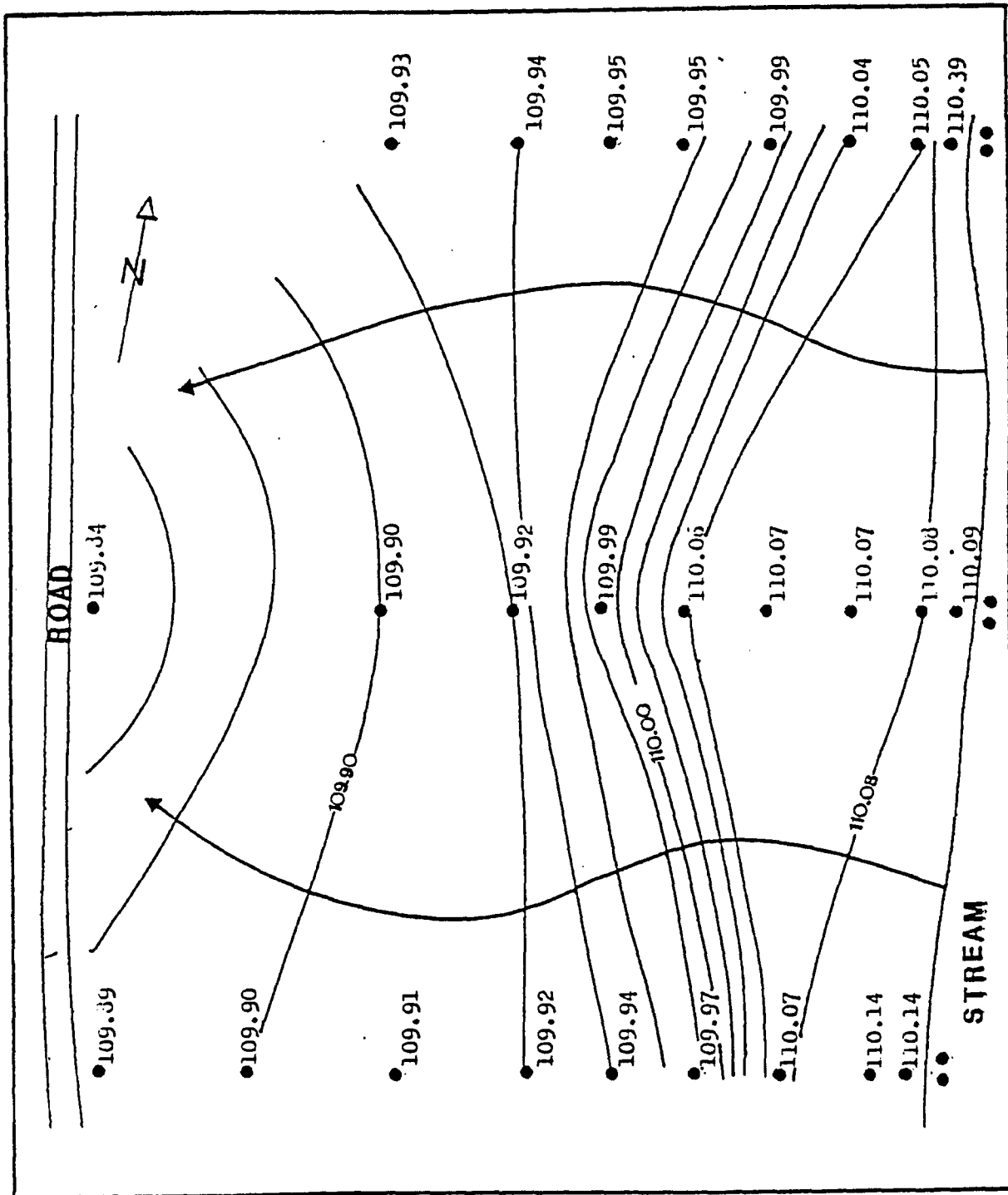


Figure 32. October 28, 1982 storm event. Flow net before the storm event.
Contour interval 0.02m

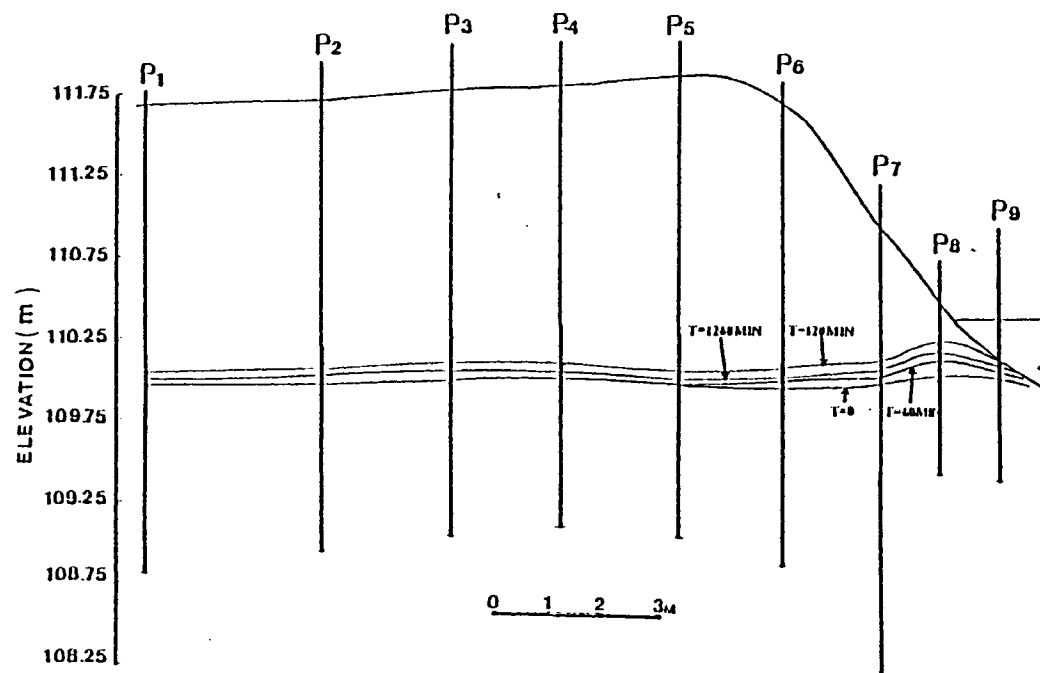


Figure 33a. October 28, 1982 storm event. Cross section 1 showing water table response during the storm event.

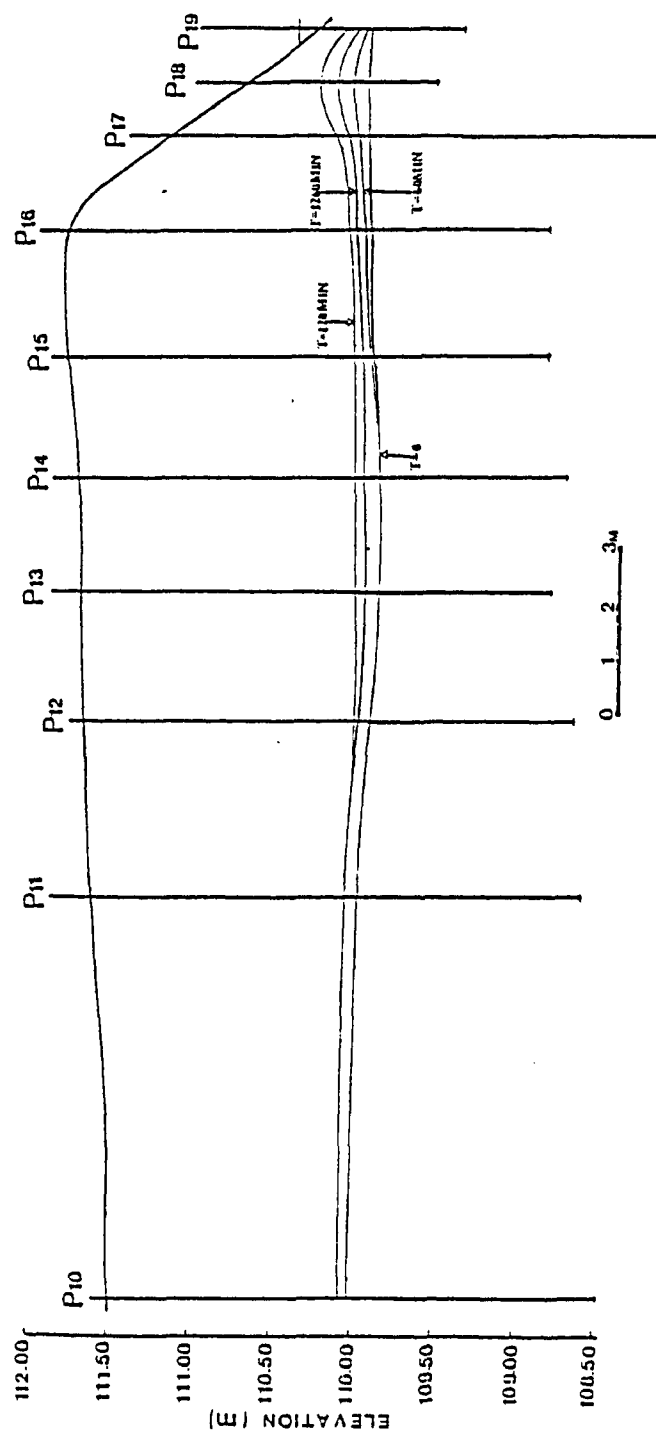


Figure 33b. October 28, 1982 storm event. Cross section 2 showing water table response during the storm event.

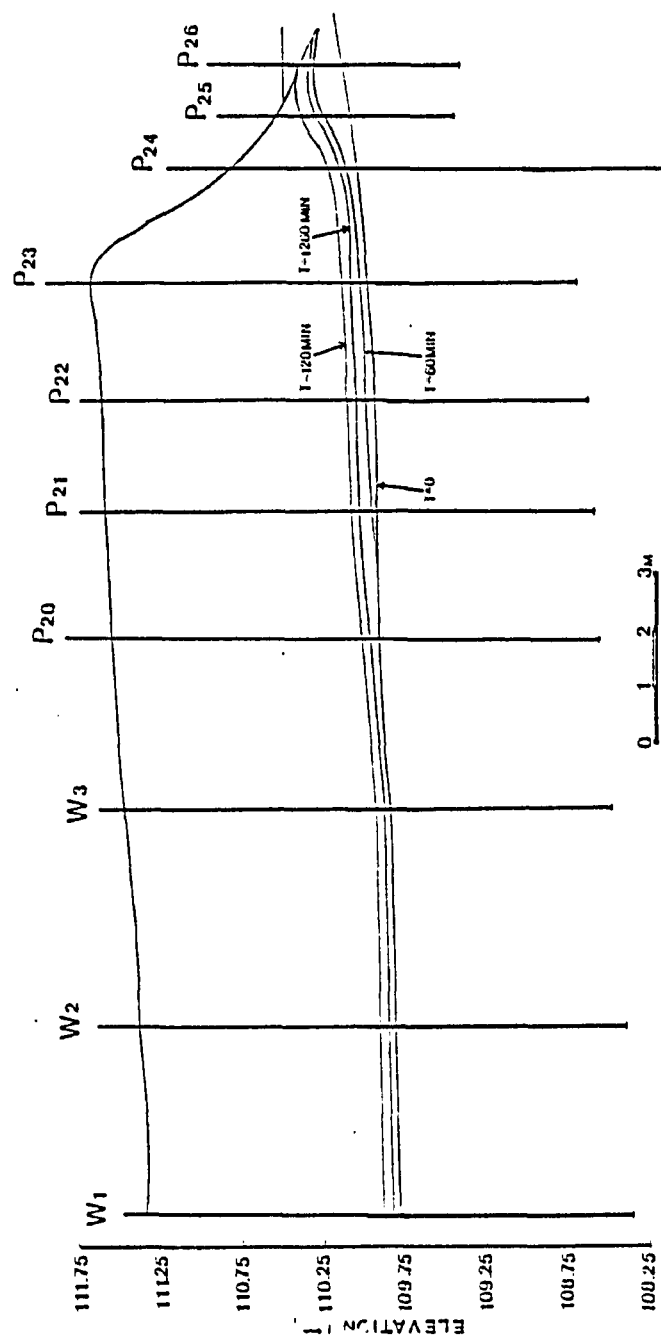


Figure 33c. October 28, 1982 storm event. Cross section 3 showing water table response during the storm event.

Table 6 . October 28,1982 storm event.Percentage rise/
decline of the water table.

Well/ piezometer.	Percentage rise(%).		percentage decline(%).
	t=60min.	t=120min.	t=1260min.
P-1	0	5.6	3.0
P-2	0	5.6	1.8
P-3	0	5.6	2.9
P-4	0	5.6	2.9
P-5	0.5	4.2	1.6
P-6	2.8	7.4	3.0
P-7	4.0	13.0	5.7
P-8	21.3	46.8	28.0
P-9	0	20.0	20.0
P-10	0	3.4	0
P-11	0	6.1	0
P-12	0	4.5	1.3
P-13	0	5.6	1.2
P-14	1.7	5.6	1.2
P-15	1.1	6.9	2.9
P-16	2.7	8.1	2.9
P-17	6.9	17.4	7.4
P-18	20.0	44.0	30.9
P-19	0	6.7	15.6
P-20	0	6.25	3.3
P-21	1.2	7.4	3.3
P-22	3.1	9.3	3.4
P-23	3.0	8.4	2.6

Table 6 cont'd

P-24	13.3	26.6	9.1
P-25	28.6	52.3	15.0
P-26	0	9.1	16.7
W-1	0	4.7	2.8
W-2	0	4.7	2.8
W-3	0	1.3	3.3

the stream on the same line of instrumentation as P-18, had no response. P-11, P-12 and P-13 showed no response. Along the No. 3 line of instrumentation, the largest water table response was recorded in P-25, where the rise was 29% (0.08 m). P-21, in which a 1.0% rise (0.02 m) occurred was the last place on that line where a significant water table response was recorded. Figure 34 shows the different responses of near-stream piezometers and piezometers remote from the stream, to the storm event. No change in the stream level was observed in P-9, P-19, and P-26.

After two hours of rain, a water table rise was observed throughout the plot. The highest recorded response was closest to the stream. In P-8, P-18, and P-25, the rises were 47% (0.22 m), 44% (0.33 m) and 52% (0.22 m). The groundwater level in P-1 and P-10 rose 6% (0.1 m) and 3% (0.05). W-1 had a 5% (0.07 m) rise. The stream level rose in P-9, P-19, and P-26 by 0.02 m.

After two hours the rain stopped. Measurements taken 21 hours later show a general decline in water level throughout the plot. The decline along the stream was far greater than in other parts of the plot. The average decline along the stream was about 25% (0.08 m), while it was 2% (0.03 m) closer to the road.

b) Neutron logging

Results of the neutron logging are presented in Figure 35 a-d. Prior to the storm event, the volumetric moisture

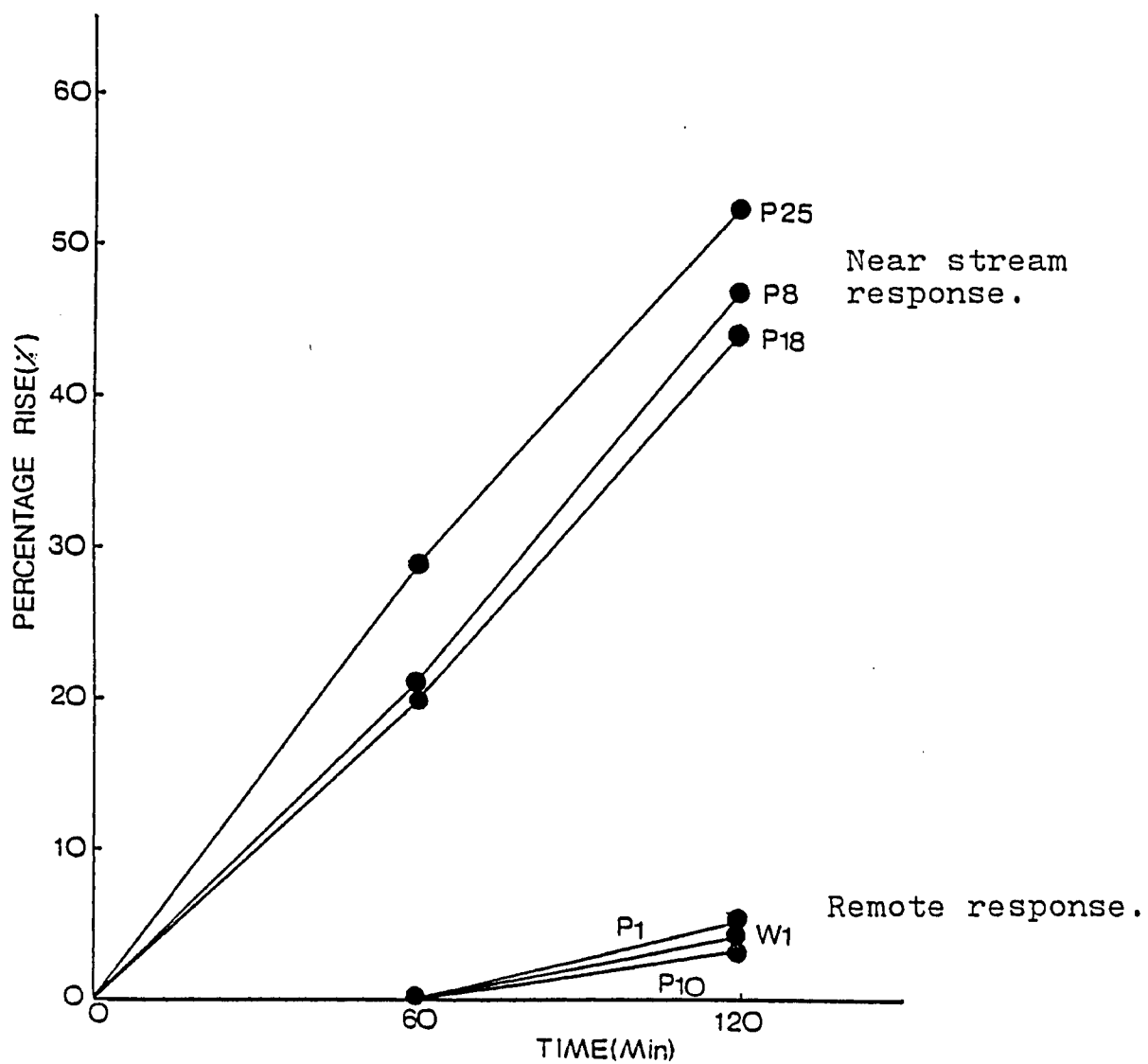


Figure 34. October 28 storm event. Groundwater response in selected wells and piezometers.

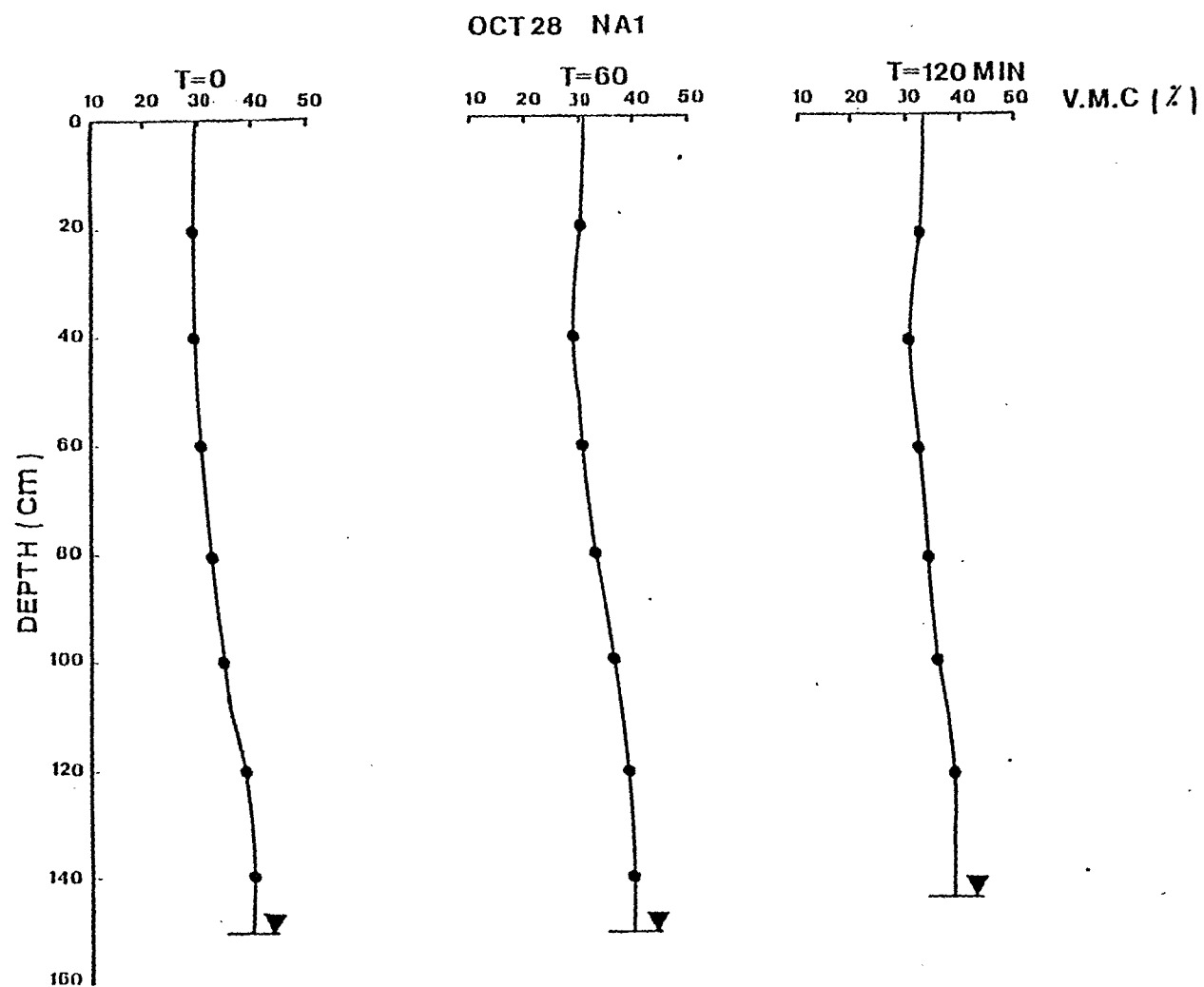


Figure 35a. October 28, 1982 storm event. Relationship of volumetric moisture content with depth.

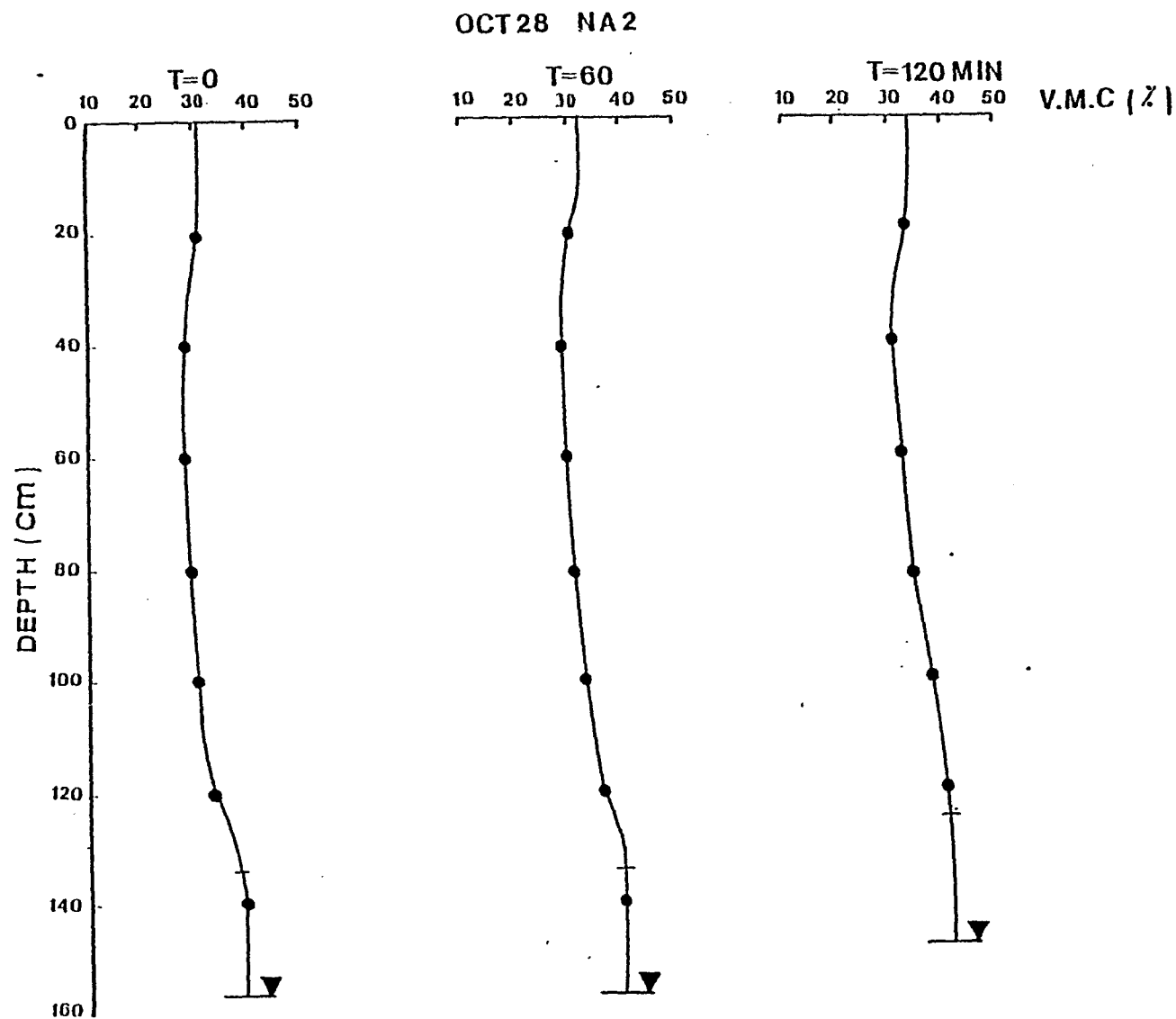


Figure 35b. October 28, 1982 storm event. Relationship of volumetric moisture content with depth.

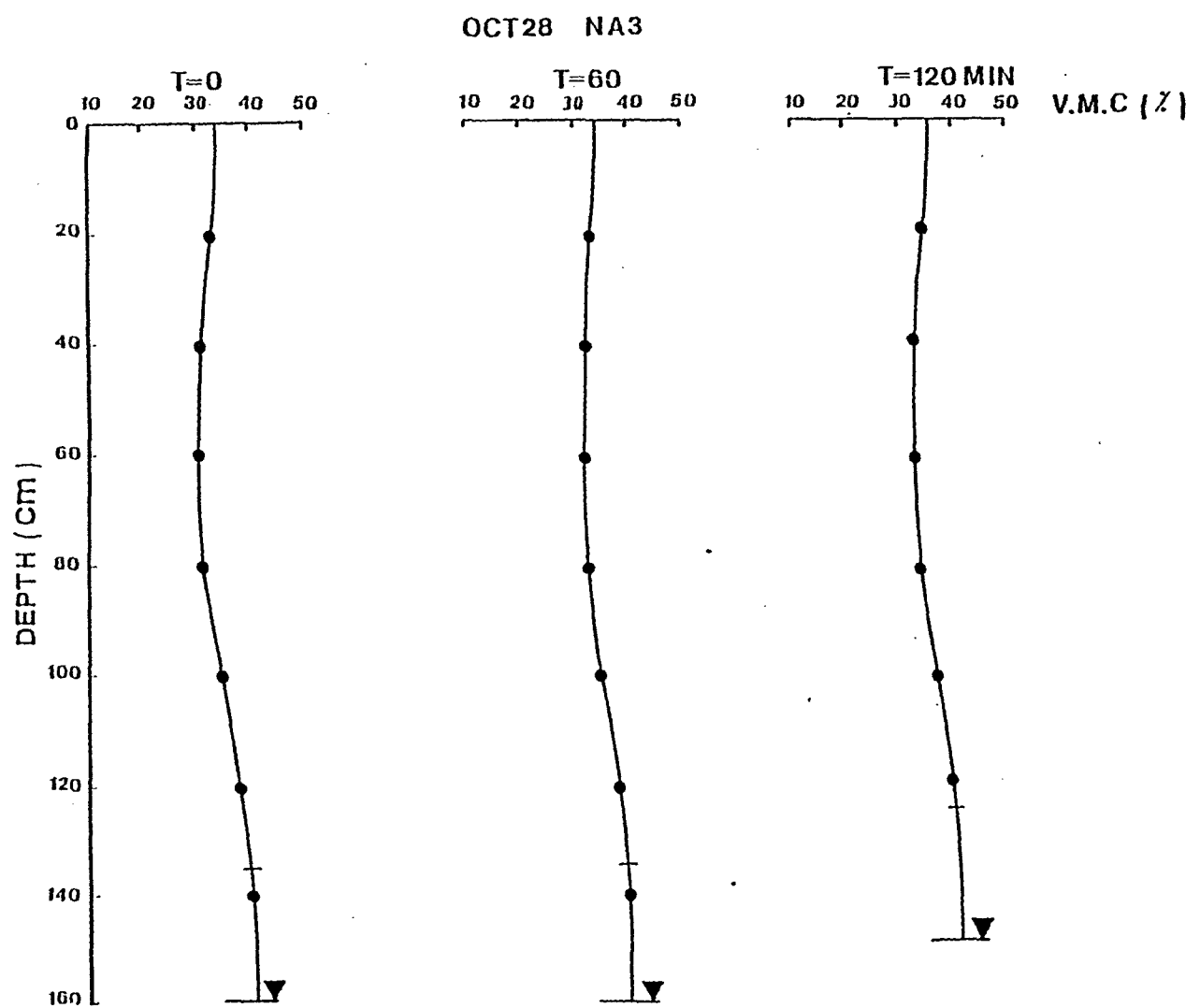


Figure 35 c. October 28,1982 storm event.Relationship of volumetric moisture content with depth.

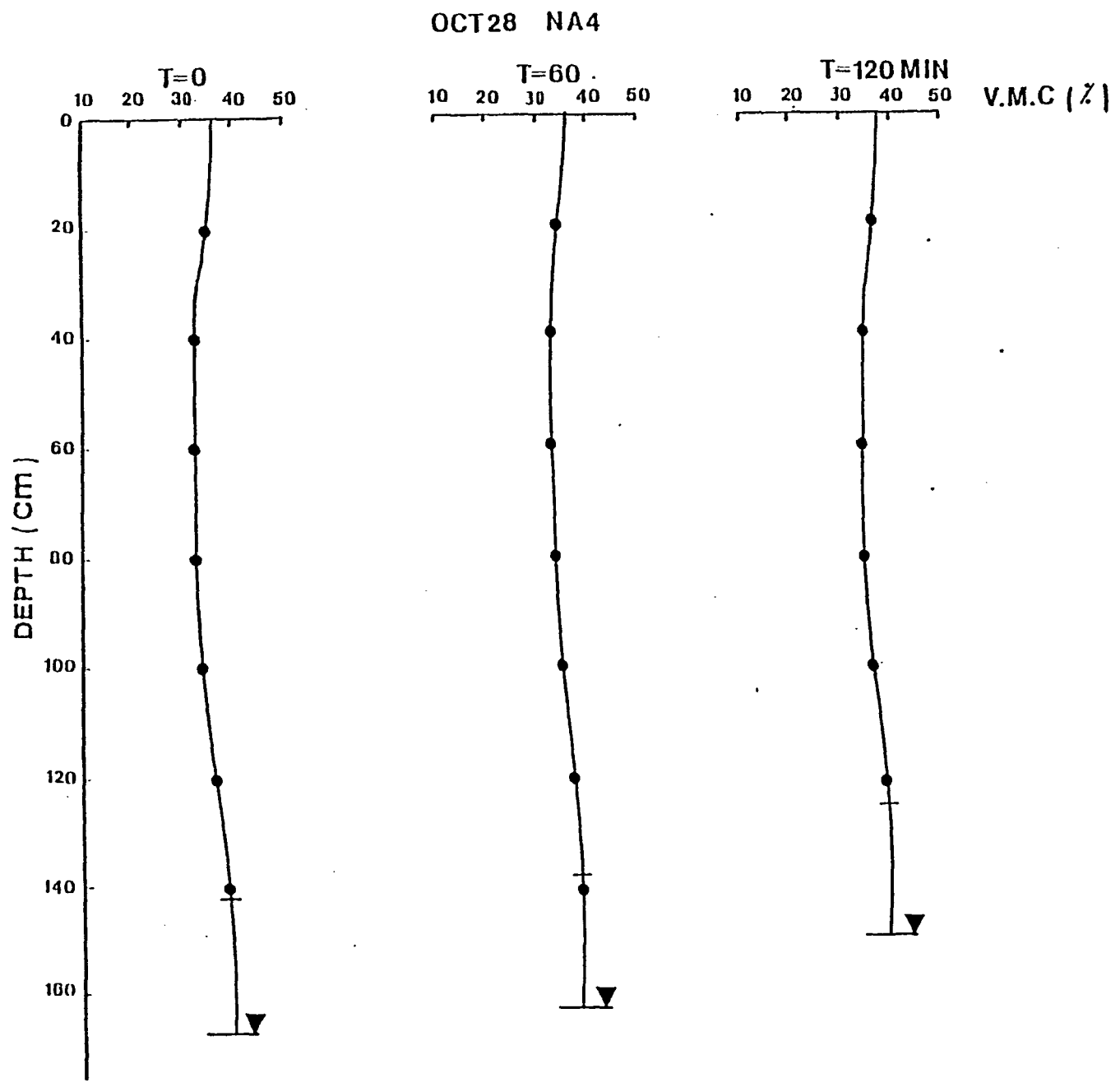


Figure 35d. October 28, 1982 storm event. Relationship of volumetric moisture content with depth.

content (V.M.C.) at the surface ranged from 30% at NA-1 to 36% at NA-4. It gradually increased with depth up to about 38% at the water table (Appendix IV-2).

The first hour of rain had only a slight effect on the V.M.C. in all four locations. The average rise of the V.M.C. in all the tested areas was about 1%. No water level rise was observed in NA-1, NA-2, or NA-3. But in NA-4, a 0.05 m rise was observed. The average height of the capillary fringe prior to the rain was about 0.24 m. After the first hour of rain event in NA-4, where a considerable water level rise was observed, the height of the capillary fringe remained unchanged.

After two hours of rain, the V.M.C. had changed considerably at the ground surface as well as below it. The rise in V.M.C. averaged 3% at the surface. A groundwater level rise was observed in all four locations. The maximum rise, 0.12 m, occurred in NA-4 while the rise in NA-3 was 0.10m. Both NA-1 and NA-2 had a water table rise of about 0.07m.

No significant change in the height of the capillary fringe was observed in all four locations,

c) Tensiometer experiments

The results of the tensiometer readings are illustrated in Figures 36 a-c. The pressure head values are given in Appendix IV-3. Prior to the storm event, the pressure head at the ground surface ranged from -130 cm at TN-1 to -150

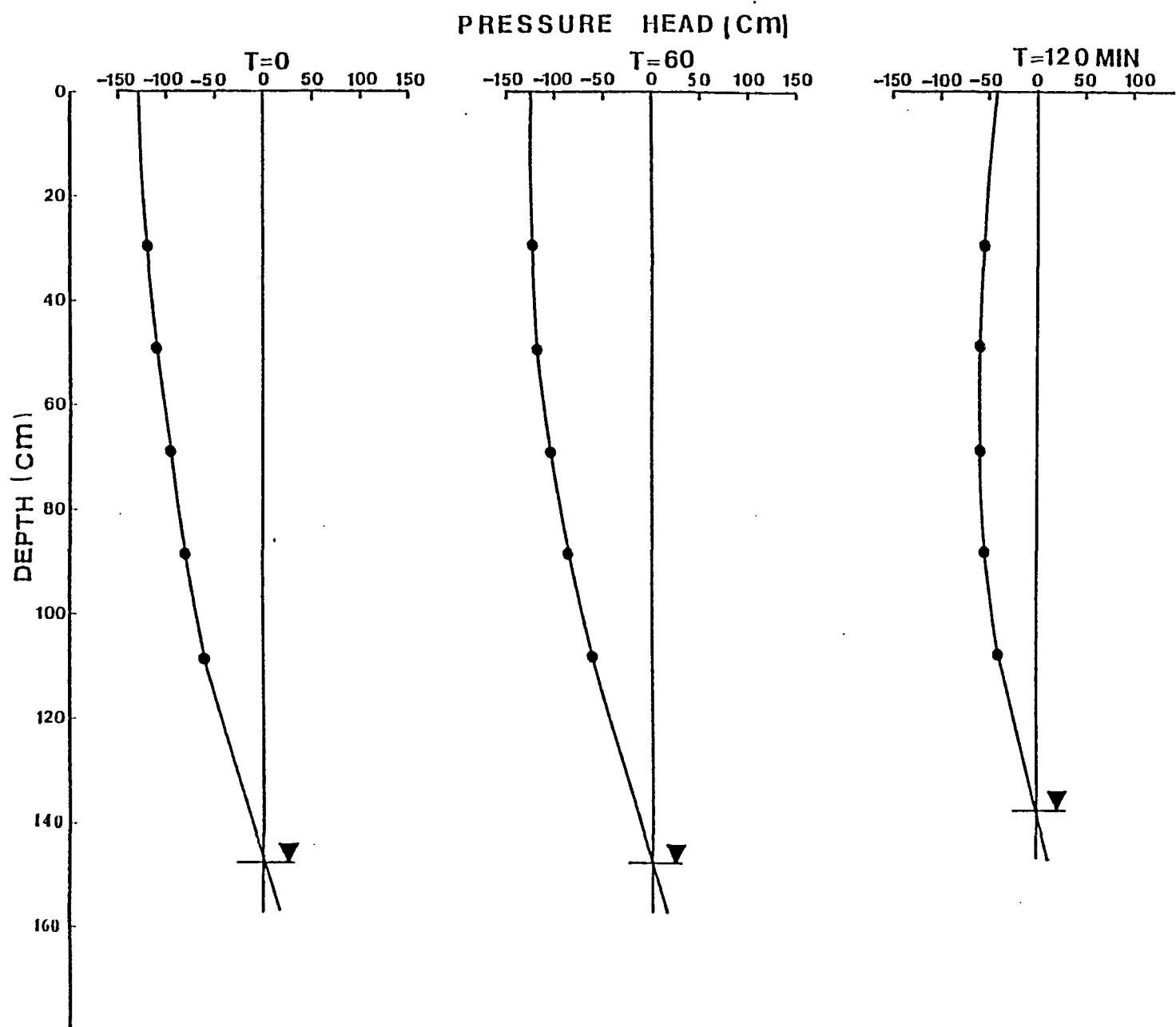


Figure 36a. October 28, 1982 storm event. Relationship of pressure head with depth. (TN1)

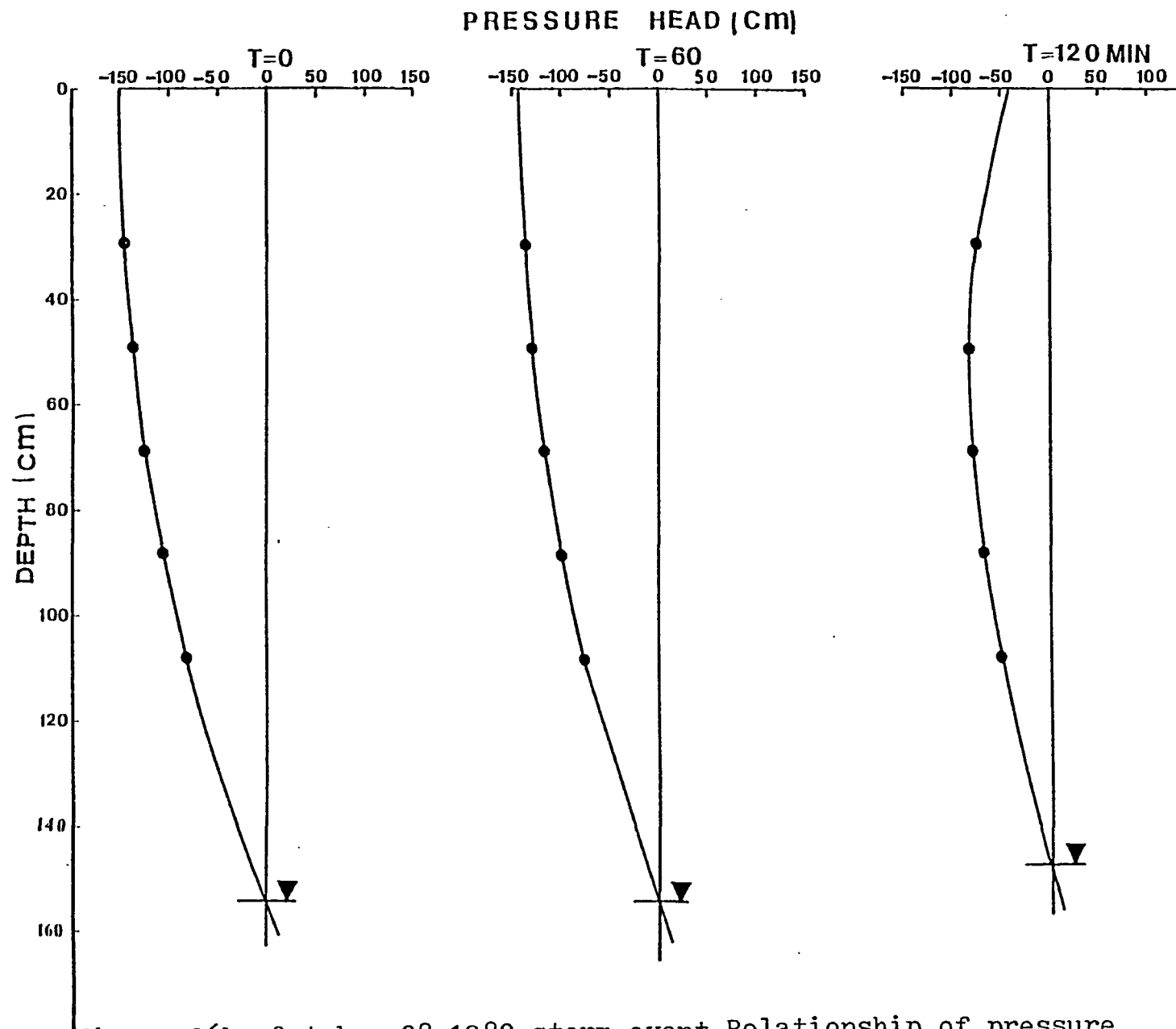


Figure 36b. October 28, 1982 storm event. Relationship of pressure head with depth. (TN2)

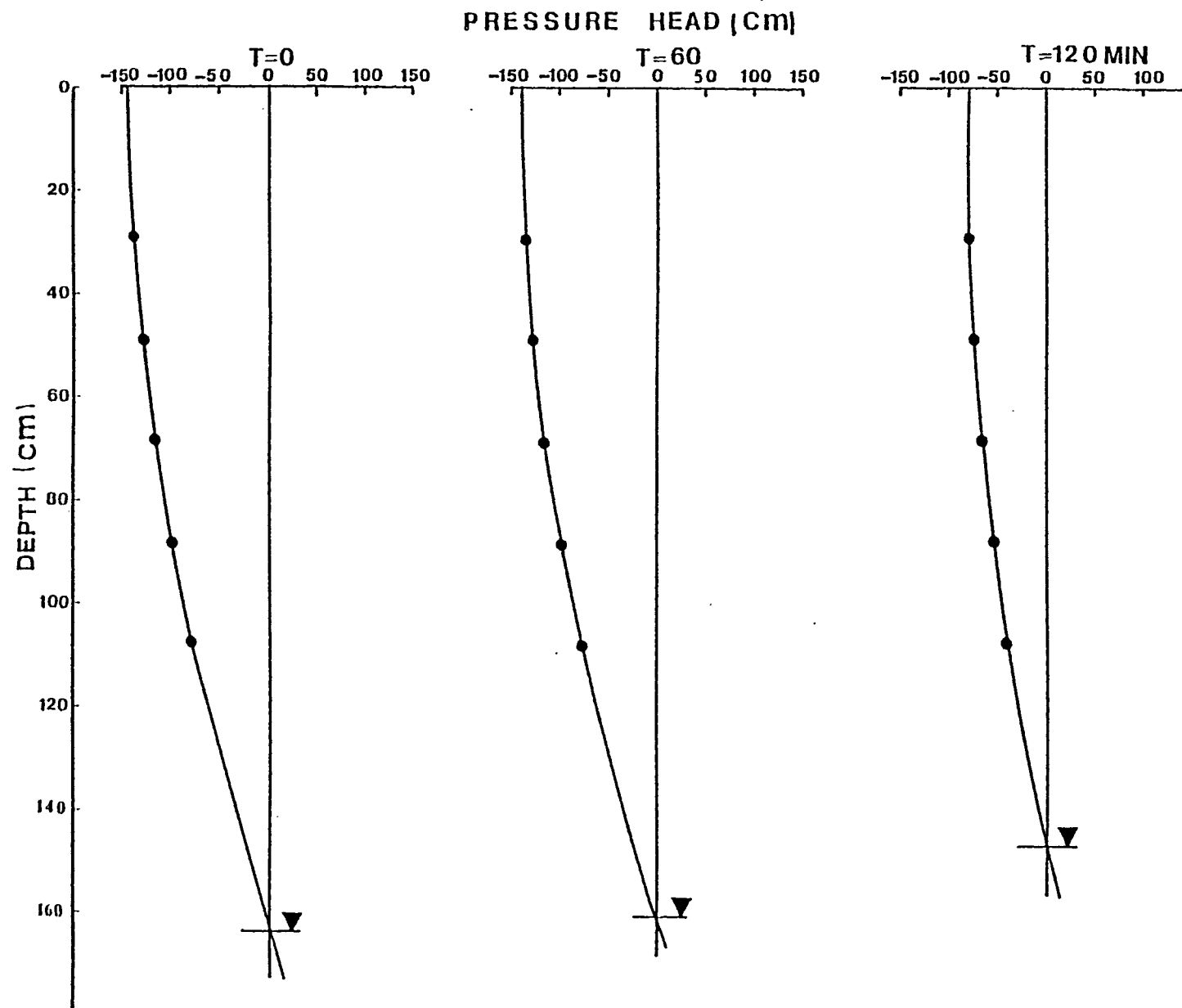


Figure 36c. October 28, 1982 storm event. Relationship of pressure head with depth. (TN4)

cm at TN-2. It gradually increased with depth reaching zero at the water table.

After the first hour of rain, the pressure head at the surface increased by about 5 cm in all three tensiometer nests, but below ground surface no significant change in pressure head was observed. After the first hour a rise in the water table was observed only at TN-4.

The second hour of rain had an apparent effect on the pressure head at and below the ground surface, in all three tested areas. The pressure head increase at the ground surface averaged about 55 cm. At all three tensiometer nests, a considerable water table rise was observed. The maximum rise of 0.12 m occurred at TN-4 while 0.07 m and 0.10 m rises were observed in TN-1 and TN-2 respectively.

Water level rises determined by neutron logging, tensiometer readings and direct observations are summarized in Table 7. The water table rises determined from different methods seem to be fairly consistent.

Table 7, October 28, 1982 storm event. Rise of the water table determined by different methods.

Location.	Distance from the stream(m).	Water table rise(m)					
		Direct observation,		Neutron logging,		Tensiometer observation,	
		t=60min	t=120min	t=60min	t=120min	t=60min	t=120min
W-1	17,5	0	0.07	0	0.07	0	0.07
W-3	11,0	0	0.07	0	0.07	0	0.1
P-20	6,5	0	0.10	0	0.10	-	-
P-23	3.0	0.05	0.14	0.05	0.12	0.04	0.12

5.2.3 October 29, 1982 Storm Event

a) Water table response

Prior to the October 29 storm, the surface soil was still wet from the artificial storm event of the 28th of October. The artificial storm event on the 29th of October lasted 3.5 hours with an average total rainfall of about 40 mm. The flow net before the storm event is given in Figure 37. The water table responses are given in Appendix V-1 and Figures 38 a-c. The percentage rise and decline for each well and piezometer are given in Table 8.

Prior to the storm event, the groundwater table was about 0.47 m below the surface level near the stream, while it was about 1.62 m deep near the road.

After the first hour of rain the water level in P-8 rose 0.1 m resulting a percentage rise of about 20%. In P-5 a 0.05 m rise was observed which is equivalent to a 3% rise. P-1 showed no significant response after the first hour of rain. In P-18, an 18% rise (0.1 m) of the water table was recorded. P-10, which is located furthest from the stream on the same line of instrumentation as P-18, had no response. P-13 showed a 3% (0.05 m) response, while P-11 and P-12 did not respond. Along the No. 3 line of instrumentation, the largest water table response was recorded in P-25, where the rise was 29% (0.1 m). P-20, in which 2% (0.05 m) rise occurred, was the last place on that line where a significant water table response was recorded. Figure 39 shows the responses of near-stream piezometers and

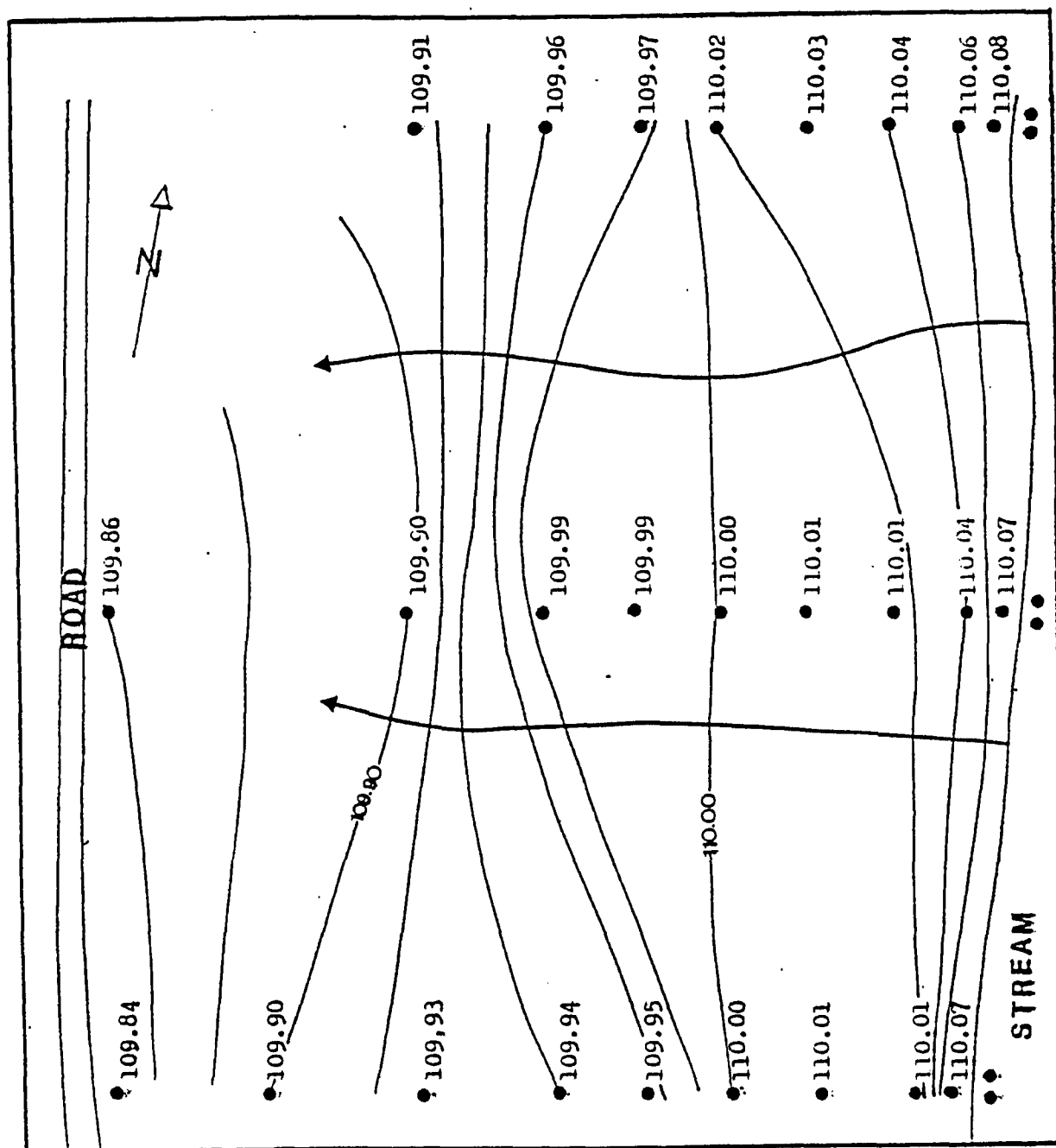


Figure 37. October 29, 1982 storm event. Flow net before the storm event.
Contour interval 0.02m

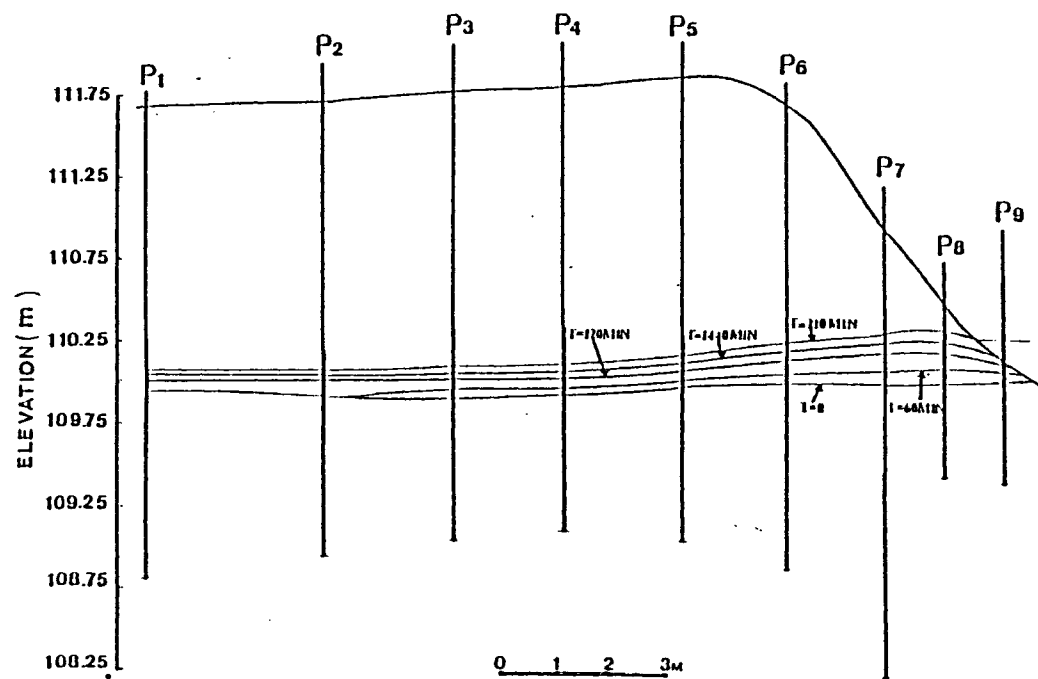


Figure 38a. October 29, 1982 storm event. Cross section 1 showing water table response during the storm event.

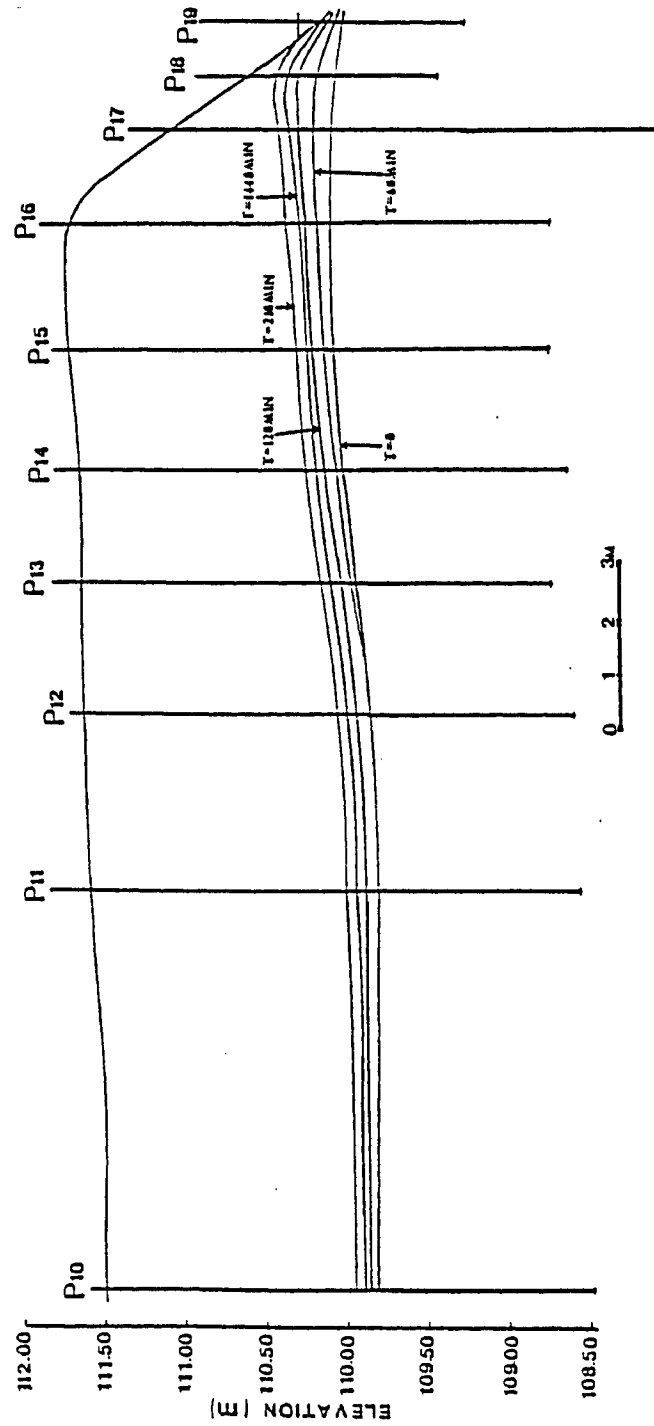


Figure 38b. October 29, 1982 storm event. Cross section 2 showing water table response during the storm event.

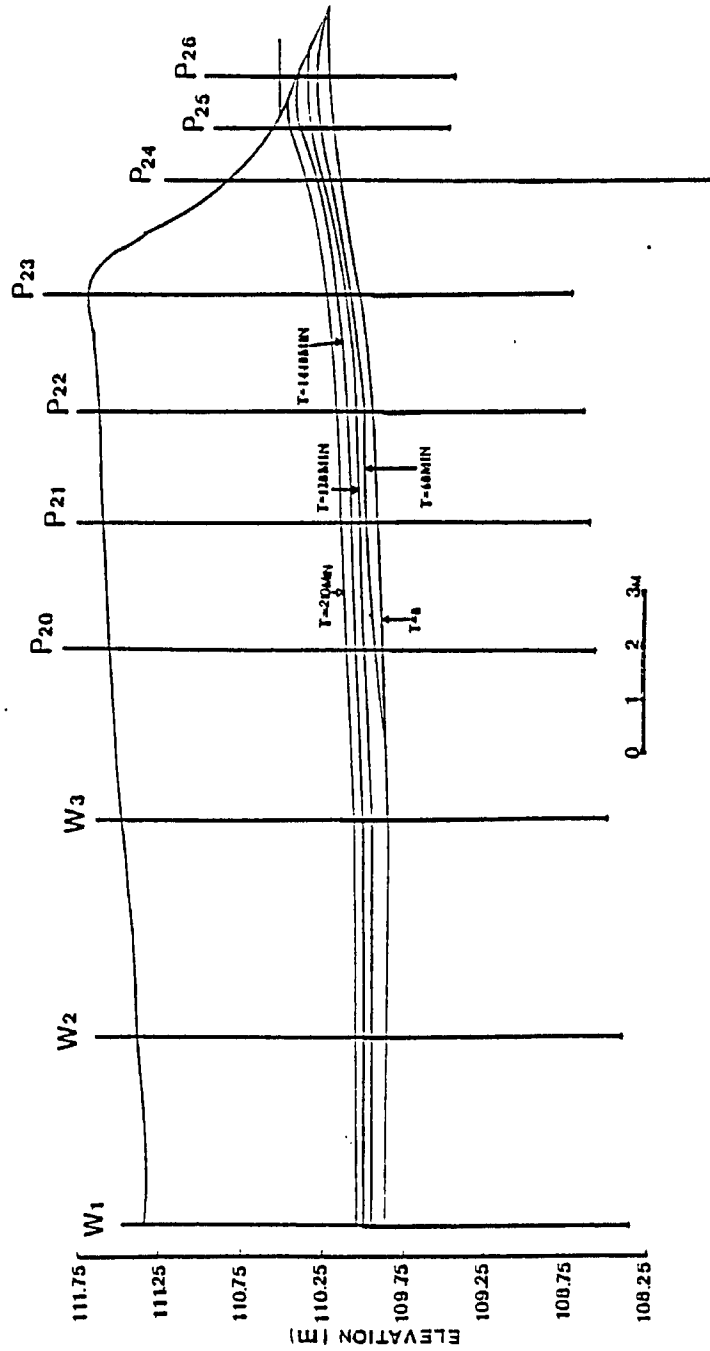


Figure 38c. October 29, 1982 storm event. Cross section 3 showing water table response during the storm event.

Table 8 . October 29,1982 storm event.Percentage rise/
decline of the water table.

Well/piezometer.	Percentage rise(%).			Percentage decline(%)
	t=60min.	t=120min.	t=210min.	t=1440min.
P-1	0	2.9	7.4	1.8
P-2	0	4.4	8.3	1.2
P-3	1.1	3.8	8.2	1.8
P-4	2.7	6.4	10.6	1.8
P-5	2.6	5.3	10.5	2.9
P-6	2.9	7.0	12.8	3.3
P-7	7.2	20.6	30.9	7.5
P-8	20.0	40.0	70.0	66.6
P-9	0	11.8	17.6	11.1
P-10	0	2.4	7.2	3.2
P-11	0	4.0	11.3	5.1
P-12	0	4.6	10.3	3.2
P-13	2.9	4.7	10.6	2.6
P-14	3.1	6.2	13.6	5.0
P-15	3.0	6.1	13.9	3.5
P-16	4.3	9.3	16.7	3.7
P-17	10.3	20.6	33.0	10.8
P-18	17.5	38.6	64.9	35.0
P-19	0	11.8	17.6	10.0
P-20	1.8	6.1	13.9	16.7
P-21	3.0	6.1	10.9	2.0
P-22	3.0	5.4	13.3	9.1
P-23	3.1	6.3	12.5	5.0

Table 8 cont'd

P-24	8.1	16.1	32.2	11.9
P-25	28.6	42.9	80.0	14.2
P-26	0	11.8	17.6	5.0
W-1	0	5.5	10.3	1.5
W-2	0	4.8	11.6	3.8
W-3	0	4.5	9.9	0.7

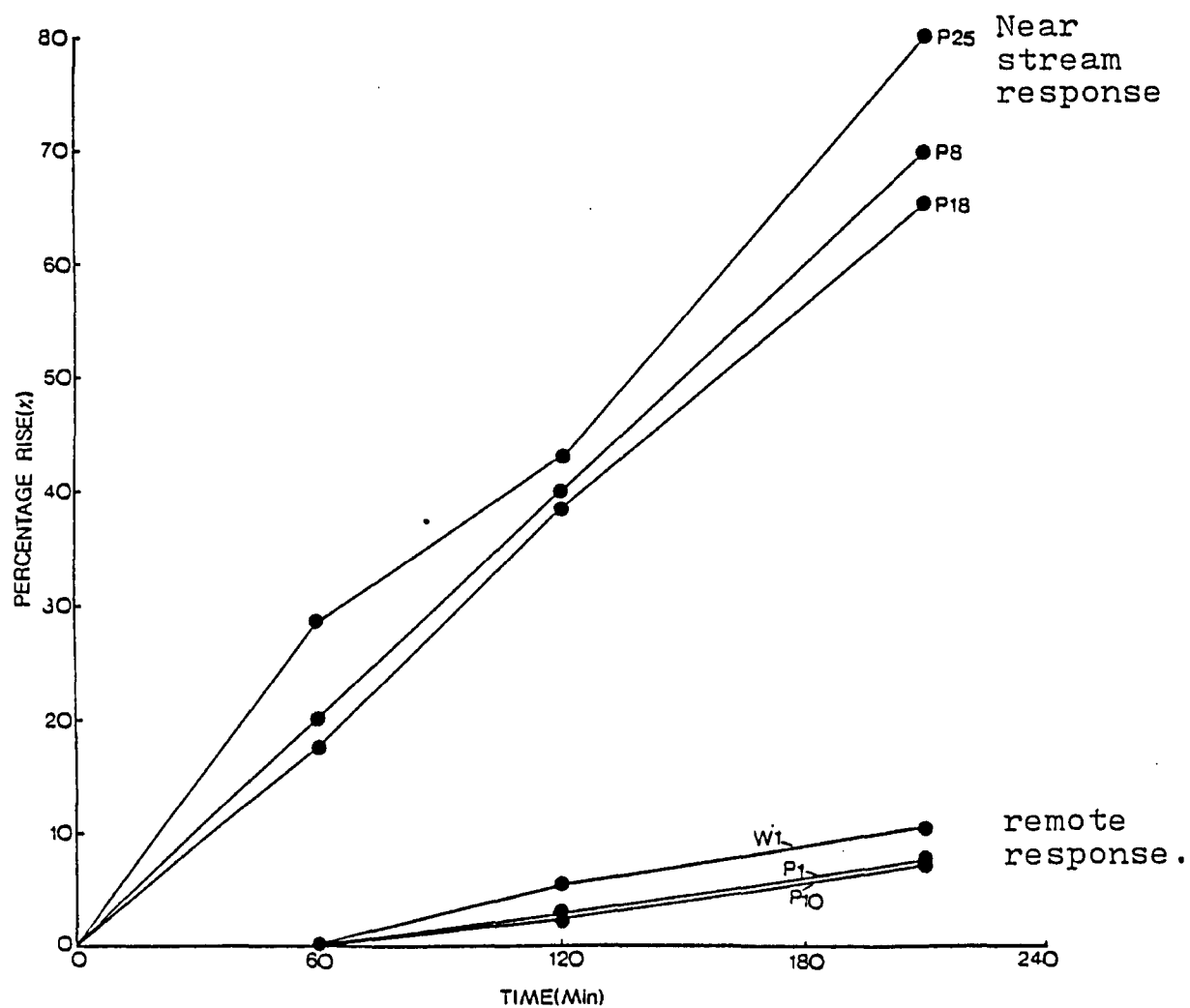


Figure 39. October 29, 1982 storm event. Groundwater table response in selected wells and piezometers.

piezometers remote from the stream, to the storm event. No change in the stream level was observed in P-9, P-19, and P-26.

After two hours of rain, a water table rise was observed throughout the plot. The highest recorded response was closest to the stream. In P-8, P-18, and P-25, the rises were 40% (0.2 m), 39% (0.22 m) and 43% (0.25 m). The groundwater level in P-1 and P-10 rose 3% (0.05 m) and 2% (0.04 m) respectively. The stream level rose in P-9, P-19 and P-26 by 0.02 m.

After 3.5 hours of rain, a significant water table rise was observed throughout the plot. In P-3, P-18, and P-25, the rises were 70% (0.35 m), 65% (0.37 m) and 80% (0.28 m). The groundwater level in P-1 and P-10 rose 7% (0.05 m). The stream level rose in P-9, P-19, and P-26 by 0.03 m.

After 3.5 hours, the rain was terminated. Measurements taken 24 hours later show a general decline in water level throughout the plot. The decline along the stream was far greater than in other parts of the plot. The average decline along the stream was about 39% (0.08 m), while it was 2% (0.03 m) closer to the road.

b) Neutron logging

Results of the neutron logging are presented in Figures 40 a-d. Prior to the storm event the volumetric moisture content (V.M.C.) at the surface ranged from 31% at NA-1 to 34% at NA-3. It gradually increased with depth up to about

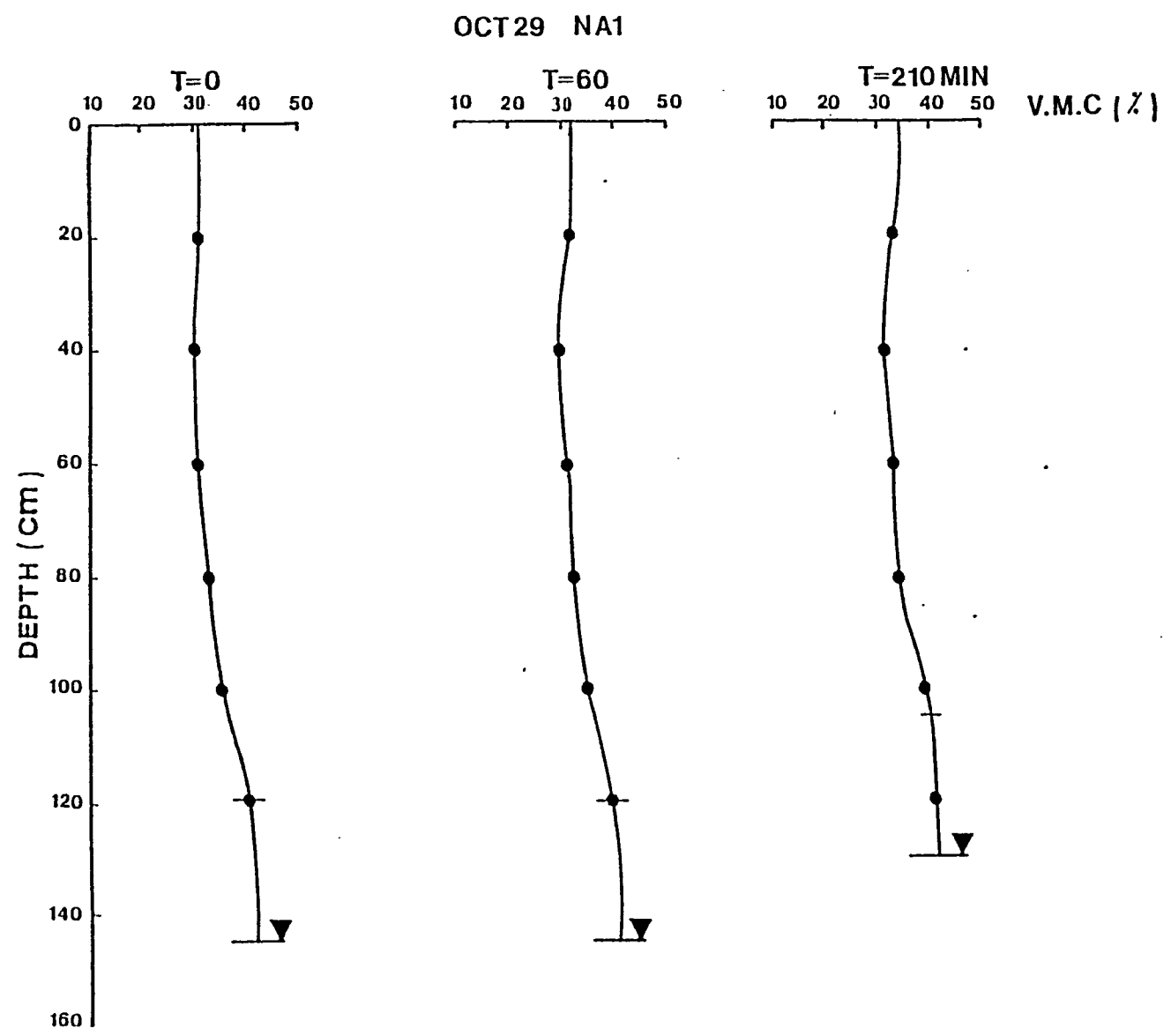


Figure 40a. October 29, 1982 storm event. Relationship of volumetric moisture content with depth.

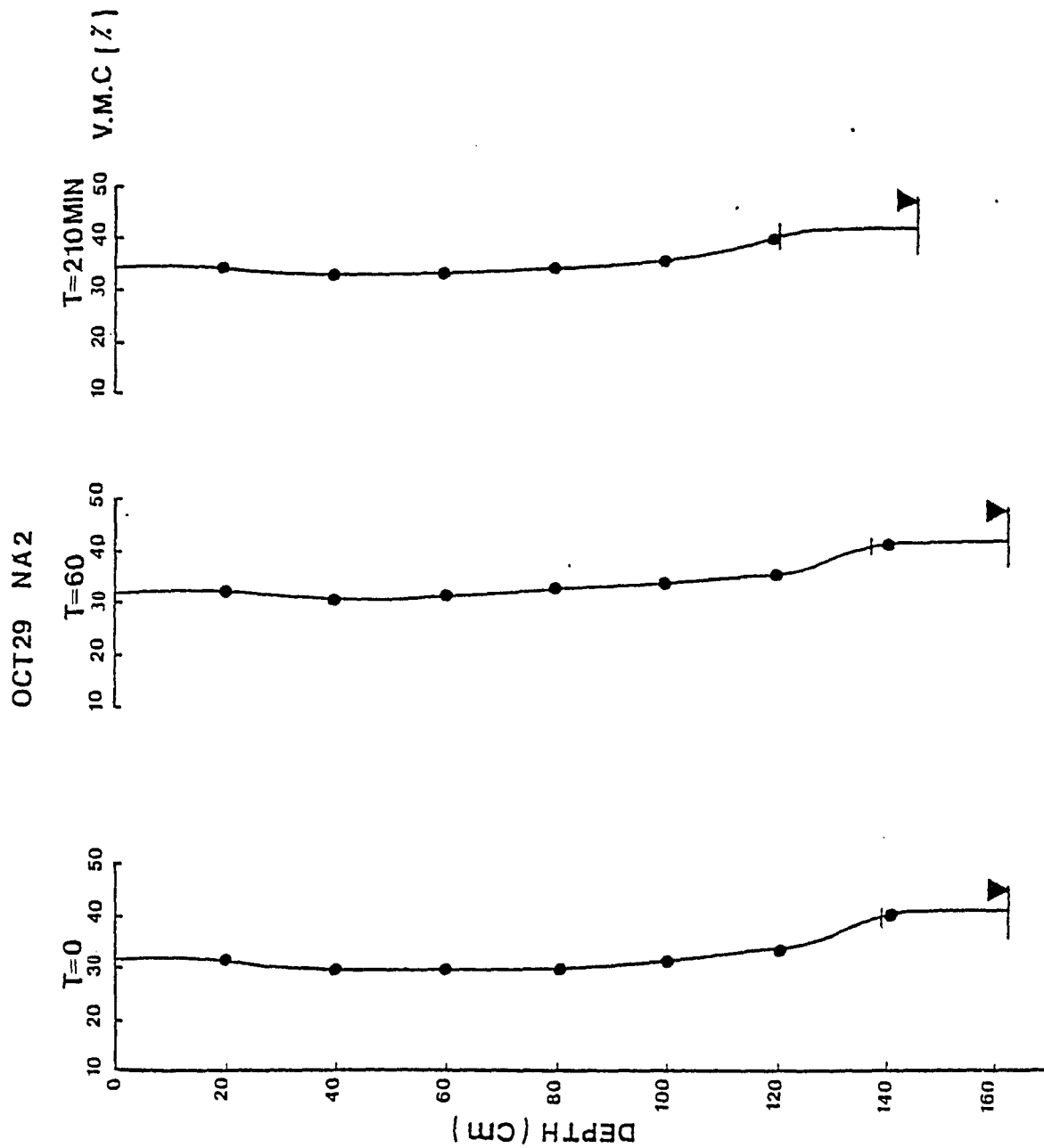


Figure 40b. October 29, 1982 storm event. Relationship of volumetric moisture content with depth.

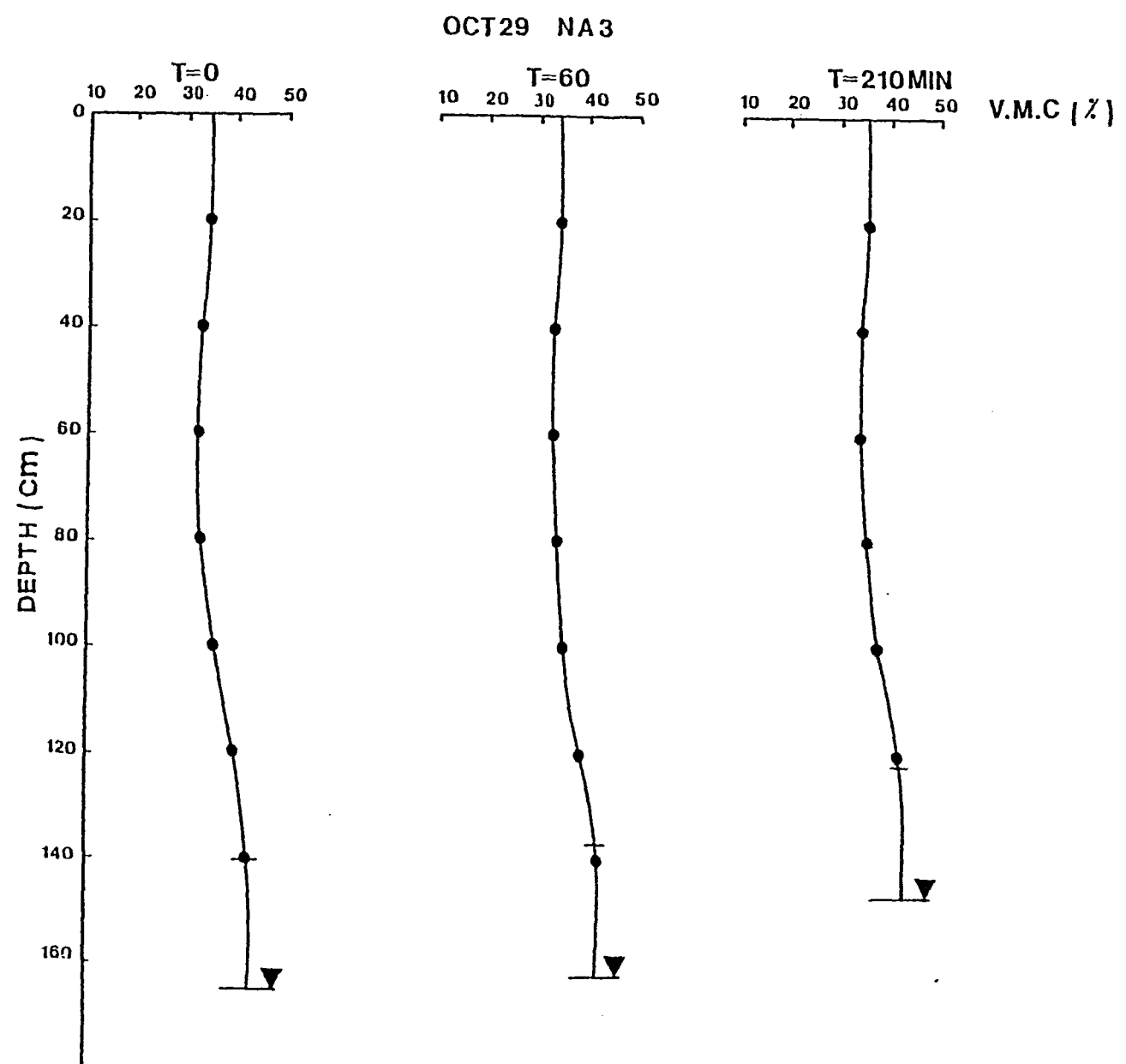


Figure 40c. October 29, 1982 storm event. Relationship of volumetric moisture content with depth.

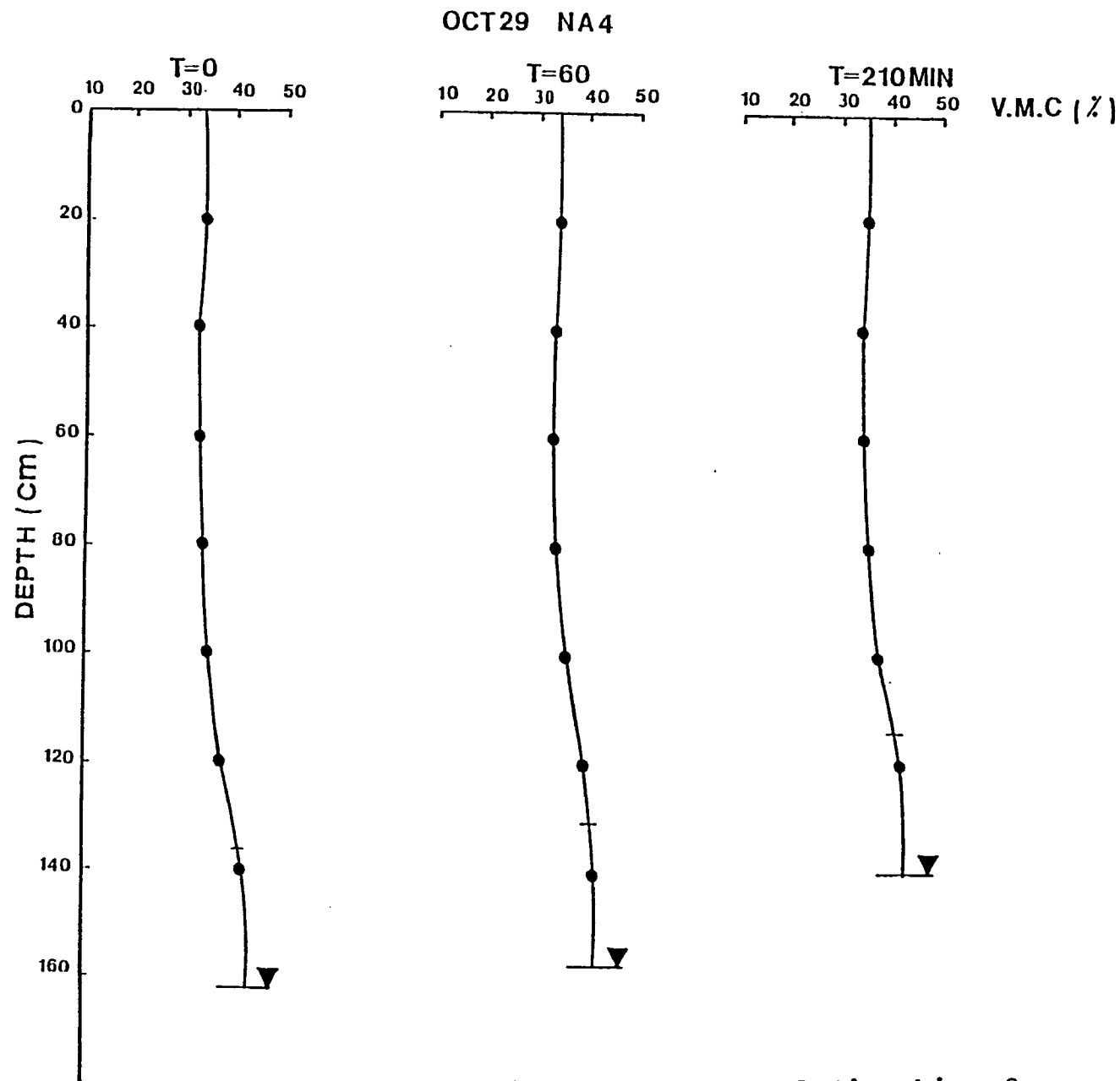


Figure 40d. October 29, 1982 storm event. Relationship of volumetric moisture content with depth.

39% at the water table (Appendix V-2).

The first hour of rain had only a slight effect on the V.M.C. in all four locations. The average rise of the V.M.C. in all tested areas was about 1% at the ground surface. No water level rise was observed in NA-1 and NA-2, but in NA-3 and NA-4, 0.03 m and 0.05 m rises were observed. The average height of the capillary fringe prior to the rain was about 0.25 m. After the first hour of rain, even in NA-3 and NA-4 where a considerable water level rise was observed, the height of the capillary fringe remained unchanged.

After 3.5 hours of rain, the V.M.C. had changed considerably at the ground surface as well as below it. The rise in V.M.C. averaged 2% at the surface. A groundwater level rise was observed in all four locations, a maximum rise of 0.17 m occurred at NA-4 and a 0.15 m rise at NA-1. Both NA-2 and NA-3 had a water table rise of about 0.16 m.

No significant change in the height of the capillary fringe was observed in all four locations.

c) Tensiometer experiments

The results of the tensiometer readings are illustrated in Figures 41 a-c. The pressure head values are given in Appendix V-3. Prior to the storm event the pressure head at the ground surface ranged from -30 cm at TN-1 to -60 cm at TN-2. It gradually increased with depth reaching zero at the water table.

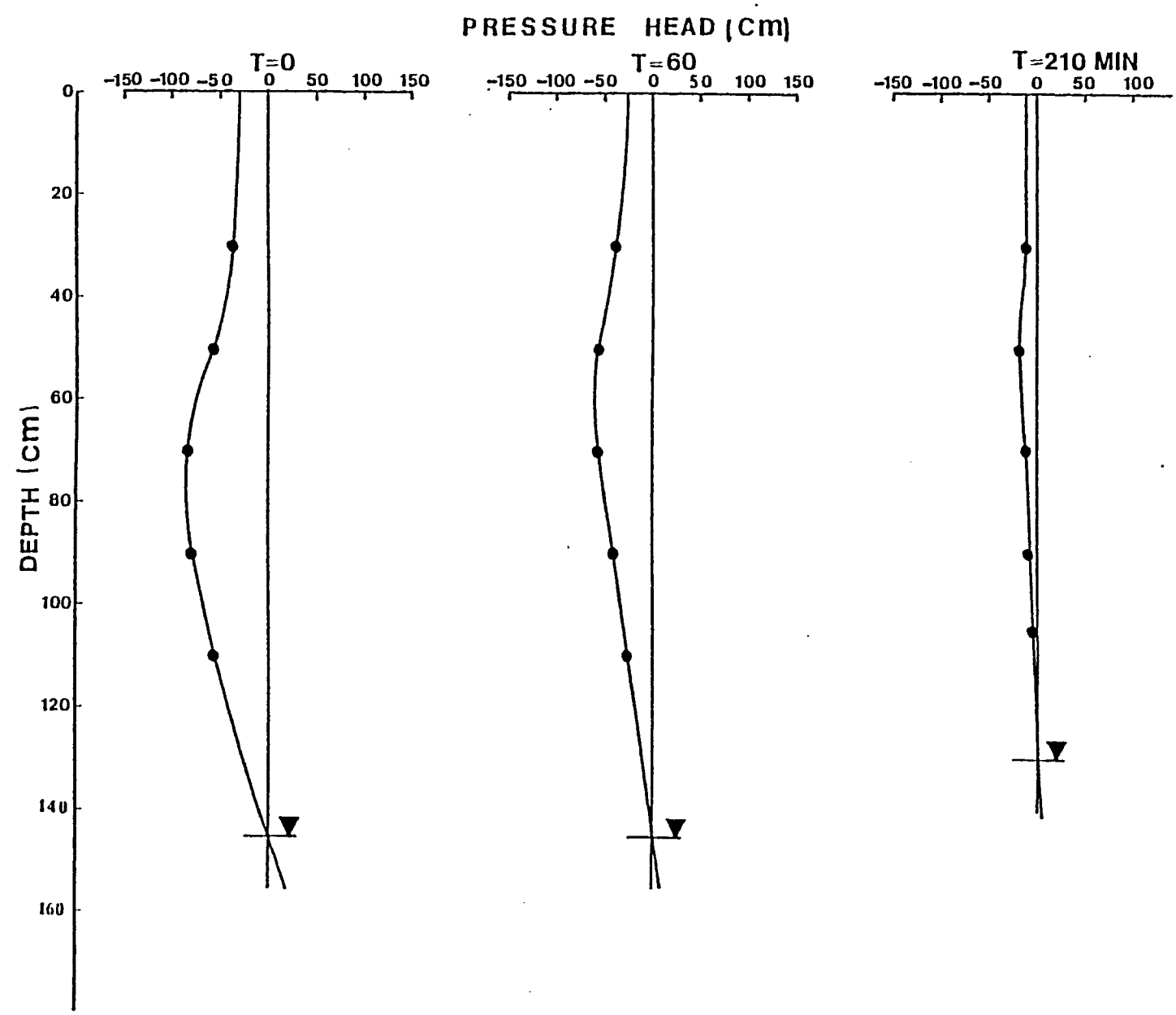


Figure 41a. October 29, 1982 storm event. Relationship of pressure head with depth. (TN1)

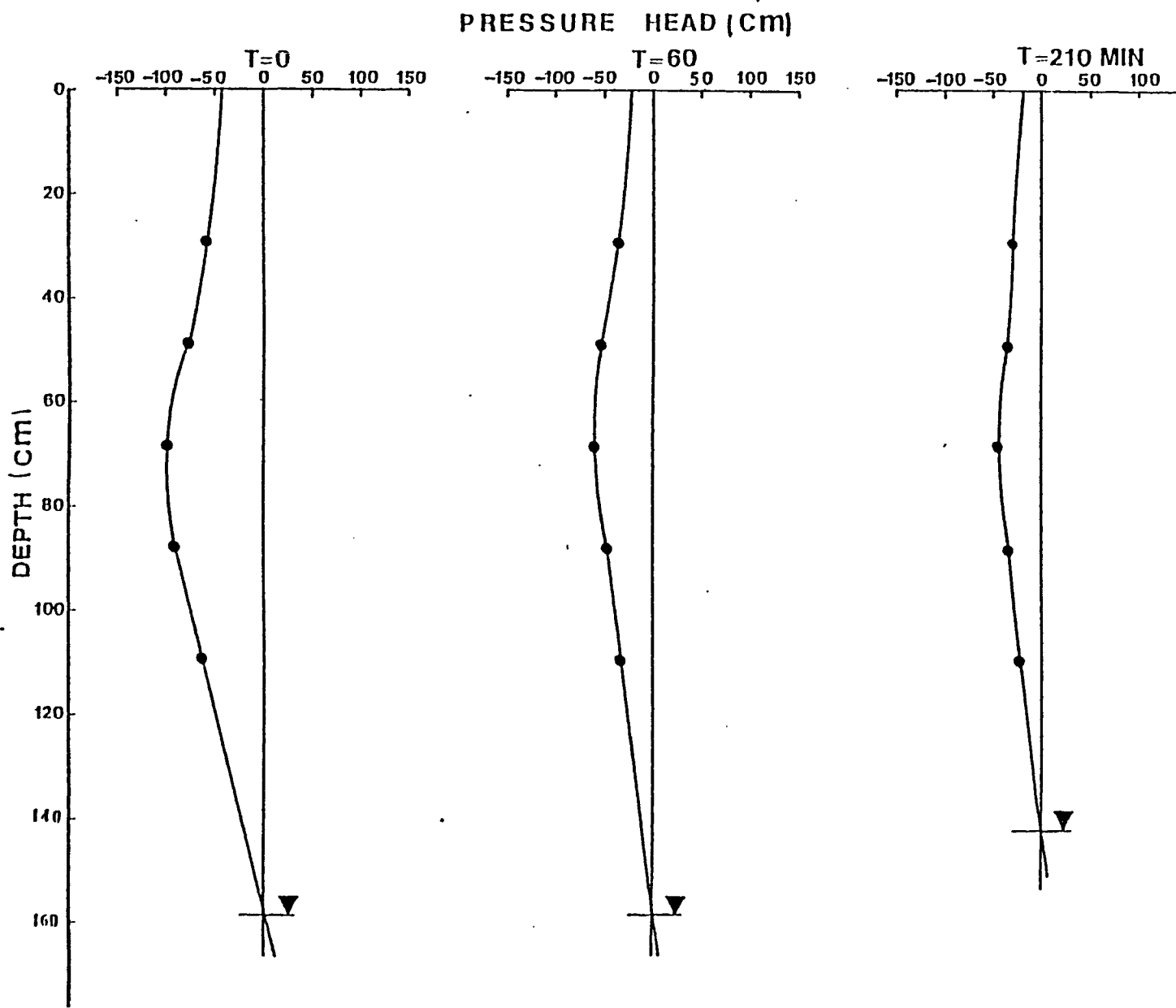


Figure 41b. October 29, 1982 storm event. Relationship of pressure head with depth. (TN2)

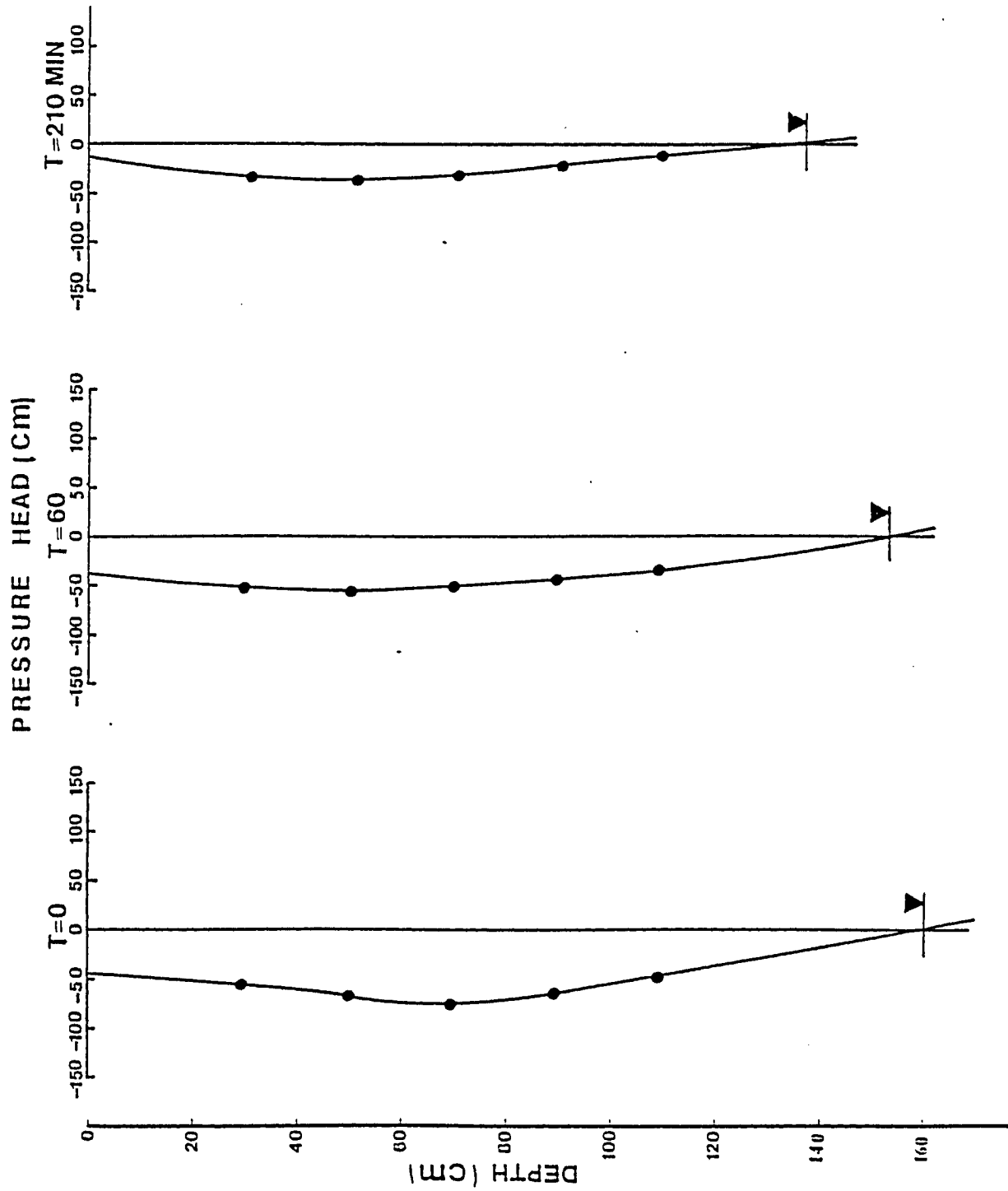


Figure 41c. October 29, 1982 storm event. Relationship of pressure head with depth. (TN4).

After the first hour of rain, the pressure head at the surface increased by about 12 cm in all three tensiometer nests; but below ground surface, no significant change in pressure head was observed. After the first hour, a rise in the water table was observed only at TN-4.

Rain in the next 2.5 hours affected the pressure head at and below the ground surface in all three tested areas. The pressure head increase at the ground surface averaged about 28 cm. At all three tensiometer nests, a considerable water table rise was observed. The maximum rise of 0.17 m occurred at TN-4, while 0.15 m and 0.16 m rise was observed in TN-1 and TN-2, respectively.

Water level rises determined by neutron logging, tensiometer readings, and direct observations are tabulated in Table 9. The water table levels determined from the different methods seem to be fairly compatible.

5.2.4 November 1 and 2, 1982 Storm Event

a) Water table response

A natural storm event which involved about 100 mm of rain occurred on the 1st and 2nd of November. The flow net on the 2nd of November is given in Figure 42. The water table responses are given in Appendix VI-1 and Figures 43 a-c. On the 2nd of November, the water table had risen so high that it emerged on the ground surface close to the stream. The depth to the water table was about 0.75 m near the road.

Table 9, October 29, 1982 storm event. Rise of the water table determined by different methods.

Location.	Distance from the stream(m).	Water table rise(m)					
		Direct observation.		Neutron logging.		Tensiometer observation.	
		t=60min	t=210min	t=60min	t=210min	t=60min	t=210min
W-1	17.5	0	0.15	0	0.15	0	0.15
W-3	11.0	0	0.16	0	0.16	0	0.16
P-20	6.5	0.03	0.23	0.03	0.16	-	-
P-23	3.0	0.05	0.20	0.05	0.17	0.05	0.17

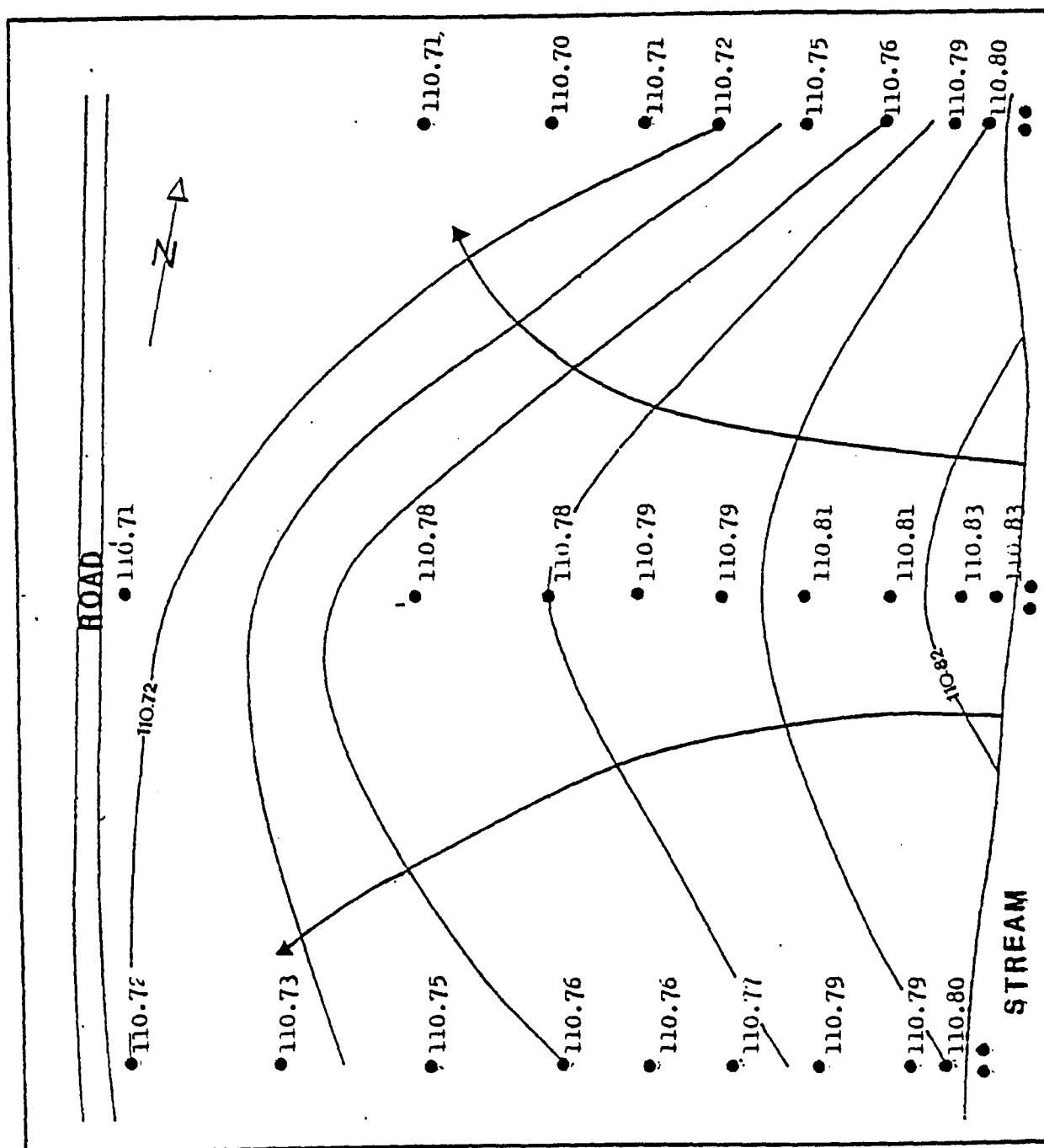


Figure 42. November 1 and 2 storm event. Flow net after the storm event. Contour interval 0.02m

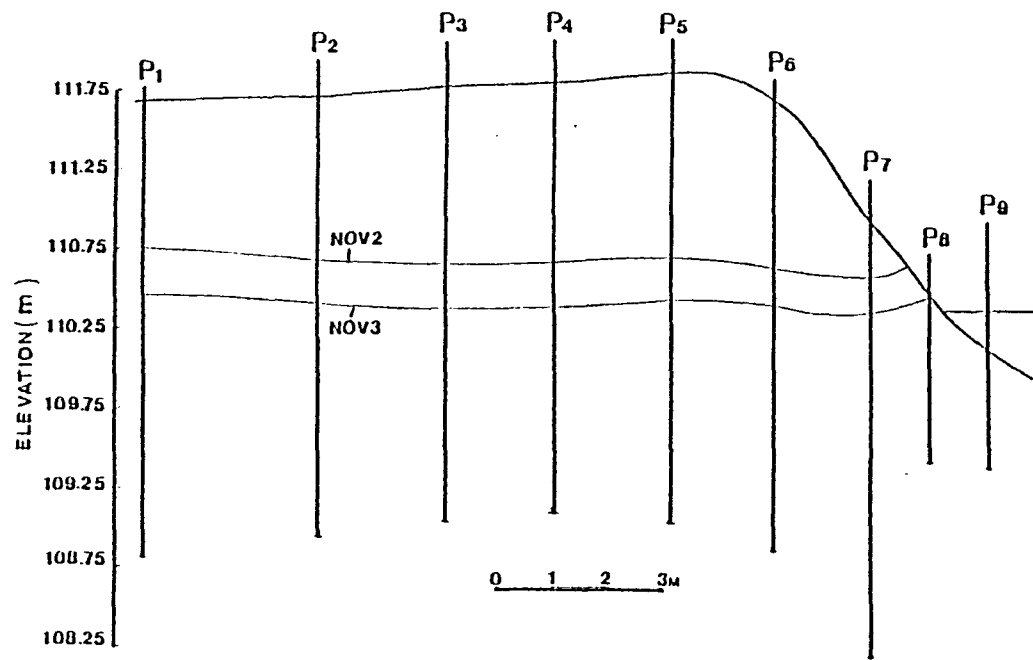


Figure 43a. November 1 and 2 storm event. Cross section 1 showing water table response.

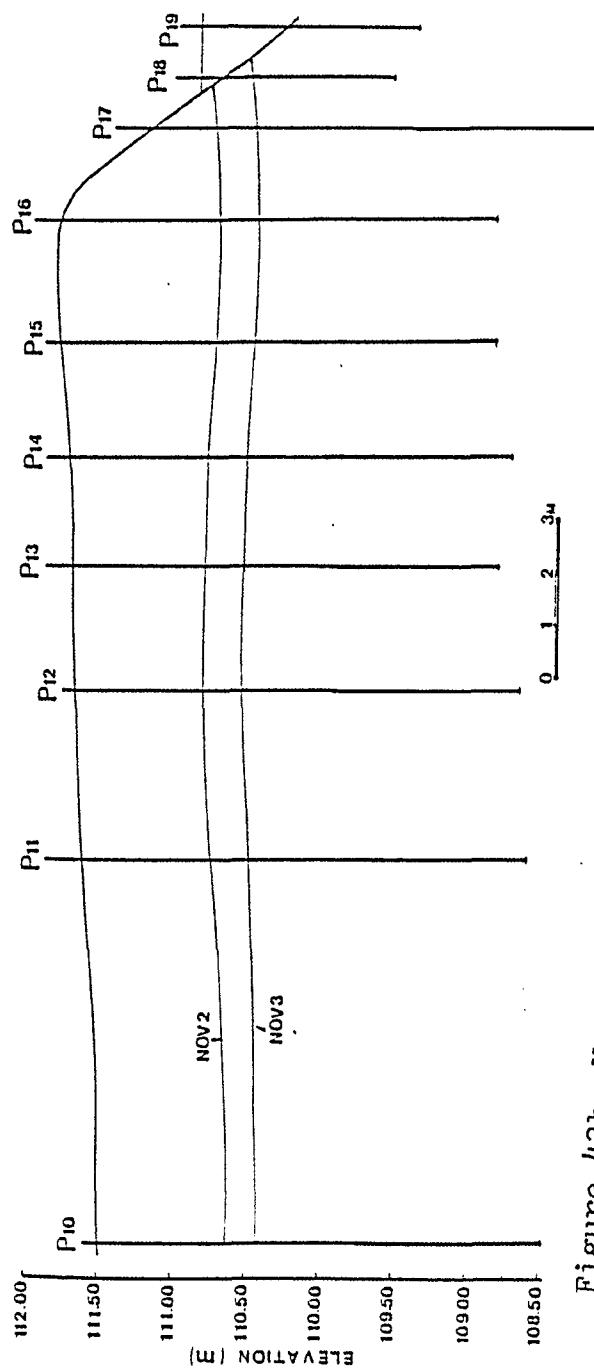


Figure 43b. November 1 and 2 storm event. Cross section 2 showing water table response.

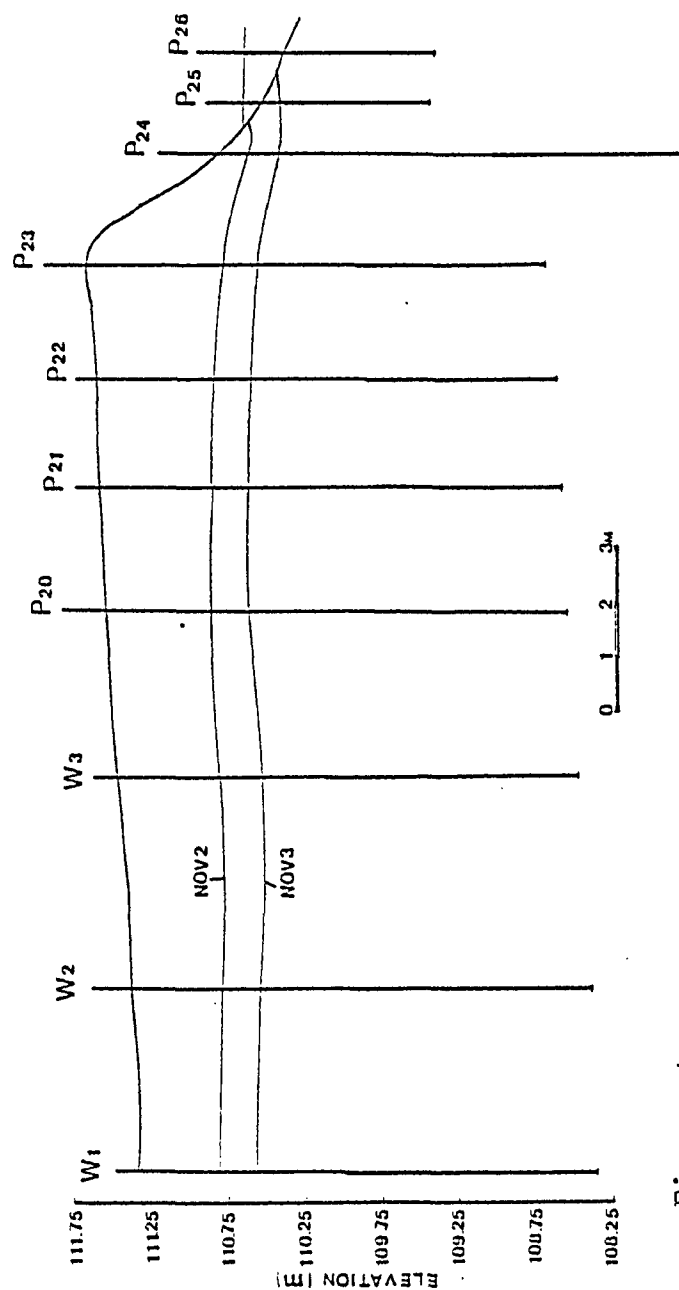


Figure 43c. November 1 and 2 storm event. Cross section 3 showing water table response.

Readings taken on the 3rd of November show a general decline in water level throughout the plot. The average decline of the water table near the stream was about 71% (0.30 m), while it was about 39% (0.29 m) at the road.

b) Tensiometer experiments

The interpretation of tensiometer experiment data is illustrated in Figure 44. The pressure head values are given in Appendix VI-2. On the 2nd of November the pressure head had risen to near saturated level at the ground surface. The pressure head at TN-1 was -5 cm, while it was -10 cm and -25 cm at TN-2 and TN-4, respectively. First a slight decrease and then an increase of the pressure head with depth was observed. Depth to the water table ranged from 52 cm at TN-1 to 85 cm at TN-4.

On the 3rd of November, the pressure head ranged from -20 cm at TN-1 to -80 cm at TN-4. At all three tensiometer nests, a considerable water table decline was observed. The maximum decline, 0.25 m, occurred at TN-2, while 0.19 and 0.22 m declines were observed in TN-1 and TN-4, respectively. The fall in the water table determined by different methods are given in Table 10. The water table decline determined from different methods seems to be compatible.

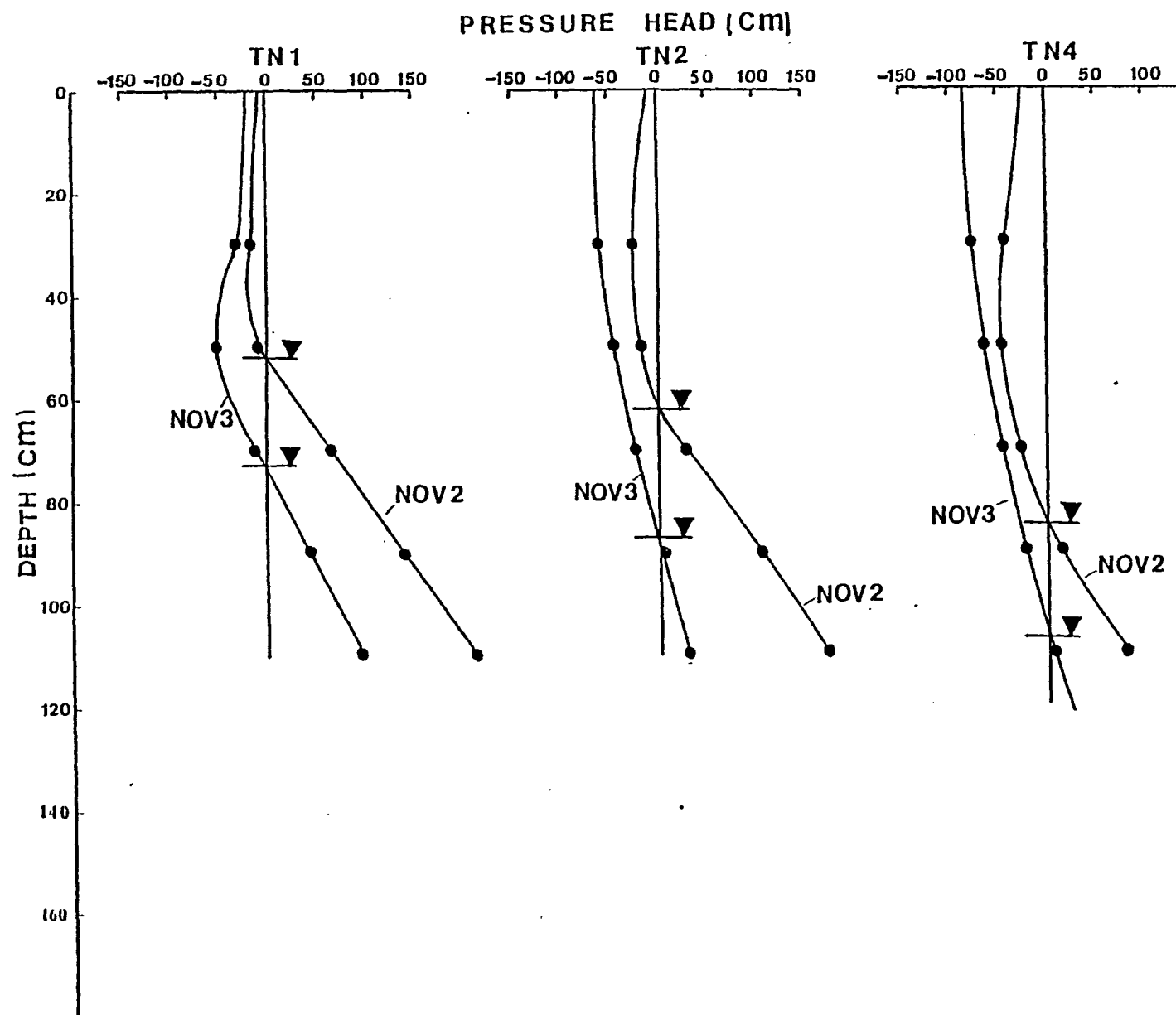


Figure 44. November 1 and 2 storm event. Relationship of pressure head with depth.

Table 10, November 1,2,1982 storm event, Decline of the water table determined by different methods.

Location.	Distance from the stream(m)	Water table rise(m)	
		Direct observation.	Tensiometer observation
W-1	17.5	0.17	0.19
W-3	11.0	0.25	0.25
P-20	6.5	0.35	-
P-23	3.0	0.22	0.22

5.3 Tracer Experiment

The objective of the tracer experiment in this study was to observe how groundwater ridging affects solute transport during storm events. This test simulates the effect of contamination spills near a stream. Ideally, the tracer should move in two directions from the groundwater ridge.

Electrical conductivity and chloride concentration values determined from water samples are tabulated in Appendix VII-1 and 2, respectively. Both electrical conductivity and chloride concentration values were plotted to study the migration of the tracer (Figure 45 a-c). A statistical analysis was carried out on 93 samples to determine the correlation between the chloride ion concentration and electrical conductivity values. Since the determined correlation coefficient was 0.98, it was decided to study the migration of the tracer on the basis of the electrical conductivity alone.

An electrical resistivity profiling survey was carried out to cross-check the earlier observations. The results of the survey are tabulated in Appendix VII-3 and plotted in Figure 46. Both the resistivity profiling survey and the water sample analyses show that the tracer generally moved in the direction of the natural water flow.

Two major problems contributed to difficulties in the tracer experiments. The number of observation wells was probably not adequate to monitor the migration of

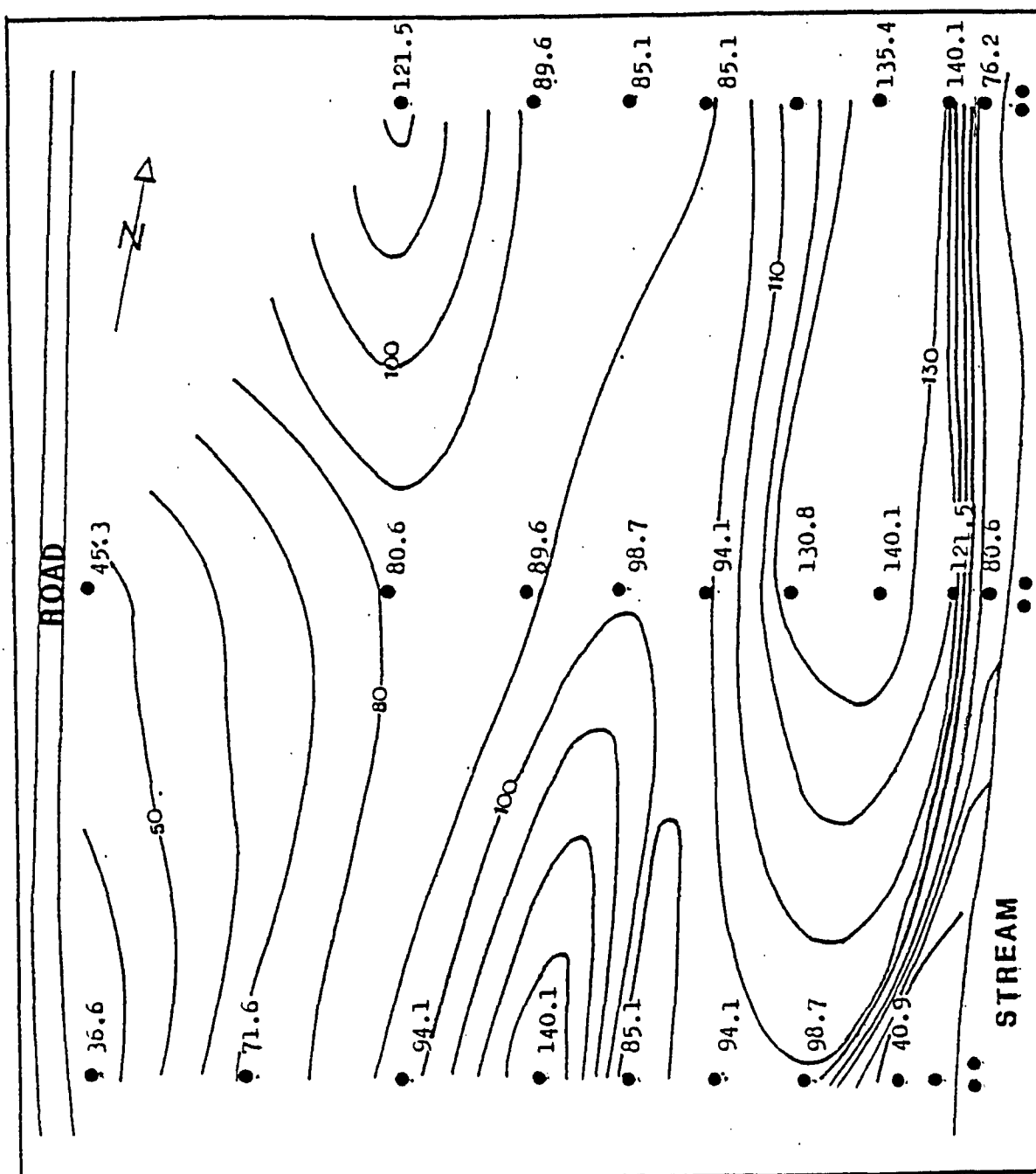


Figure 45a. Migration of the tracer based on the chemical analyses. (November 5, 1982.)
Contour interval 10 ppm.

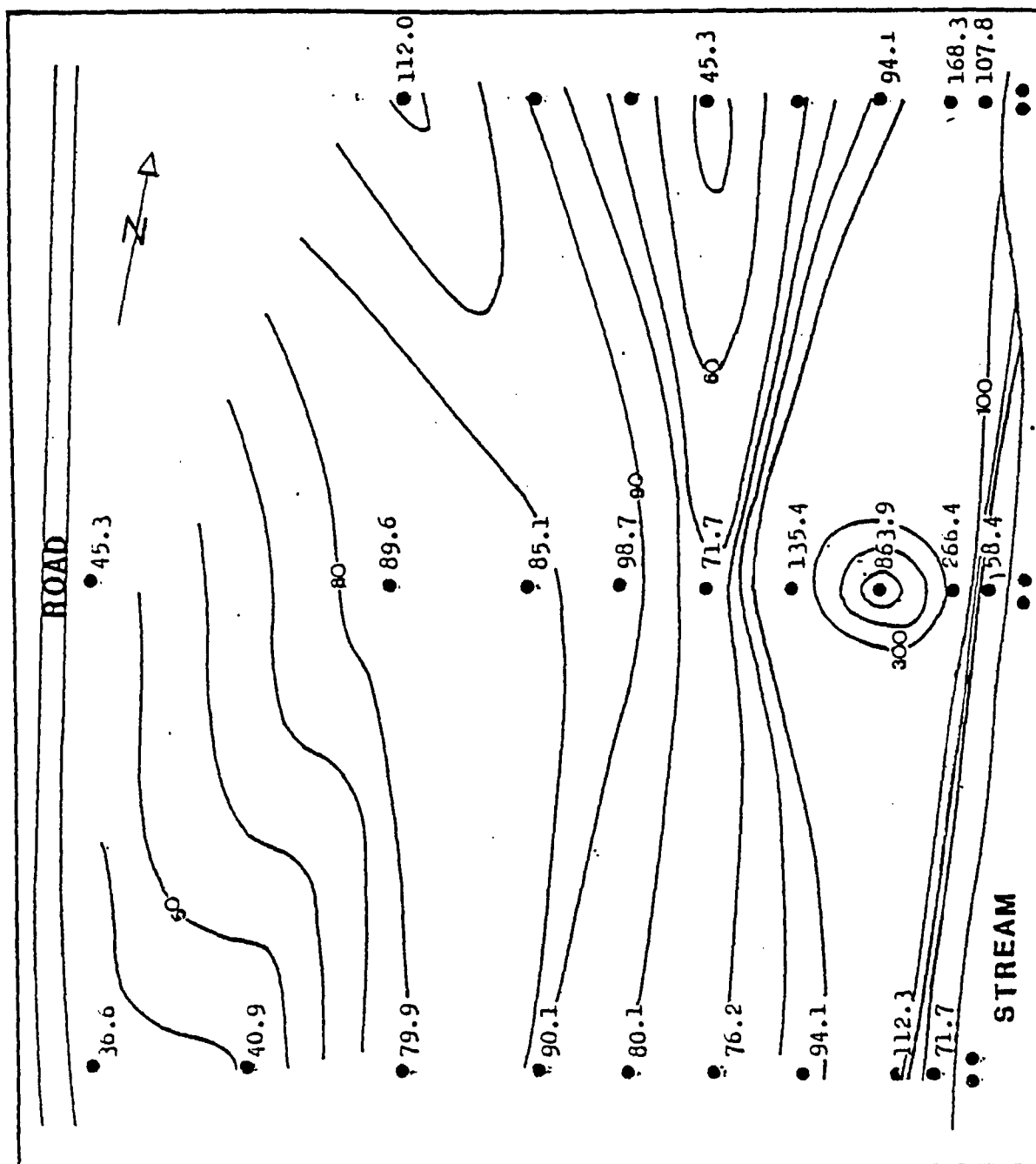


Figure 45 c Migration of the tracer based on the chemical analyses. (November 24, 1982.)
 Contour interval; 10 ppm below 100 ppm
 200 ppm above 100 ppm

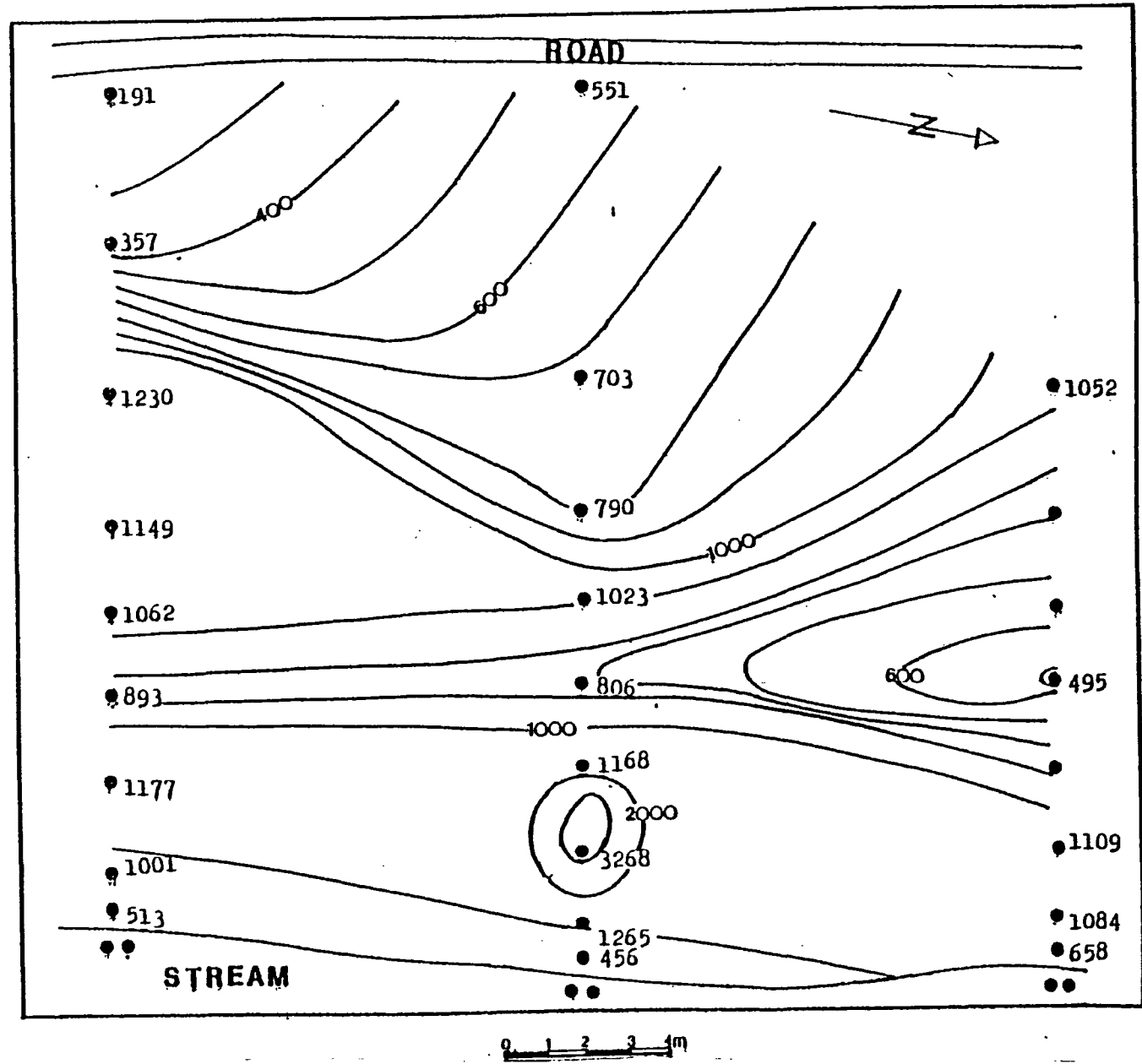


Figure 45d. Migration of the tracer based on the electrical conductivity values.(November 24,1982.)
Contour interval; 100 micro siemens below 1000
1000 micro siemens above 1000.

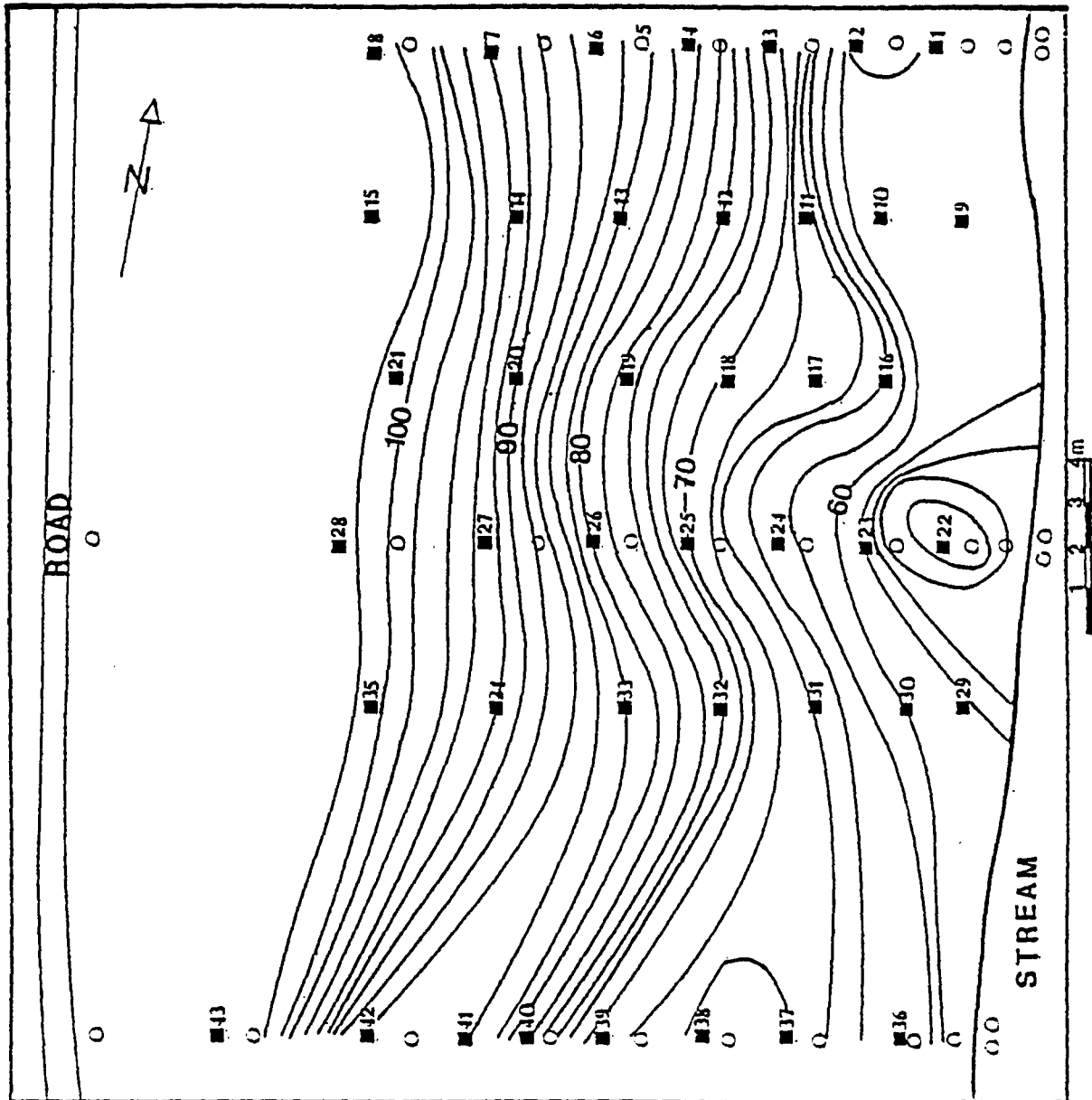


Figure 46. Migration of the tracer based on the electrical resistivity profiling. (December 17, 1982.)
Contour interval 2 micro siemens.

the tracer and the timing of sampling was probably not appropriate. In this study, samples were collected on a weekly basis in the first phase and on a monthly basis later on. No sampling was done during or immediately after the storm events. Even if the tracer had moved against the natural hydraulic gradient during the storm events, the groundwater flow may have masked it before the samples were collected.

5.4 Summary of Results

1. Groundwater response to the precipitation events occurred in piezometers nearest the stream first. Piezometers and wells located farther from the stream started responding later.

2. The water level response depended on the depth to the water table.

3. With the continuing precipitation, a general water table rise occurred and the groundwater ridge near the stream became masked.

4. Groundwater levels began declining after the rain stopped with the maximum decline along the stream where the groundwater ridge was formed during the storm.

5. Conversion of the tension-saturated capillary fringe into a pressure-saturated zone was noted through tensiometer and neutron logging observations.

6. The capillary fringe moves upward with the rising water table.

The results of the storm responses are summarized in Table 11.

5.5 Discussion of Results

The groundwater ridging hypothesis is based on the following main points (Sklash and Farvolden 1979):

1. Groundwater level response starts near the stream and it is followed by the other parts of the watershed.

2. The water table response is controlled by the depth to the water table.

3. The groundwater ridge formed during the initial stage of the storm event provides the early impetus for groundwater discharge while later high groundwater discharge is sustained by a basin-wide water table rise.

4. Formation of a groundwater ridge happens through the conversion of the tension saturated capillary fringe into a pressure saturated zone.

5. Formation of a groundwater ridge results in a rapid and significant discharge of groundwater into the stream.

The results obtained from the present study substantiate the first four points of the groundwater ridging hypothesis. The fifth point, namely the rapid groundwater discharge as a result of the groundwater ridge could not be supported due to the hydrogeological regime of the experimental plot. The groundwater flow at the site is normally away from the stream towards the road. The hydraulic gradient generated by the groundwater ridge was not great enough to change the direction of flow.

Table 11. Summary Table

Event	Pre-event Conditions		Event Description		Near Stream response	Remote response
	Rain	Depth to the water table (m)	Amount of rain (m)	Duration (hours)		
12 Oct. 1982	On 3rd Oct. 0.008 m	0.6 near stream 1.8 near the road	0.028	2	After the first hour - rapid response After the second hour rapid response continued.	No response after the first hour. Slight response after the second hour.
28 Oct. 1982	Artificial rain on Oct. 12	0.4 near stream 1.6 near the road	0.018	2	After the first hour - rapid response. After the second hour - rapid response.	No response after the first hour. Slight response after the second hour.
29 Oct. 1982	Artificial rain on 28th Oct.	0.47 near stream 1.62 near the road	0.04	3,5	After the first hour - rapid response. After the second hour - rapid response. After 3.5 hours, rapid response continued.	No response after the first hour. Slight response after the second hour. Fairly high response after 3.5 hours.
1 & 2 Nov. 1982	Artificial rain on Oct. 29	---	0.1	approx. 12	General rise of the water table was observed throughout the plot.	

The observed rise of the capillary fringe also supports the groundwater ridging hypothesis. The newly formed capillary fringe could be converted to phreatic water giving an opportunity for a continuous growth of the groundwater ridge.

The results of the present study show that the groundwater ridging hypothesis could be an acceptable theory to explain the rapid groundwater discharge during storm events.

6.0 CONCLUSIONS AND RECOMMENDATIONS

6.1 Conclusions

Based on the results of this study, the following conclusions can be made.

a) There are three layers present at the study area. The topsoil is underlain by a medium-fine sand layer about 2.5 m thick. This sand layer is underlain by a sandy silt layer which gradually changes into silt at a depth of about 4.5 m. The average hydraulic conductivity of the sand layer is about 4.3×10^{-6} m/sec. Hydraulic conductivity of the silt layer averages about 2.1×10^{-6} m/sec. The groundwater flows away from the stream to west.

b) During the four monitored storm events, water table response started near the stream first.

c) Water table response is a function of the initial depth to the water table.

d) Water table rises as a result of the conversion of the tension saturated capillary fringe into a pressure saturated zone.

e) The height of the capillary fringe is about 0.24 m at the site. The capillary fringe rises with the rising water table.

f) When the rain events stop, the water table declines with the maximum decline near the stream where the groundwater ridge formed during storm event.

In summary, it can be concluded that the groundwater

ridging hypothesis appears to be an acceptable explanation for the mechanism of the rapid and significant groundwater contribution to the storm runoff.

In light of the results obtained from the present study, the existing models on runoff generation and chemical variation in the streams during storm events, should be reevaluated. As it was shown by Pinder and Jones (1969), Walling and Foster (1975), Sklash et al. (1978), Reid et al. (1981) and others, the dilution models based on current theories of storm runoff generation do not account for the chemical behaviour of the storm runoff. This is probably because these models do not consider groundwater as a significant contributor to storm runoff.

It is important to recognize the paths through which the agricultural chemicals are being washed to streams for an effective practice of agriculture. Development of a reliable dilution model will facilitate the understanding of this migration of the chemicals.

Although the existing theories on runoff generation can explain the quantitative aspect of the storm runoff peaks, they are unable to account for the observed stream chemistry variation during runoff events. Most of these theories neglect the role of groundwater in storm runoff (Horton 1933, Betson 1964, Hewlett and Hibbert 1967, Dunne and Black 1970a, b). All these models should be modified using real proportions of the surface water and groundwater in the storm runoff.

6.2 Recommendations

Based on the results of the present study, it is recommended to carry out similar research in different hydrogeological and topographical surroundings. The use of continuous water level recorders should give better results than taking readings after a specific time. Isotope tracers are recommended for future studies as a substitute for sodium chloride. Although chloride tracers are less expensive and more easily accessible, in order to get a detectable amount of it in observation wells, a large amount of tracer should be applied. It is also recommended to apply the tracer well ahead of storm events and the sampling should be done both before and frequently during the storm events. By doing so, the chances of detecting the tracer movement against the natural hydraulic gradient due to the groundwater ridge, will be increased.

LIST OF REFERENCES

- Anderson, M. G. and Burt, T. P., 1977. A laboratory model to investigate the soil moisture conditions on a draining slope. *J. Hydrology* 33, pp. 383-390.
- Bernier, P. Y., 1982. A revised source area simulator for small forested basins. Unpubl. Ph.D. thesis, University of Georgia, Athens, Georgia, U.S.A., 143 p.
- Betson, R. P., 1964. What is watershed runoff? *J. Geophys. Res.* 69(8), pp. 1541-1551.
- Betson, R. P., and Marius, J. B., 1969. Source areas of storm runoff. *Water Resour. Res.*, 5(3), pp. 574-582.
- Chapman, L. J., and Putnam, D. F., 1966. The physiography of Southern Ontario. University of Toronto Press, 306 p.
- Clark, S. P., 1966. Handbook of physical constants. *Geolog. Society of America*, 523 p.
- Corey, J. C., 1970. Determination of soil density and water content by fast neutrons and gamma rays. *Water Resour. Res.*, 6(1), pp. 223-229.
- Crouzet, E., Hubbert, P., Olive, P., Siwertz, E., and Marce, A., 1970. Le tritium dans les mesures d'hydrologie de surface. Determination experimentale du coefficient de ruissellement. *J. Hydrol.* 11, pp. 217-229.
- Dincer, T., Payne, B. R., Flowkowski, T., Martinec, J., and Tongiorgi, E., 1970. Snowmelt runoff from measurements of tritium and oxygen -18. *Water Resour. Res.* 6, pp. 110-124.

- Dobrin, M. B., 1976. Introduction to geophysical prospecting. McGraw Hill, Inc. New York, 630 p.
- Dunne, T., and Black, R. D., 1970a. An experimental investigation of runoff production in permeable soils. Water Resour. Res., 6, pp. 478-490.
- _____, 1970b. Partial area contributions to storm runoff in a small New England watershed. Water Resour. Res., 6, pp. 1296-1311.
- Dunne, T., Moore, T. R., and Taylor, C. H., 1975. Recognition and prediction of runoff producing zones in humid regions. Bull. Int. Ass. Sci. Hydrol., 20(3), pp. 305-327.
- Elrick, D. E., and Lawson, D. W., 1967. Tracer techniques in hydrology. Hydrology Symposium, N.R.C., Victoria, B. C., Canada, pp. 178-187.
- Engman, T. E., and Rogowski, A. S., 1974. A partial area model for storm flow synthesis. Water Resour. Res. 10, pp. 464-472.
- Foster, S.S.D., 1974. Groundwater storage-river flow relationship in a chalk catchment. J. Hydrol. 23, pp. 299-311.
- Freeze, R. A., 1971. Three dimensional, transient, saturated unsaturated flow in a groundwater basin. Water Resour. Res. 8, pp. 609-623.
- _____, 1972a. Role of subsurface flow in generating surface runoff. Baseflow contributions to channel flow. Water Resour. Res., 8, pp. 609-623.

- _____, 1972b. Role of subsurface flow in generating surface runoff 2. Baseflow contributions to channel flow. Water Resour. Res. 8, pp. 1072-1283.
- _____, 1974. Streamflow generation. Rev. Geophys. Space Phys. 12, pp. 627-647.
- Freeze, R. A., and Cherry, J. A., 1979. Groundwater. Prentice-Hall Inc., Englewood Cliffs, New Jersey, 604 p.
- Glover, B. J., and Johnson, P., 1974. Variations in the natural chemical concentrations of river water during flood flows and the lag effect. J. Hydrol., V.22, pp. 303-316.
- Guiton, T. S., 1978. A groundwater study of the Ojibway prairie. Waterloo Research Institute, Waterloo.
- Hall, F. R., 1971. Dissolved solids-discharge relationships-2, applications to field data. Water Resour. Res. 7, 591-601.
- Hewlett, J. D., 1961. Soil moisture as a source of base flow from steep mountain watersheds. G.S. Forest Serv. Southeast Forest Exp. Sta., Res. paper S.E.132, 11 pp.
- Hewlett, J. D., 1969. Tracing storm base flow to variable source areas on forested headwaters. Tech. report., No. 2, School of Forest Resources, University of Georgia, Athens, Georgia, 14 p.

- Hewlett, J. D., and Hibbert, A. R., 1967. Factors effecting the response of small watersheds to precipitation in humid areas. In: International Symposium on Forest Hydrology. W. E. Sopper and H. W. Lull (Eds.), Permagon, New York, pp. 275-290.
- Hewlett, J. D., and Nutter, W. L., 1970. The varying source area of streamflow from upland areas. In: Symposium on Interdisciplinary Aspects of Watershed Management, Mont. State Univ., Bozeman, Montana, pp. 65-83.
- Hills, R. C., 1971. The influence of land management and soil characteristics on infiltration and the occurrence of overland flow. J. of Hydrol. 13, pp. 163-181.
- Horton, R. E., 1933. The role of infiltration in the hydrologic cycle. Trans. AGU, 14, pp. 446-460.
- Hvorslev, M. J., 1951. Time lag and soil permeability in groundwater observations. Bulletin 86, Waterways experiment station, Corps. of Engineers, Vicksburg, Mississippi, 49 p.
- Klute, A., Scott, E. J., and Whisler, F. D. (1965). Steady state water flow in a saturated inclined soil slab. Water Resour. Res., 1, pp. 287-294.
- Lambe, T. W. and Whiteman, R. V., 1976. Soil testing for engineers. John Wiley and Sons, Inc., New York, 165 p.
- Larzeg, H., 1972. Master curves for the Wenner array. Inland Waters Directorate, Water Resources Branch, Ottawa, Canada, 104 p.

- Lee, D. B., Cherry, J. A., and Pickens, J. F., 1980. Ground-water transport of a salt tracer through a sandy lake bed. *Limnol. Oceanogr.* 25(1), pp. 45-61.
- Manual of Technicon Autoanalyzer II, 1973. Technicon Instruments Corporation, Tarrytown, New York, U.S.A., 3p.
- Manual of Neutron Depthprobe 501, 1982. Campbell Pacific Nuclear Corporation, U.S.A., 3 p.
- Martinec, J., 1975. Subsurface flow from snowmelt traced by tritium. *Water Resour. Res.* 11, pp. 496-497.
- Martinec, J., Oeschger, H., Schotterer, U., Siegenthaler, U., Nuti, S., and Tongiorgi, E., 1981. Example of a separation of runoff components by environmental isotopes. *Rivista Italiana Di Geofisica E Science Affini*, vol. V (Bossolasco-Anniversary) (1978-79), 6 p.
- Nakamura, R., 1971. Runoff analyses by electrical conductance of water. *J. Hydrol.*, 14, pp. 197-212.
- O'Brien, A. L., 1980. The role of groundwater in stream discharges from two small wetland controlled basins in Eastern Massachusetts. *Groundwater*, 18, pp. 359-365.
- Ontario Water Resources Commission, 1971. Groundwater probability map of Essex County.
- Pilgrim, D. H., and Huff, D. D., 1979. Use of specific conductance and contact time relations for separation flow components in storm runoff. *Water Resour. Res.* 15(2), pp. 329-339.

- Pinder, G. F., and Jones, J. F., 1969. Determination of the groundwater component of peak discharge from the chemistry of total runoff. *Water Resour. Res.* 5, pp. 438-445.
- Ragan, R. M., 1968. An experimental investigation of partial area contributions. *Publ. 76 Int. Ass. Sci. Hydrol. Berne*, pp. 241-249.
- Reid, J. M., Macleod, D. A., and Cresser, M. S., 1981. Factors affecting the chemistry of precipitation and river water in an upland catchment. *J. of Hydrology*, 50, pp. 129-145.
- Richards, N. R., and Caldwell, A. G., 1949. Soils survey of Essex County. Experimental farms service, Dominion Dept. of Agriculture and Ontario Agricultural College.
- Sanderson, M., 1980. The climate of the Essex region-Canada's southern land. *Dept. of Geography, University of Windsor*, 104 p.
- Sklash, M. G., 1978. The role of groundwater in storm and snowmelt runoff generation. Unpubl. Ph.D. thesis, University of Waterloo, Waterloo, Ontario, 261 p.
- Sklash, M. G., and Farvolden, R. N., 1979. The role of groundwater in storm runoff. *J. Hydrol.* 43, pp. 45-65.
- Sklash, M. G., Farvolden, R. N., and Fritz, P., 1976. A conceptual model of watershed response to rainfall developed through the use of oxygen-18 as a natural tracer. *Can. J. Earth Sci.*, 13, pp. 271-283.

- Sklash, M. G., Gillham, R. W., and Cherry, J. A., 1978. Studies of the agricultural contribution to nitrate enrichment of groundwater and the subsequent nitrate loading to surface waters. Part III: Mechanisms of runoff generation and nitrate flux to streams during runoff events. Waterloo Research Institute, University of Waterloo, Waterloo, Ontario, 104 p.
- Sklash, M. G. and Wilson, B. A., 1982. An investigation of the groundwater ridging hypothesis for storm runoff generation. Canadian Hydrology Symposium, June 14-15, 1982, Fredericton, New Brunswick, pp. 575-596.
- Standard methods for the examination of water and wastewater, 1971. American Public Health Association, Water Works Association and Pollution Control Federation, 327 p.
- Steppuhn, H., 1975. Contributions to runoff from a melting prairie snow patch as traced by O-18. 43rd Annual Meeting, Western Snow Conference, 14 p.
- Telford, W. M., Geldarl, L. P., Sheriff, R. E., and Keys, D. A., 1976. Applied Geophysics. Vail-Ballou Press, Inc., Binghamton, New York, 860 p.
- Toler, L. G., 1965. Relation between chemical quality and water discharge in Spring creek, Southwestern Georgia. U.S. Geol. Survey, Prof. paper 525-c, pp. c209-c213.
- Toth, J., 1962. A theory of groundwater motion in small drainage basins in central Alberta, Canada. J. Geophys. Res. 67, pp. 4375-4387.

- Vagners, U. S., 1972. Quaternary geology of Windsor-Essex area, Prelim. map, p. 749, Geolog. ser., scale 1:50,000, Geology, 1970, 1971.
- Walling, D. E., and Foster, I.D.L., 1975. Variations in the natural chemical concentration of river water during flows, and the lag effect, some further comments. J. Hydrol., V26, pp. 244-277.
- Ward, R. C., 1982. The fountains of the deep and the windows of Heaven. Perplexity and progress in explaining the response of rivers to precipitation. University of Hull, an inaugural lecture delivered at the University of Hull, 30 p.
- Weyman, D. R., 1970. Throughflow on hillslopes and its relation to the stream hydrograph. Bull. Int. Ass. Sci. Hydrol. 15(2), pp. 25-33.
- Whipkey, R. Z., 1965. Subsurface storm flow from forested slopes. Bull. Int. Assoc. Sci. Hydrol. 3, pp. 74-85.
- Wilson, B. A., 1981. An investigation of the groundwater ridging theory for large groundwater contributions to streams during storm runoff events. Unpubl. M.A.Sc. thesis, University of Windsor, Windsor, Ontario, 94 p.
- Zaslavsky, D., and Sinai, G., 1981. Surface hydrology 1-Explanation of phenomena, ASCE, J. Hydraulics Div., 107 (HY1), pp. 1-16.

APPENDIX I

Analyses of Data

I.1 Seismic Method (Dobrin, 1976, Telford, et al. 1976)

The velocity of the seismic waves and the depth to the interfaces were calculated from the first arrival times plotted against geophone distance. The velocities were calculated by taking the inverse of the slope of the plot. Depth to the first interface was calculated using the following formula:

$$z_0 = \frac{1}{2} x_c \sqrt{\frac{v_1 - v_0}{v_1 + v_0}}$$

where: x_c is the critical distance and z_0 is the depth to the interface and v_0 and v_1 are the velocities of the upper and lower units.

The thickness of the following layer was calculated using the relationship given below:

$$z_1 = \frac{1}{2} \left[T_i - 2z_0 \sqrt{\frac{v_2^2 - v_0^2}{v_2 v_0}} \right] \frac{v_2 v_1}{\sqrt{v_2^2 - v_1^2}}$$

where T_i is the intercept time of the third segment of the plot, and v_2 is the velocity of the third layer.

I.2 Electrical Resistivity Method (Dobrin, 1976, Telford et al. 1976)

The apparent resistivity values were plotted against the distance between electrodes on a log-log paper. The apparent resistivity of the first layer was readily determined from the graph. Then the field data curve was matched with standard type curves, and the apparent

resistivity and the thickness of subsequent layers were determined.

I.3 Neutron Logging (Manual of Neutron Depthprobe Model 501)

Ten standard counts were averaged to obtain a standard count for each test day. Then the following formula was used to determine the volumetric moisture content:

$$\text{moisture content (gr/cu cm)} = 0.304 \times \frac{\text{Reading}}{\text{Standard}} - 0.0026$$

The plot of moisture content against the depth below the ground surface was used to determine the height of the capillary fringe. The height of the capillary fringe was determined from the plot where moisture content equals to 99% of its maximum value.

I.4 Tensiometer Experiment (Manual of Tensiometer Model 2325)

Tensiometer readings (Figure 1-1) and the depth to the porous cups were used in the equation given below to calculate the negative pressure head.

$$h = -12.6 a + c$$

The resulting pressure head was plotted against the depth.

I.5 Testing for hydraulic conductivity (Hvorscev 1951)

The logarithm of unrecovered head/initial head difference $(H-h/H-H_0)$ was plotted against the time on a semi-log paper. The basic time lag (T) , which is the

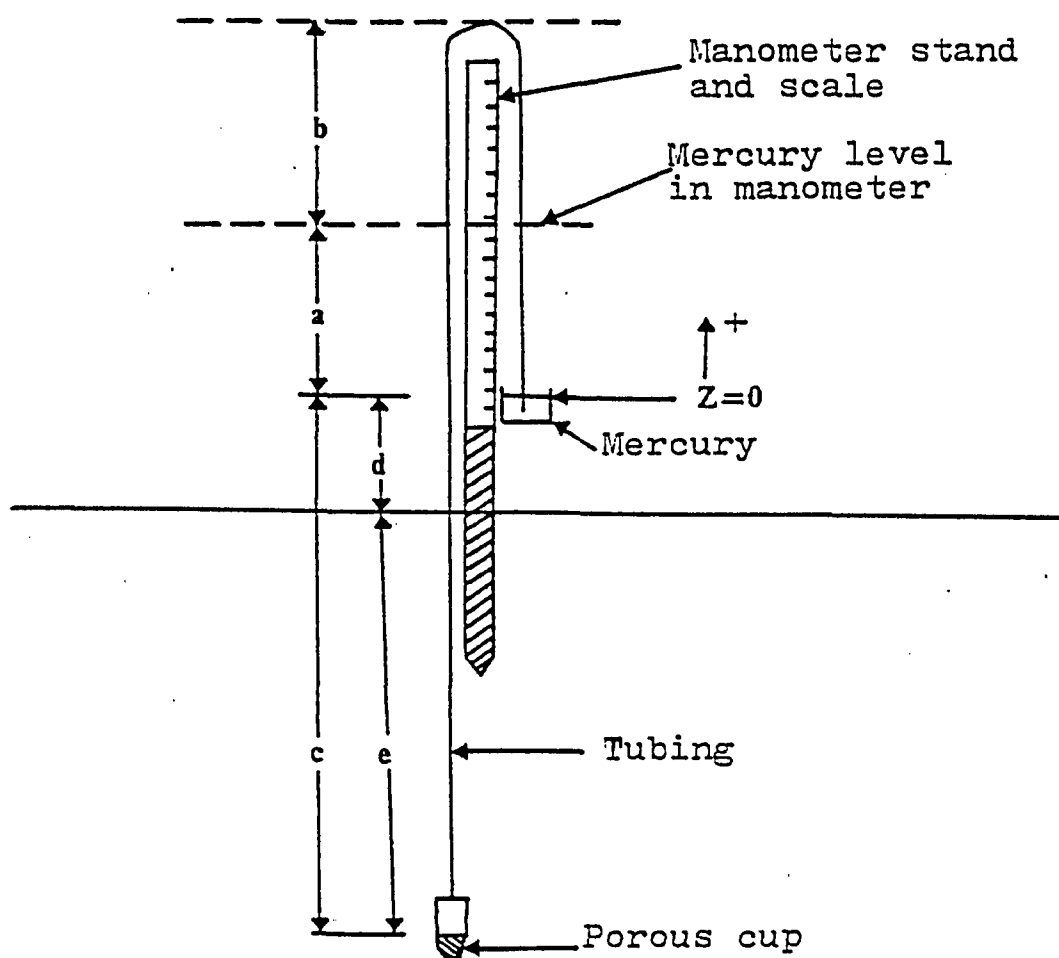


Figure I-1 Schematic diagram of a tensiometer-mercury manometer system for measuring negative pressure head.

corresponding time to the $H-h/H-H_0$ value of 0.37 was determined from the graph. The hydraulic conductivity was calculated using the formula given below,

$$K = \frac{r^2 \ln (L/R)}{2LT}$$

where:

r = radius of casing

L = length of the intake zone

R = radius of the piezometer

T = Basic time lag

I.6 Grain size analyses (Lambe, 1976)

The Hazen formula ($K = A d_{10}^2$), where the hydraulic conductivity of a soil is proportional to the square of an effective particle diameter, was used. The diameter read from a grain size curve at the 10% finer point was used as the effective diameter. The following procedure was used to analyze the hydrometer test data to obtain the diameter of the particles and the percentage of soil remaining in suspension.

Hydroscopic moisture correction factor (A) = $\frac{\text{mass of oven dried sample}}{\text{mass of sample before drying}}$

Oven dry mass of soil = Air dry mass $\times A$

$$P = \frac{(100,000/W) G}{G - G_1}$$

where:

P = percentage of soil remaining in suspension at level at which hydrometer measures the density of suspension.

W = oven dry mass of total test sample.

G = unit weight of soil particles.

G₁ = unit weight of water.

$$D = R \sqrt{L/T} = 30 \sqrt{4/980 (G-G_1) L/T}$$

where D = diameter of particle, mm.

μ = viscosity of water.

L = distance from surface of suspension to level at which density of suspension is measured, cm.

T = time reading in minutes.

R = constant.

I.7 Chloride and Electrical Conductivity Measurements

(Standard Methods For Examination of Water And Waste Water, 1971)

Both chloride concentration values and corrected electrical conductivity values were examined to study the migration of the tracer. Conductivity measurements were corrected for temperature as well as equipment errors. The following formula was used to calculate the temperature correction:

$$\text{Temperature correction} = \text{Reading} \times 0.02 (25 - T^{\circ}\text{C})$$

where: T°C - room temperature in celsius.

The readings corrected for temperature were again corrected for equipment errors by multiplying them by the ratio 1413/Reading KCl.

Where Reading KCl - is the conductivity of a standard KCl solution at the room temperature.

Appendix 11. Results of the investigation of the site.

Appendix 11-1. Electrical sounding measurements-Line 1

Electrode spacing(m)	Apperent resistivity (Ohm-m)
0.61	250.00
1.22	225.96
1.83	179.26
2.44	131.13
3.05	117.97
3.66	102.50
4.27	84.72
4.88	72.62
5.49	70.67
6.10	64.35
7.32	52.56
8.53	56.63
9.75	53.93
11.00	51.71
12.20	50.71
15.20	51.13
18.30	47.11
21.34	56.30
24.38	59.49
27.43	63.77
30.48	67.03
36.58	62.05

Appendix 11-1 cont'd

42.67	64.35
48.77	82.73
54.86	89.62
60.96	99.58

Appendix 11-2 Results of the seismic survey -line 1.

Distance(m)	Arrival time(sec $\times 10^{-3}$)	
	upshot	downshot
0.91	3.66	6.54
1.96	11.08	11.12
2.95	11.76	15.81
3.94	13.70	17.76
4.92	16.93	18.12
5.90	20.48	18.98
6.89	21.74	20.34
7.87	22.07	19.18
8.86	22.95	20.16
9.84	23.13	23.00
10.8	22.94	22.77
11.8	22.91	23.49
12.79	23.31	22.6
13.78	24.07	23.36
14.76	24.12	25.27
16.4	24.39	25.30
19.68	28.59	26.73
12.32	28.90	26.73
22.96	28.55	27.40

Appendix 11-2.cont'd

22.6	29.58	29.90
26.25	30.00	30.11
27.89	31.61	31.03
29.53	32.80	32.42
31.17	34.90	33.67
32.80	35.10	35.30
31.08	36.65	37.06
39.39	38.73	38.21
42.65	40.37	40.12
49.21	44.73	44.25
52.49	46.26	46.95
55.77	48.20	48.55
59.06	49.76	50.85
62.34	52.45	53.11
65.60	54.00	54.61
72.18	55.25	59.65
78.75	62.95	62.51
85.30	65.3	65.23

Appendix 11-3. Results of the seismic survey-line 2.

Distance(m)	Arrival time(sec $\times 10^{-3}$)	
	up shot	down shot.
0.98	4.40	7.88
1.96	9.75	12.60
2.95	14.01	16.03
3.95	17.55	19.16
4.92	20.17	21.07
5.90	22.05	22.17
6.89	21.89	23.63
7.87	23.45	24.72
8.86	23.15	24.11
9.84	24.55	25.79
10.80	25.04	25.79
11.80	24.37	26.86
12.76	26.85	27.17
13.78	27.27	27.67
14.76	29.77	28.74
16.40	31.94	29.67
18.04	31.09	30.98
19.68	31.28	31.79
22.32	32.04	30.69
22.96	33.72	30.65

Appendix 11-3 cont'd

24.60	36.88	32.78
26.25	37.86	34.62
27.89	39.46	34.42
29.53	39.98	34.17
31.17	40.03	34.46
32.80	41.55	37.47
31.08	42.45	38.02
39.37	43.96	40.22
42.65	44.14	44.46

Appendix 11-4. Elevation of piezometers and wells.

Well/piezometer.	Elevation (m)
P-1	111.68
P-2	111.73
P-3	111.77
P-4	111.82
P-5	111.89
P-6	111.76
P-7	110.96
P-8	110.42
P-9	110.22
P-10	111.51
P-11	111.63
P-12	111.67
P-13	111.69
P-14	111.71
P-15	111.81
P-15	111.76
P-16	111.10
P-17	110.63
P-18	110.22
P-19	110.57
P-20	111.57
P-21	111.57

Appendix 11-4 cont'd.

P-22	111.62
P-23	111.67
P-24	110.76
P-25	110.45
P-26	110.22
W-1	111.34
W-2	111.37
W-3	111.50

Relative to an arbitrary datum 100m below the ground surface.

Appendix 11-5. Hydraulic conductivity values determined using Hvorslev's method.

well/ piezometer	K (m/sec)
P-1	6.2×10^{-6}
P-2	2.6×10^{-6}
P-3	4.2×10^{-6}
P-4	3.8×10^{-6}
P-5	3.4×10^{-6}
P-6	5.2×10^{-6}
P-7	2.5×10^{-6}
P-8	3.3×10^{-6}
P-10	2.3×10^{-6}
P-11	1.5×10^{-6}
P-12	2.3×10^{-6}
P-13	2.4×10^{-6}
P-14	8.3×10^{-7}
P-15	6.3×10^{-7}
P-16	2.4×10^{-7}
P-17	2.4×10^{-7}
P-18	3.3×10^{-7}
P-20	3.4×10^{-7}
P-21	4.7×10^{-7}
P-22	2.4×10^{-7}
P-23	2.5×10^{-7}
P-24	2.0×10^{-6}

Appendix 11-5 cont'd

P-24	2.0×10^{-6}
P-25	2.3×10^{-6}
W-1	8.9×10^{-7}
W-2	4.7×10^{-7}
W-3	6.7×10^{-7}

Appendix 11-6
Hydraulic conductivity values determined using
Hazen's formula.

well/ auger hole	sample No.	Interval(m)	hydraulic conductivity(m/s)
Deep well	1	0 -0.45	5.2×10^{-5}
	2	0.45-0.91	3.8×10^{-5}
	3	0.91-1.37	6.7×10^{-5}
	4	1.37-1.87	5.2×10^{-5}
	5	1.87-2.28	3.2×10^{-4}
	6	2.28-2.74	6.4×10^{-5}
	7	2.74-3.20	6.1×10^{-5}
	8	3.20-3.65	4.9×10^{-5}
	9	3.65-4.11	3.4×10^{-5}
	10	4.11-4.57	7.3×10^{-6}
	11	4.57-5.02	4.0×10^{-6}
	12	5.02-5.48	2.3×10^{-6}
Auger hole 1	1	0 -0.40	1.7×10^{-4}
	2	0.40-0.80	1.0×10^{-4}
	3	0.80-1.20	4.6×10^{-5}
Auger hole 2	1	0 -0.40	7.8×10^{-6}
	2	0.40-0.80	2.25×10^{-4}
	3	0.80-1.20	3.6×10^{-5}
Auger hole 3	1	0 -0.40	1.4×10^{-4}
	2	0.40-0.80	1.4×10^{-5}
	3	0.80-1.20	7.0×10^{-5}
Auger hole 4	1	0 -0.40	6.4×10^{-5}
	2	0.40-0.80	1.7×10^{-4}
	3	0.80-1.20	3.4×10^{-5}

Appendix III. Results of the October 12, 1982 storm event.

Appendix III-1 October 12, 1982 storm event. Depth to the water table.

Well/ piezometer.	t=0	t=60min.	t=120min.	t=1080min.
P-1	1.95	1.95	1.87	1.90
P-2	1.97	1.97	1.90	1.92
P-3	2.02	2.02	1.95	1.97
P-4	2.05	2.05	1.97	2.00
P-5	2.15	2.12	2.07	2.10
P-6	1.97	1.92	1.85	1.87
P-7	1.15	1.00	0.87	0.92
P-8	0.60	1.45	0.32	0.37
P-9*	0.30	0.30	0.32	0.25
P-10	1.85	1.85	1.77	1.80
P-11	1.92	1.92	1.82	1.87
P-12	1.90	1.90	1.80	1.85
P-13	1.90	1.87	1.77	1.82
P-14	1.87	1.82	1.72	1.75
P-15	1.90	1.85	1.75	1.77
P-16	1.87	1.80	1.72	1.75
P-17	1.12	1.02	0.90	0.97
P-18	0.70	0.55	0.45	0.55
P-19*	0.27	0.27	0.29	0.27
P-20	1.80	1.75	1.69	1.70
P-21	1.75	1.70	1.60	1.65
P-22	1.72	1.67	1.55	1.62
P-23	1.70	1.62	1.52	1.60

Appendix III-1cont'd

P-24	0.75	0.67	0.57	0.62
P-25	0.47	0.34	0.20	0.27
P-26*	0.27	0.27	0.29	0.25
W-1	1.56	1.56	1.51	1.51
W-2	1.62	1.62	1.55	1.55
W-3	1.77	1.77	1.72	1.71

* above the ground level.

Appendix 111-2 October 12, 1982 storm event. Volumetric moisture content.(%).

Neutron access tube.	Depth(m).	t=0	t=60min.	t=120min.
NA-1	0.20	29	30	31
	0.40	32	32	33
	0.60	37	37	38
	0.80	41	41	42
	1.00	45	45	46
	1.20	47	47	49
	1.40	50	50	50
NA-2	0.20	26	27	32
	0.40	29	29	30
	0.60	32	32	34
	0.80	36	36	37
	1.00	40	39	39
	1.20	43	42	42
	1.40	46	45	46
NA-3	0.20	27	28	32
	0.40	28	28	30
	0.60	31	31	32
	0.80	36	36	38
	1.00	42	42	44
	1.20	45	46	48
	1.40	48	49	50

Appendix 111-2 cont'd

NA-4	0.20	26	28	31
	0.40	28	28	29
	0.60	32	32	34
	0.80	38	38	39
	1.00	42	43	44
	1.20	47	46	49
	1.40	49	50	50

Appendix 111-3 October 12, 1982 storm event. Pressure head(cm).

Tensiometer nest.	Depth(m).	t=0	t=120min.	t=1080min.
TN-1	0.30	-155	-140	-60
	0.50	-145	-125	-130
	0.70	-110	-110	-90
	0.70	-75	-75	-65
	1.10	-50	-45	-40
TN-2	0.30	-160	-150	-60
	0.50	-140	-145	-95
	0.70	-125	-130	-105
	0.90	-110	-110	-100
	1.10	-85	-80	-80
TN-4	0.30	-155	-145	-75
	0.50	-140	-135	-85
	0.70	-125	-120	-105
	0.90	-110	-105	-105
	1.10	-90	-70	-80

Appendix IV. Results of the October 28, 1982 storm event.

Appendix IV-1 October 28, 1982 storm event. Depth to the water table. (m)

Well/ Piezometer.	t=0	t=60min.	t=120min.	t=1260min.
P-1	1.77	1.77	1.67	1.72
P-2	1.77	1.77	1.67	1.70
P-3	1.80	1.80	1.70	1.75
P-4	1.80	1.80	1.70	1.75
P-5	1.90	1.89	1.82	1.85
P-6	1.75	1.70	1.62	1.67
P-7	1.00	0.96	0.87	0.92
P-8	0.47	0.37	0.25	0.32
P-9*	0.15	0.15	0.17	0.15
P-10	1.50	1.50	1.45	1.45
P-11	1.65	1.65	1.55	1.55
P-12	1.62	1.62	1.55	1.57
P-13	1.80	1.80	1.70	1.72
P-14	1.80	1.77	1.70	1.72
P-15	1.87	1.85	1.75	1.80
P-16	1.85	1.80	1.70	1.75
P-17	1.15	1.07	0.95	1.02
P-18	1.15	0.60	0.42	0.55
P-19*	0.75	0.30	0.32	0.27
P-20	0.30	1.60	1.50	1.55
P-21	1.60	1.60	1.50	1.55
P-22	1.62	1.57	1.47	1.52
P-23	1.62	1.62	1.57	1.57

Appendix IV-1cont'd

P-24	0.75	0.65	0.55	0.60
P-25	0.42	0.30	0.20	0.17
P-26*	0.22	0.22	0.24	0.20
W-1	1.50	1.50	1.43	1.47
W-2	1.50	1.50	1.43	1.47
W-3	1.57	1.57	1.50	1.55

* Above the ground level.

Appendix 1V-2 October 28, 1982 storm event. Volumetric moisture content. (%)

Neutron access tube.	Depth(m)	t=0	t=60min.	t=120min
NA-1	0.20	30	31	33
	0.40	29	29	30
	0.60	31	32	33
	0.80	33	33	35
	1.00	35	36	36
	1.20	37	39	40
	1.40	40	40	-
NA-2	0.20	31	32	33
	0.40	28	29	30
	0.60	28	30	32
	0.80	30	31	33
	1.00	32	33	36
	1.20	34	35	39
	1.40	40	40	40
NA-3	0.20	33	34	35
	0.40	31	32	33
	0.60	31	33	33
	0.80	31	33	35
	1.00	34	35	36
	1.20	37	39	40
	1.40	41	41	-

Appendix 1V-2 cont'd

NA-4	0.20	35	35	37
	0.40	32	34	35
	0.60	32	34	35
	0.80	33	35	35
	1.00	33	36	36
	1.20	36	38	39
	1.40	39	40	40

Appendix 1V-3 October 28, 1982 storm event. Pressure head(cm).

Tensiometer nest.	Depth(m).	t=0	t=60min.	t=120min.
TN-1	0.30	-125	-125	-65
	0.50	-110	-120	-70
	0.70	-95	-105	-60
	0.90	-85	-85	-55
	1.10	-60	-60	-40
TN-2	0.30	-150	-135	-75
	0.50	-135	-130	-80
	0.70	-125	-120	-75
	0.90	-105	-100	-65
	1.10	-85	-75	-55
TN-4	0.30	-140	-140	-85
	0.50	-130	-130	-75
	0.70	-115	-120	-65
	0.90	-100	-95	-55
	1.10	-80	-75	-40

Appendix V. Results of the October 29, 1982 storm event.

Appendix V-1 October 29, 1982 storm event. Depth to the water table.

Well/ piezometer.	t=0	t=60min.	t=120min.	t=210min.	t=1440min.
P-1	1.75	1.65	1.70	1.62	1.65
P-2	1.80	1.80	1.72	1.65	1.67
P-3	1.82	1.80	1.75	1.67	1.70
P-4	1.87	1.82	1.75	1.67	1.70
P-5	1.90	1.85	1.80	1.70	1.75
P-6	1.72	1.67	1.60	1.50	1.55
P-7	0.97	0.90	0.77	0.67	0.72
P-8	0.50	0.40	0.30	0.15	0.25
P-9*	0.17	0.17	0.19	0.20	0.18
P-10	1.67	1.67	1.63	1.55	1.60
P-11	1.77	1.77	1.70	1.57	1.65
P-12	1.75	1.75	1.67	1.57	1.62
P-13	1.70	1.65	1.62	1.52	1.56
P-14	1.62	1.57	1.52	1.40	1.47
P-15	1.65	1.60	1.55	1.42	1.47
P-16	1.62	1.55	1.47	1.35	1.40
P-17	0.97	0.87	0.77	0.65	0.72
P-18	0.57	0.47	0.35	0.20	0.27
P-19*	0.17	0.17	0.19	0.20	0.18
P-20	1.65	1.62	1.55	1.42	1.50
P-21	1.65	1.60	1.55	1.47	1.50
P-22	1.65	1.60	1.56	1.43	1.50
P-23	1.60	1.55	1.50	1.40	1.47

Appendix V-1 cont'd

P-24	0.62	0.57	0.52	0.42	0.47
P-25	0.35	0.25	0.20	0.07	0.12
P-26*	0.17	0.17	0.19	0.20	0.19
W-1	1.45	1.45	1.37	1.30	1.32
W-2	1.47	1.47	1.40	1.30	1.35
W-3	1.62	1.62	1.55	1.46	1.47

* Above the ground level.

Appendix V-2 October 29, 1982 storm event. Volumetric moisture content.

Neutron access tube.	Depth(m)	t=0	t=60min.	t=210min.
NA-1	0.20	31	32	33
	0.40	30	30	31
	0.60	31	32	33
	0.80	33	33	34
	1.00	34	35	39
	1.20	40	40	40
	1.40	-	-	-
NA-2	0.20	31	32	34
	0.40	29	30	32
	0.60	29	31	33
	0.80	30	32	33
	1.00	32	32	34
	1.20	33	34	38
	1.40	40	40	40
NA-3	0.20	33	34	35
	0.40	32	33	34
	0.60	33	33	34
	0.80	33	34	35
	1.00	34	36	37
	1.20	37	40	42
	1.40	42	42	-

Appendix V-2cont'd

NA-4	0.20	34	34.5	35
	0.40	32	33	34
	0.60	32	33	34
	0.80	32	34	35
	1.00	35	36	37
	1.20	39	39	42
	1.40	42	42	-

Appendix V-3 October 29, 1982 storm event. Pressure head(cm).

Tensiometer nest.	Depth(m)	t=0	t=60min.	t=120min.
TN-1	0.30	-35	-40	-10
	0.50	-55	-60	-20
	0.70	-85	-55	-10
	0.90	-80	-40	-8
	1.10	-50	-25	-5
TN-2	0.30	-65	-35	-30
	0.50	-80	-55	-35
	0.70	-105	-60	-45
	0.90	-95	-45	-30
	1.10	-65	-30	-20
TN-4	0.30	-60	-55	-30
	0.50	-65	-60	-40
	0.70	-75	-50	-35
	0.90	-65	-40	-25
	1.10	-50	-35	-15

Appendix VI. Results of the November 1 and 2 storm event.
 Appendix VI-1 November 1, 2 storm event. Depth to
 the water table.

Well/ piezometer.	November 2	November 3
P-1	0.95	1.30
P-2	1.05	1.32
P-3	1.07	1.32
P-4	1.15	1.42
P-5	1.17	1.42
P-6	1.07	1.32
P-7	0.37	0.58
P-8	0.24*	0.05
P-9	0.65*	0.35*
P-10	0.85	1.15
P-11	0.85	1.12
P-12	0.85	1.12
P-13	0.90	1.15
P-14	0.92	1.17
P-15	1.05	1.30
P-16	1.05	1.30
P-17	0.37	0.65
P-18	0.17*	0.17
P-19	0.65*	0.38*
P-20	0.65	0.90
P-21	0.67	0.92
P-22	0.75	1.00
P-23	0.85	1.07

Appendix VI-1cont'd

P-24	0.12	0.22
P-25	0.17*	0.10
P-26	0.65*	0.38*
W-1	0.52	0.75
W-2	0.57	0.72
W-3	0.62	0.87

* Above the ground level.

Appendix VI-2 November 1,2 storm event.Pressure head.(cm)

Date	Depth(m)	TN-1	TN-2	TN-4
Nov.2	0.30	-15	-25	-40
	0.50	-5	-20	-45
	0.70	+65	+30	-25
	0.90	+145	+110	+20
	1.10	+220	+175	+85
Nov.3	0.30	-30	-60	-80
	0.50	-50	-45	-65
	0.70	-10	-20	-45
	0.90	+45	+5	-20
	1.10	+95	+30	+10

Appendix VII. Results of the tracer experiment.

Appendix VII-1 Electrical conductivity of water samples (micro seimens)

Well/piezometer.	Nov. 5*	Nov. 16**	Nov. 24	Nov. 30	Dec. 10	Dec. 17	Feb. 16
P-1	871	1027	1052	862	690	757	573
P-2	781	727	-	636	570	591	444
P-3	806	968	-	964	819	1381	636
P-4	739	983	495	627	618	811	766
P-5	916	-	-	-	-	1511	-
P-6	1072	1275	1109	1153	1497	1184	766
P-7	995	1200	1084	1141	1057	935	1844
P-8	949	1043	658	1113	624	682	1279
P-10	401	508	551	538	535	519	505
P-11	585	-	703	749	662	626	596
P-12	696	891	790	1035	852	780	655
P-13	1011	1050	1023	1053	945	904	677
P-14	981	998	806	951	997	924	783
P-15	899	1116	1168	1550	1009	989	1142
P-16	1059	3606	3268	12266	19858	12311	4708
P-17	921	1200	1285	1819	2949	1889	1295

Appendix Vll-1 cont'd

P-18	876	917	456	874	770	642	1959
P-20	1271	1361	1149	1279	1212	1190	990
P-21	921	1069	1062	1069	1098	1101	969
P-22	879	953	893	1062	954	1045	1014
P-23	925	1151	1177	1192	1096	1026	1006
P-24	324	904	1001	-	-	1012	952
P-25	-	923	513	641	578	845	904
W-1	279	-	191	279	281	335	-
W-2	522	621	357	492	671	665	869
W-3	912	1164	1230	1185	914	897	803
stream	-	703	-	-	-	-	-

* tracer application.

** natural rain took place.

Appendix VII-2 Concentration of chloride ions(ppm).

Well/ piezometer.	Nov.5*	Nov.16**	Nov.24	Nov.30
P-1	121.5	135.4	112.0	86.9
P-2	89.6	76.2	-	66.0
P-3	85.1	80.6	-	96.8
P-4	85.1	89.6	45.3	55.0
P-5	-	-	-	242.0
P-6	135.4	112.3	94.1	79.2
P-7	140.1	176.7	168.3	203.5
P-8	76.2	157.9	107.8	188.1
P-10	45.3	49.6	45.3	28.6
P-11	80.6	-	89.6	71.5
P-12	89.6	-	85.1	77.0
P-13	98.7	98.6	98.7	90.2
P-14	94.1	76.1	71.7	55.0
P-15	130.8	116.9	135.4	107.8
P-16	140.1	773.6	863.9	4174.5
P-17	121.5	163.6	266.4	420.2
P-18	80.6	98.7	58.4	143.0
P-20	140.1	112.3	90.1	91.2
P-21	85.1	80.6	80.1	77.0
P-22	94.1	89.6	76.2	68.2
P-23	98.7	103.2	94.1	90.2
P-24	40.9	121.5	112.3	110.0
P-25	-	97.1	71.7	79.2

Appendix V11-2 cont'd

W-1	36.6	-	36.6	19.8
W-2	71.6	85.1	40.9	33.0
W-3	94.1	94.1	79.9	77.0
stream	-	173.1	-	-

Appendix VII-3 Results of the electrical resistivity survey.

Station No.	Resistivity. (ohm-m)
1	59.96
2	56.15
3	58.74
4	80.23
5	86.79
6	94.84
7	104.61
8	59.58
9	59.67
10	67.20
11	76.11
12	84.36
13	93.96
14	105.54
15	63.86
16	67.44
17	6972
18	77.36
19	91.02
20	100.77
21	51.55
22	58.92

Appendix VII-3.cont'd

23	62.26
24	69.94
25	80.12
26	92.54
27	103.14
28	58.61
29	60.08
30	66.35
31	74.83
32	82.39
33	92.15
34	100.98
35	63.61
36	64.98
37	66.29
38	65.10
39	70.31
40	78.35
41	84.17
42	86.23
43	108.75

CURRICULUM VITAE.

BORN: August 6, 1951 in Badulla, Sri Lanka.

Education:

Secondary school:

Bandarawela Maha Vidyalaya. Bandarawela. Sri Lanka.

University Education:

People's Friendship University, Moscow, Soviet Union.

Master of Science Degree in Petroleum Engineering, 1978.

Professional experience:

Three years of experience as an engineering geologist with
Foundations and geoscience consultants, P.O. Box 1048, Agodi,
Ibadan, Nigeria.

Home address: Hegoda, Badulla. Sri Lanka.